periodic table) and ZnSe is a 2–6 compound. The degree of ionic character in the bonding of these compounds increases as the electronegativity between the atoms in the compounds increases. Thus, one would expect a 2-6 compound to have more ionic character than a 3-5 compound because of the greater electronegativity difference in the 2-6 compound. Example Problem 2.9 illustrates this.

EXAMPLE PROBLEM 2.9

Calculate the percentage ionic character of the semiconducting compounds GaAs (3–5) and ZnSe (2–6) by using Pauling's equation

$$\% \text{ ionic character} = (1 - e^{(-1/4)(X_A - X_B)^2})(100\%)$$

a. For GaAs, electronegativities from Fig. 2.14 are $X_{Ga} = 1.6$ and $X_{As} = 2.0$. Thus,

$$\begin{aligned} \% \text{ ionic character} &= (1 - e^{(-1/4)(1.6-2.0)^2})(100\%) \\ &= (1 - e^{(-1/4)(-0.4)^2})(100\%) \\ &= (1 - 0.96)(100\%) = 4\% \end{aligned}$$

b. For ZnSe, electronegativities from Fig. 2.14 are $X_{Zn} = 1.6$ and $X_{Se} = 2.4$. Thus,

$$\begin{aligned} \% \text{ ionic character} &= (1 - e^{(-1/4)(1.6-2.4)^2})(100\%) \\ &= (1 - e^{(-1/4)(-0.8)^2})(100\%) \\ &= (1 - 0.85)(100\%) = 15\% \end{aligned}$$

Note that as the electronegativities differ, more for the 2–6 compound, the percentage ionic character increases.

Metallic-Covalent Mixed Bonding Mixed metallic-covalent bonding occurs commonly. For example, the transition metals have mixed metallic-covalent bonding involving dsp bonding orbitals. The high melting points of the transition metals are attributed to mixed metallic-covalent bonding. Also in group 4A of the periodic table, there is a gradual transition from pure covalent bonding in carbon (diamond) to some metallic character in silicon and germanium. Tin and lead are primarily metallically bonded.

Metallic-Ionic Mixed Bonding If there is a significant difference in electronegativity in the elements that form an intermetallic compound, there may be a significant amount of electron transfer (ionic binding) in the compound. Thus, some intermetallic compounds are good examples for mixed metallic-ionic bonding. Electron transfer is especially important for intermetallic compounds such as $NaZn_{13}$ and less important for compounds Al_9Co_3 and Fe_5Zn_{21} since the electronegativity differences for the latter two compounds are much less.

2.6 SECONDARY BONDS

Until now, we have considered only primary bonding between atoms and showed that it depends on the interaction of their valence electrons. The driving force for primary atomic bonding is the lowering of the energy of the bonding electrons. Secondary bonds are relatively weak in contrast to primary bonds and have energies of

only about 4 to 42 kJ/mol (1 to 10 kcal/mol). The driving force for secondary bonding is the attraction of the electric dipoles contained in atoms or molecules.

An electric dipole moment is created when two equal and opposite charges are separated, as shown in Fig. 2.29*a*. Electric dipoles are created in atoms or molecules when positive and negative charge centers exist (Fig. 2.29*b*).

Dipoles in atoms or molecules create dipole moments. A *dipole moment* is defined as the charge value multiplied by the separation distance between positive and negative charges, or

$$\mu = qd \tag{2.13}$$

where μ = dipole moment
q = magnitude of electric charge
d = separation distance between the charge centers

Dipole moments in atoms and molecules are measured in Coulomb-meters (C · m) or in debye units, where 1 debye = 3.34×10^{-30} C · m.

Electric dipoles interact with each other by electrostatic (Coulombic) forces, and thus atoms or molecules containing dipoles are attracted to each other by these forces. Even though the bonding energies of secondary bonds are weak, they become important when they are the only bonds available to bond atoms or molecules together.

In general, there are two main kinds of secondary bonds between atoms or molecules involving electric dipoles: fluctuating dipoles and permanent dipoles. Collectively, these secondary dipole bonds are sometimes called *van der Walls bonds (forces)*.

Very weak secondary bonding forces can develop between the atoms of noble-gas elements that have complete outer-valence-electron shells (s^2 for helium and s^2p^6 for Ne, Ar, Kr, Xe, and Rn). These bonding forces arise because the asymmetrical distribution of electron charges in these atoms creates electric dipoles. At any instant, there is a high probability that there will be more electron charge on one side of an atom than on the other (Fig. 2.30). Thus, in a particular atom, the electron charge cloud will change with time, creating a "fluctuating dipole." Fluctuating dipoles of nearby atoms can attract each other, creating weak interatomic nondirectional bonds. The liquefaction and solidification of the noble gases at low temperatures and high pressures are attributed to fluctuating dipole bonds. The melting and boiling points of the noble gases at atmospheric pressure are listed in Table 2.8. Note that as the atomic size of the noble gases increases, the melting and boiling points also increase due to stronger bonding forces since the electrons have more freedom to create stronger dipole moments.

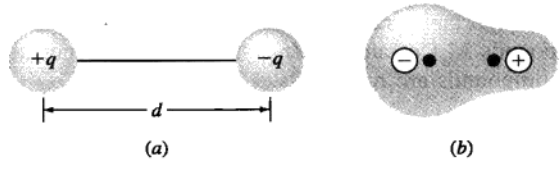

Figure 2.29
(*a*) An electric dipole. The dipole moment is *qd*.
(*b*) An electric dipole moment in a covalently bonded molecule.

Table 2.8 The melting and boiling points of various noble gases.

Noble gas	Melting point (°C)	Boiling point (°C)
Helium	−272.2	−268.9
Neon	−248.7	−245.9
Argon	−189.2	−185.7
Krypton	−157.0	−152.9
Xenon	−112.0	−107.1
Radon	−71.0	−61.8

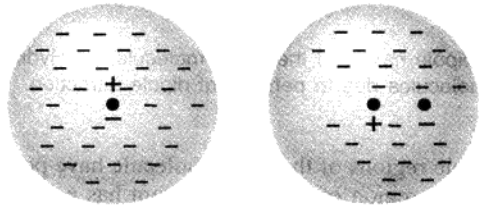

(*a*) (*b*)

Figure 2.30
Electron charge distribution in a noble gas atom. (a) An idealized symmetric charge distribution in which the negative and positive charge centers are superimposed at the center. (b) The actual asymmetric distribution of electrons causing a temporary dipole.

Weak bonding forces among covalently bonded molecules can be created if the molecules contain **permanent dipoles.** For example, the methane molecule, CH_4, with its four C–H bonds arranged in a tetrahedral structure (Fig. 2.24), has a zero dipole moment because of its symmetrical arrangement of four C–H bonds. That is, the vectorial addition of its four dipole moments is zero. The chloromethane molecule, CH_3Cl, in contrast, has an asymmetrical tetrahedral arrangement of three C–H bonds and one C–Cl bond, resulting in a net dipole moment of 2.0 debyes. The replacement of one hydrogen atom n methane with one chlorine atom raises the boiling point from −128°C for methane to −14°C for chloromethane. The much higher boiling point of chloromethane is due to the permanent dipole bonding forces among the chloromethane molecules.

The **hydrogen bond** is a special case of a permanent dipole-dipole interaction between polar molecules. Hydrogen bonding occurs when a polar bond containing the hydrogen atom, O–H or N–H, interacts with the electronegative atoms O, N, F, or Cl. For example, the water molecule, H_2O, has a permanent dipole moment of 1.84 debyes due to its asymmetrical structure with its two hydrogen atoms at an angle of 105° with respect to its oxygen atom (Fig. 2.31*a*).

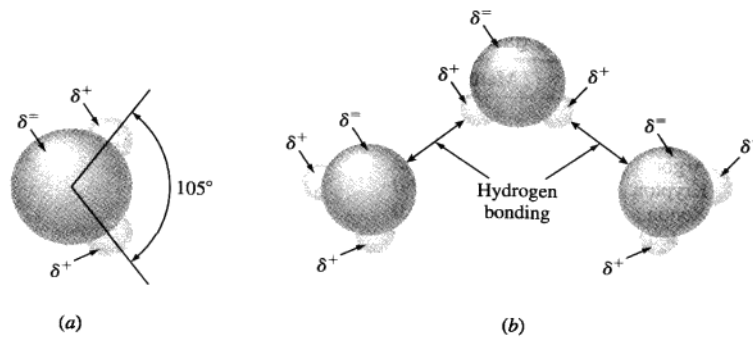

Figure 2.31
(*a*) Permanent dipole nature of the water molecule. (*b*) Hydrogen bonding among water molecules due to permanent dipole attraction.

The hydrogen atomic regions of the water molecule have positively charged centers, and the opposite end region of the oxygen atom has a negatively charged center (Fig. 2.31*a*). In hydrogen bonding between water molecules, the negatively charged region of one molecule is attracted by coulombic forces to the positively charged region of another molecule (Fig 2.31*b*).

In liquid and solid water, relatively strong intermolecular permanent dipole forces (hydrogen bonding) are formed among the water molecules. The energy associated with the hydrogen bond is about 29kJ/mol (7 kcal/mol) as compared to about 2 to 8 kJ/mol (0.5 to 2 kcal/mol) for fluctuating dipole forces in the noble gases. The exceptionally high boiling point of water (100°C) for its molecular mass is attributed to the effect of hydrogen bonding. Hydrogen bonding is also very important for strengthening the bonding between molecular chains of some types of polymeric materials.

2.7 SUMMARY

Atoms consist mainly of three basic subatomic particles: *protons, neutrons,* and *electrons.* The electrons are envisaged as forming a cloud of varying density around a denser atomic nucleus containing almost all the mass of the atom. The outer electrons (high energy electrons) are the valence electrons, and it is mainly their behavior that determines the chemical reactivity of each atom.

Electrons obey the laws of quantum mechanics, and as a result, the energies of electrons are *quantized.* That is, an electron can have only certain allowed values of energies. If an electron changes its energy, it must change to a new allowed energy level. During an energy change, an electron emits or absorbs a photon of energy according to Planck's equation $\Delta E = h\nu$, where ν is the frequency of the radiation. Each electron is associated with four quantum numbers: the principal quantum number n, the subsidiary quantum number l, the magnetic quantum number m_l, and the spin quantum number m_s. According to Pauli's exclusion principle, *no two electrons in the same atom can have all four quantum numbers the same.* Electrons also obey Heisenberg's uncertainty principle, which states that it is impossible to determine the momentum and position of an electron simul-

taneously. Thus, the location of electrons in atoms must be considered in terms of electron density distributions.

There are two main types of atomic bonds: (1) *strong primary bonds* and (2) *weak secondary bonds*. Primary bonds can be subdivided into (1) *ionic*, (2) *covalent*, and (3) *metallic bonds*, and secondary bonds can be subdivided into (1) *fluctuating dipoles* and (2) *permanent dipoles*.

Ionic bonds are formed by the transfer of one or more electrons from an electropositive atom to an electronegative one. The ions are bonded together in a solid crystal by electrostatic (coulombic) forces and are *nondirectional*. The size of the ions (geometric factor) and electrical neutrality are the two main factors that determine the ion packing arrangement. *Covalent bonds* are formed by the sharing of electrons in pairs by half-filled orbitals. The more the bonding orbitals overlap, the stronger the bond. Covalent bonds are *directional*. *Metallic bonds* are formed by metal atoms by a mutual sharing of valence electrons in the form of delocalized electron charge clouds. In general, the fewer the valence electrons, the more delocalized they are and the more metallic the bonding. *Metallic bonding* only occurs among an aggregate of atoms and is *nondirectional*.

Secondary bonds are formed by the electrostatic attraction of electric dipoles within atoms or molecules. *Fluctuating dipoles* bond atoms together due to an asymmetrical distribution of electron charge within atoms. These bonding forces are important for the liquefaction and solidification of noble gases. *Permanent dipole* bonds are important in the bonding of polar covalently bonded molecules such as water and hydrocarbons.

Mixed bonding commonly occurs between atoms and in molecules. For example, metals such as titanium and iron have mixed metallic-covalent bonds; covalently bonded compounds such as GaAs and ZnSe have a certain amount of ionic character; some intermetallic compounds such as $NaZn_{13}$ have some ionic bonding mixed with metallic bonding. In general, bonding occurs between atoms or molecules because their energies are lowered by the bonding process.

2.8 DEFINITIONS

Sec. 2.1

Law of multiple proportions: when atoms are combined, in specific simple fractions, they form different compounds.

Law of mass conservation: a chemical reaction does not lead to creation or destruction of matter.

Sec. 2.2

Atomic number (Z): the number of protons in the nucleus of an atom.

Atomic mass unit: defined as 1/12 the mass of a carbon atom.

Mass number (A): the sum of protons and neutrons in the nucleus of an atom.

Isotopes: atoms of the same element that have the same number of protons but not the same number of neutrons.

Mole: the amount of substance that contains 6.02×10^{23} elementary entities (atoms or molecules).

Law of chemical periodicity: properties of elements are functions of their atomic number in a periodic manner.

Sec. 2.3

Quanta: a discrete (specific) amount of energy emitted by atoms and molecules.

Electromagnetic radiation: energy released and transmitted in the form of electromagnetic waves.

Photon: quantum of energy emitted or released in the form of electromagnetic radiation with a specific wavelength and frequency.
Ionization energy: the minimum energy required to separate an electron from its nucleus.
Uncertainty principle: it is impossible to simultaneously determine the exact position and the exact momentum of a body (for instance an electron).
Electron density: the probability of finding an electron of a given energy level in a given region of space.
Orbitals: different wave functions that are solutions to the wave equation and can be presented as electron density diagrams.
Boundary surface: an alternative to the electron density diagram showing the area inside which one can find an electron with a probability of 90 percent.
Principal quantum number: A quantum number representing the energy level of the electron.
Orbital quantum number: the shape of the electron cloud or the boundary space of the orbital is determined by this number.
Magnetic quantum number: represents the orientation of the orbitals within each subshell.
Spin quantum number: represents the spin of the electron.
Pauli's exclusion principle: no two electrons can have the same set of four quantum numbers.
Nucleus charge effect: the higher the charge of the nucleus, the higher is the attraction force on an electron and the lower the energy of the electron.
Shielding effect: when two electrons within the same energy level repel each other and thus counteract the attraction force of the nucleus.

Sec. 2.4
Metallic radius: half the distance between the nuclei of two adjacent atoms in a sample of a metallic element.
Covalent radius: half the distance between the nuclei of the identical atoms within the covalent molecule.
First ionization energy: the energy required for the removal of the outermost electron.
Second ionization energy: the energy required to remove a second outer core electron (after the first one has been removed).
Positive oxidation number: the number of outer electrons that an atom can give up through the ionization process.
Electron affinity: the tendency of an atom to accept one or more electrons and release energy in the process.
Negative oxidation number: the number of electrons that an atom can gain.
Reactive metals: metals with low ionization energies and little or no electron affinity.
Reactive nonmetals: nonmetals with high ionization energies and extensive electron affinity.
Metalloids: elements that can behave either in a metallic or a nonmetallic manner.
Electronegativity: the degree by which atoms attract electrons to themselves.
Hess Law: the total heat of formation is equal to the sum of the heat of formation in the five steps of ionic solid formation.

Sec. 2.5
Primary bonds: strong bonds that form between atoms.
Ionic bonding: a primary bond that forms between metals and nonmetals or atoms with large differences in their electronegativities.
Equilibrium interionic distance: the distance between the cation and the anion when the bond is formed (at equilibrium).
Lattice energy: energy associated with formation of a 3-D solid from gaseous ions through ionic bonding.
Covalent bonding: a type of primary bond typically observed between atoms with small differences in their electronegativities and mostly between nonmetals.

Shared pair (bonding pair): the pair of electrons in the formed covalent bond.
Bond order: the number of shared pairs (covalent bonds) formed between two atoms.
Bond energy: the energy required to overcome the attraction force between the nuclei and the shared pair of electrons in a covalent bond.
Bond length: the distance between the nuclei of two bonded atoms at the point of minimum energy in a covalent bond.
Hybrid orbitals: when two or more atomic orbitals mix to form new orbitals.
Network covalent solids: materials that are made up entirely of covalent bonds.
Metallic bonds: example of a primary bond that forms due to tight packing of atoms in metals during solidification.

Sec. 2.6
Secondary bonds: comparatively weak bonds that form between molecules (and atoms of noble gasses) due to electrostatic attraction electric dipoles.
Fluctuating dipole: a changing dipole created by instantaneous changes in the electron charge clouds.
Permanent dipole: a stable dipole created due to structural asymmetries in the molecule.
Hydrogen bond: a special case of permanent dipole interaction between polar molecules.

2.9 PROBLEMS

Answers to problems marked with an asterisk are given at the end of the book.

Knowledge and Comprehension Problems

2.1 Describe the laws of (*a*) multiple proportions and (*b*) mass conservation as related to atoms and their chemical properties.

2.2 How did scientists find out that atoms themselves are made up of smaller particles?

2.3 How was the existence of electrons first verified? Discuss the characteristics of electrons.

2.4 How was the existence of protons first verified? Discuss the characteristics of protons.

2.5 What are the similarities and differences among protons, neutrons, and electrons? Compare in detail.

2.6 One mole of iron atoms has a mass of 55.85 g; without any calculations determine the mass in amu of one iron atom.

2.7 One atom of oxygen has a mass of 16.00 amu; without any calculations determine the mass in grams of one mole of oxygen atoms.

2.8 Define (*a*) atomic number, (*b*) atomic mass, (*c*) atomic mass unit (amu), (*d*) mass number, (*e*) isotopes, (*f*) mole, (*g*) relative atomic mass, (*h*) average relative atomic mass, and (*i*) Avogadro's number.

2.9 Explain the law of chemical periodicity.

2.10 What is the nature of visible light? How is the energy released and transmitted in visible light?

2.11 (*a*) Rank the following emissions in increasing magnitude of wavelength: microwave oven emissions, radio waves, sun lamp emissions, X-ray emissions, and gamma ray emissions from the sun. (*b*) Rank the same emissions in terms of frequency. Which emission has the highest energy?

2.12 Describe the Bohr model of the hydrogen atom. What are the shortcomings of the Bohr model?

2.13 Describe the uncertainty principle. How does this principle contradict Bohr's model of the atom?

2.14 Describe the following terms (give a diagram for each): (*a*) electron density diagram, (*b*) orbital, (*c*) boundary surface representation, and (*d*) radial probability.

2.15 Name and describe all the quantum numbers.

2.16 Explain Pauli's exclusion principle.

2.17 Describe (*a*) the nucleus charge effect, and (*b*) the shielding effect in multi-electron atoms.

2.18 Describe the terms (*a*) metallic radius, (*b*) covalent radius, (*c*) first ionization energy, (*d*) second ionization energy, (*e*) oxidation number, (*f*) electron affinity, (*g*) metals, (*h*) nonmetals, (*i*) metalloids, and (*j*) electronegativity.

2.19 Compare and contrast the three primary bonds in detail (draw a schematic for each). Explain the driving force in the formation of such bonds or in other words why do atoms want to bond at all?

2.20 Describe the factors that control packing efficiency (number of neighbors) in ionic and covalent solids. Give an example of each type of solid.

2.21 Describe the five stages leading to formation of an ionic solid. Explain which stages require energy and which stages release energy.

2.22 Describe (*a*) Hess Law, (*b*) lattice energy, and (*c*) heat of formation.

2.23 Describe the terms (*a*) shared pair, (*b*) bond order, (*c*) bond energy, (*d*) bond length, (*e*) polar and non-polar covalent bonds, and (*f*) network covalent solid.

2.24 Explain the hybridization process in carbon. Use orbital diagrams.

2.25 Describe the properties (electrical, mechanical, etc.) of materials that are exclusively made up of (*a*) ionic bonds, (*b*) covalent bonds, and (*c*) metallic bonds Name a material for each type

2.26 What are secondary bonds? What is the driving force for formation of such bonds? Give examples of materials in which such bonds exist.

2.27 Discuss various types of mixed bonding.

2.28 Define the following terms: (*a*) dipole moment, (*b*) fluctuating dipole, (*c*) permanent dipole, (*d*) van der Waals bonds, and (*e*) hydrogen bond.

Application and Analysis Problems

***2.29** The diameter of a soccer ball is approximately 0.279 m (11 in.). The diameter of the moon is 3.476×10^6 m. Give an "estimate" of how many soccer balls it will take to cover the surface of the moon (assume the moon is a sphere with a flat terrain). Compare this number to Avogadro's number. What is your conclusion?

***2.30** Each quarter produced by the U.S. mint is made up of a copper and nickel alloy. In each coin, there is 0.00740 moles of Ni and 0.0886 moles of copper. (*a*) What is the total mass of a quarter? (*b*) What percentage of the mass of a quarter is nickel and what percentage is copper?

2.31 Sterling silver contains 92.5 wt % silver and 7.5 wt % copper. Copper is added to silver to make the metal stronger and more durable. A small sterling silver spoon has a mass of 100 g. Calculate the number of copper and silver atoms in the spoon.

***2.32** There are two naturally occurring isotopes for boron with mass numbers 10 (10.0129 amu) and 11 (11.0093 amu); the percentages are 19.91 and 80.09, respectively

(*a*) Find the average atomic mass and (*b*) the relative atomic mass (or atomic weight) of boron. Compare your value with that presented in the periodic table.

2.33 A monel alloy consists of 70 wt % Ni and 30 wt % Cu. What are the atomic percentages of Ni and Cu in this alloy?

***2.34** What is the chemical formula of an intermetallic compound that consists of 15.68 wt % Mg and 84.32 wt % Al?

2.35 In order to raise the temperature of 100 g of water from room temperature (20°C) to boiling temperature (100°C), an energy input of 33,440.0 J is required. If one uses a microwave oven (λ of radiation of 1.20 cm) to achieve this, how many photons of the microwave radiation is required?

2.36 For Prob. 2.35, determine the number of photons to achieve the same increase in temperature if (*a*) ultraviolet ($\lambda = 1.0 \times 10^{-8}$ m), visible ($\lambda = 5.0 \times 10^{-7}$ m), and infrared ($\lambda = 1.0 \times 10^{-4}$ m) lights were used. What important conclusions can you draw from this exercise?

***2.37** In order for the human eye to detect the visible light, its optical nerves must be exposed to a minimum energy of 2.0×10^{-17} J. (*a*) Calculate the number of photons of red light needed to achieve this ($\lambda = 700$ nm). (*b*) Without any additional calculations, determine if you would need more or less photons of blue light to excite the optical nerves?

2.38 Represent the wave length of the following rays by comparing each to the length of a physical object (e.g., a ray with a wavelength of 1 m (100 cm) would be approximately that of a baseball bat): (*a*) rays from a dental ray, (*b*) rays in a microwave oven, (*c*) rays in a sun lamp, (*d*) rays in a heat lamp, and (*e*) an FM radio wave.

2.39 For the rays in Prob. 2.38, without any calculations, rank them in increasing order of the energy of the radiation.

2.40 In a commercial x-ray generator, a stable metal such as copper (Cu) or tungsten (W) is exposed to an intense beam of high-energy electrons. These electrons cause ionization events in the metal atoms. When the metal atoms regain their ground state they emit x-rays of characteristic energy and wavelength. For example, a "tungsten" atom struck by a high-energy electron may lose one of its K shell electrons. When this happens, another electron, probably from the tungsten L shell will "fall" into the vacant site in the K shell. If such a $2p \rightarrow 1s$ transition occurs in tungsten, a tungsten K_α x-ray is emitted. A tungsten K_α x-ray has a wavelength λ of 0.02138 nm. What is its energy? What is its frequency?

2.41 A hydrogen atom exists with its electron in the $n = 4$ state. The electron undergoes a transition to the $n = 3$ state. Calculate (*a*) the energy of the photon emitted, (*b*) its frequency, and (*c*) its wavelength in nanometers (nm).

***2.42** A hydrogen atom exists with its electron in the $n = 6$ state. The electron undergoes a transition to the $n = 2$ state. Calculate (*a*) the energy of the photon emitted, (*b*) its frequency, and (*c*) its wavelength in nanometers.

2.43 Using the information given in Example Problems 2.4 and 2.5 to determine the uncertainty associated with the electron's position if the uncertainty in determining its velocity is 1 percent. Compare the calculated uncertainty in the position with the estimated diameter of the atom. What is your conclusion?

2.44 Repeat Prob. 2.43 to determine the uncertainty associated with the electron's position if the uncertainty in determining its velocity is 2%. Compare the calculated uncertainty in the position with that of Prob. 2.43. What is your conclusion?

*2.45 For the principal quantum number, n, of value 4, determine all other possible quantum numbers for ℓ and m_ℓ.

2.46 For each pair of n and ℓ given below, give the sublevel name, possible values of m_ℓ, and the corresponding number of orbitals.

(*a*) n = 1, $\ell = 0$

(*b*) n = 2, $\ell = 1$

(*c*) n = 3, $\ell = 2$

(*d*) n = 4, $\ell = 3$

2. 47 Determine if the following combinations of quantum numbers are acceptable.

(*a*) $n = 3$, $\ell = 0$, $m_\ell = +1$

(*b*) $n = 6$, $\ell = 2$, $m_\ell = -3$

(*c*) $n = 3$, $\ell = 3$, $m_\ell = -1$

(*d*) $n = 2$, $\ell = 1$, $m_\ell = +1$

2.48 In each row (a through *d*) there is only one piece of information that is wrong. Highlight the information that is wrong (explain why).

	n	ℓ	m_ℓ	Name
(*a*)	3	0	1	3s
(*b*)	2	1	−1	2s
(*c*)	3	1	+2	3d
(*d*)	3	3	0	4f

*2.49 Determine the four quantum numbers for the third, fifteenth, and seventeenth electrons of the Cl atom.

2.50 Determine the electron configuration and group number of the atom in the ground state based on the given partial (valence level) orbital diagram. Identify the element.

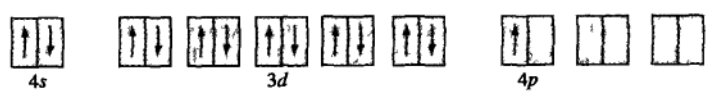

2.51 Write the electron configurations of the following elements by using spdf notation: (*a*) yttrium, (*b*) hafnium, (*c*) samarium, (*d*) rhenium.

2.52 Write the electron configuration of the following ions using the spdf notation: (*a*) Cr^{2+}, Cr^{3+}, Cr^{6+}; (*b*) *Mo^{3+}, Mo^{4+}, Mo^{6+}; (*c*) Se^{4+}, Se^{6+}, Se^{2-}.

2.53 Rank the following atoms in (*a*) increasing atomic size and (*b*) decreasing first ionization energy, IE1. Use only the periodic table to answer the questions. Check your answer using Figs. 2.10 and 2.11.

(*i*) K, Ca, Ga

(*ii*) Ca, Sr, Ba

(*iii*) I, Xe, Cs

2.54 Rank the following atoms in (*a*) increasing atomic size and (*b*) decreasing first ionization energy, IE1. Use only the periodic table to answer the questions. Check your answer using Figs. 2.10 and 2.11.

(*i*) Ar, Li, F, O, Cs C

(*ii*) Sr, H, Ba, He, Mg, Cs

2.55 The first ionization energies of two atoms with electronic configurations (*a*) $1S^22s^22p^6$ and (*b*) $1s^22s^22p^63s^1$ are given to be 2080 kJ/mol and 496 kJ/mol. Determine which IE1 belongs to which electronic structure and justify your answer.

2.56 The first ionization energies of three atoms with electronic configurations (*a*) $[He]2s^2$, (*b*) $[Ne]3s^1$, (*c*) $[Ar]4s^1$, and (*d*) $[He]2s^1$ are given to be 496 kJ/mol, 419 kJ/mol, 520 kJ/mol, and 899 kJ/mol. Determine which IE1 belongs to which electronic structure and explain your answer.

2.57 Similar to Fig 2.15, use (*a*) orbital diagrams and (*b*) Lewis symbols to explain the formation of Na^+ and O^{2-} ions and the corresponding bonding What is the formula of the compound?

2.58 Calculate the attractive force ($\bullet\!\!\rightarrow \leftarrow\!\!\bullet$) between a pair of Ba^{2+} and S^{2-} ions that just touch each other. Assume the ionic radius of the Ba^{2+} ion to be 0.143 nm and that of the S^{2-} ion to be 0.174 nm.

2.59 Calculate the net potential energy for a $Ba^{2+}S^{2-}$ ion pair by using the b constant calculated from Prob. 2.58. Assume $n = 10.5$.

2.60 If the attractive force between a pair of Cs^+ and I^- ions is 2.83×10^{-9} N and the ionic radius of the Cs^+ ion is 0.165 nm, calculate the ionic radius of the I^- ion in nanometers.

***2.61** For the each pair of bonds presented below, determine which has the higher lattice energy (more negative) Explain your answer. Also, which of the five ionic compounds do you think has the highest melting temperature and why? Verify your answer.

(*a*) LiCl and CsCl

(*b*) CsCl and RbCl

(*c*) LiF and MgO

(*d*) MgO and CaO

***2.62** Calculate the lattice energy for the formation of solid NaF if the following information is given. What does the calculated lattice energy tell you about the material?

109 kJ is required to convert solid Na to gaseous Na

243 kJ is required to convert gaseous F_2 to two monatomic F atoms

496 kJ is required to remove the $3s^1$ electron of Na (form Na^+ cation)

−349 kJ of energy (energy is released) to add an electron to the F (form Na^- anion)

−411 kJ of energy to form gaseous NaF (heat of formation of NaF)

2.63 Calculate the lattice energy for the formation of solid NaCl if the following information is given. What does the calculated lattice energy tell you about the material?

(*i*) 109 kJ is required to convert solid Na to gaseous Na

(*ii*) 121 kJ is required to convert gaseous Cl2 to two monatomic Cl atoms

(*iii*) 496 kJ is required to remove the 3s1 electron of Na (form Na+ cation)

(*iv*) −570 kJ of energy (energy is released) to add an electron to the Cl

(*v*) −610 kJ of energy to form gaseous NaCl (heat of formation of NaCl)

2.64 For each bond in the following series of bonds, determine the bond order, rank bond length, and rank bond strength. Use only the periodic table. Explain your answers.

(*a*) S−F; S−Br; S−Cl

(*b*) C−C; C=C; C≡C

2.65 Rank the following covalently bonded atoms according to the degree of polarity· C−N; C−C; C−H; C−Br.

2.61 List the number of atoms bonded to a C atom that exhibits sp^3, sp^2, and sp hybridization. For each, give the geometrical arrangement of the atoms in the molecule.

2.67 Is there a correlation between the electron configurations of the elements scandium (Z = 21) through copper (Z = 29) and their melting points? (See Table 2.7.)

***2.68** Compare the percentage ionic character in the semiconducting compounds CdTe and InP.

Synthesis and Evaluation Problems

2.69 ^{39}K, ^{40}K, and ^{41}K are the three isotopes of potassium. If ^{40}K has the lowest abundance, which other isotope has the highest?

***2.70** Most modern *scanning electron microscopes* (SEMs) are equipped with energy-dispersive x-ray detectors for the purpose of chemical analysis of the specimens. This x-ray analysis is a natural extension of the capability of the SEM because the electrons that are used to form the image are also capable of creating characteristic x-rays in the sample. When the electron beam hits the specimen, X-rays specific to the elements in the specimen are created. These can be detected and used to deduce the composition of the specimen from the well-known wavelengths of the characteristic x-rays of the elements. For example:

Element	Wavelength of K_α x-rays
Cr	0.2291 nm
Mn	0.2103 nm
Fe	0.1937 nm
Co	0.1790 nm
Ni	0.1659 nm
Cu	0.1542 nm
Zn	0.1436 nm

Suppose a metallic alloy is examined in an SEM and three different x-ray energies are detected. If the three energies are 7492, 5426, and 6417 eV, what elements are present in the sample? What would you call such an alloy? (Look ahead to Chap. 9 in the textbook.)

2.71 According to Sec. 2.5.1, in order to form monatomic ions from metals and nonmetals, energy must be added. However, we know that primary bonds form because the involved atoms want to lower their energies. Why then do ionic compounds form?

2.72 Of the noble gases Ne, Ar, Kr, and Xe, which should be the most chemically reactive?

***2.73** The melt temperature of Na is (89°C) and is higher than the melt temperature of K (63.5°C). Can you explain this in terms of the differences in electronic structure?

***2.74** The melt temperature of Li (180°C) is significantly lower than the melt temperature of its neighbor Be (1287°C). Can you explain this in terms of the differences in electronic structure?

2.75 The melting point of the metal potassium is 63.5°C, while that of titanium is 1660°C. What explanation can be given for this great difference in melting temperatures?

2.76 Cartridge brass is an alloy of two metals: 70 wt % copper and 30 wt % zinc. Discuss the nature of the bonds between copper and zinc in this alloy.

2.77 After ionization, why is the sodium ion smaller than the sodium atom? After ionization, why is the chloride ion larger than the chlorine atom?

2.78 Regardless of the type of primary bond, why does the tendency exist for atoms to bond?

***2.79** Pure aluminum is a ductile metal with low tensile strength and hardness. Its oxide Al_2O_3 (alumina) is extremely strong, hard, and brittle. Can you explain this difference from an atomic bonding point of view?

2.80 Graphite and diamond are both made from carbon atoms. (*a*) List some of the physical characteristics of each. (*b*) Give one application for graphite and one for diamond. (*c*) If both materials are made of carbon, why does such a difference in properties exist?

2.81 Silicon is extensively used in the manufacture of integrated circuit devices such as transistors and light-emitting diodes. It is often necessary to develop a thin oxide layer (SiO_2) on silicon wafers. (*a*) What are the differences in properties between the silicon substrate and the oxide layer? (*b*) Design a process that produces the oxide layer on a silicon wafer. (*c*) Design a process that forms the oxide layer only in certain desired areas.

2.82 How can the high electrical and thermal conductivities of metals be explained by the "electron gas" model of metallic bonding? Ductility?

2.83 Describe fluctuating dipole bonding among the atoms of the noble gas neon. Of a choice between the noble gases krypton and xenon, which noble gas would be expected to have the strongest dipole bonding and why?

2.84 Carbon tetrachloride (CCl_4) has a zero dipole moment. What does this tell us about the C—Cl bonding arrangement in this molecule?

2.85 Methane (CH_4) has a much lower boiling temperature than does water (H_2O). Explain why this is true in terms of the bonding between molecules in each of these two substances.

2.86 For each of the following compounds, state whether the bonding is essentially metallic, covalent, ionic, van der Waals, or hydrogen: (*a*) Ni, (*b*) ZrO_2, (*c*) graphite, (*d*) solid Kr, (*e*) Si, (*f*) BN, (*g*) SiC, (*h*) Fe_2O_3, (*i*) MgO, (*j*) W, (*k*) H_2O within the molecules, (*l*) H_2O between the molecules.

If ionic and covalent bonding are involved in the bonding of any of the compounds listed, calculate the percentage ionic character in the compound.

***2.87** In the manufacturing of a light bulb, the bulb is evacuated of air and then filled with argon gas. What is the purpose of this?

2.88 Stainless steel is a corrosion-resistant metal because it contains large amounts of chromium. How does chromium protect the metal from corrosion?

2.89 Robots are used in auto industries to weld two components at specific locations. Clearly, the end position of the arm must be determined accurately in order to weld the components at the precise position. (*a*) In selecting the material for the arm of such robots, what factors must be considered? (*b*) Select a proper material for this application.

2.90 A certain application requires a material that is lightweight, an electrical insulator, and has some flexibility. (*a*) Which class of materials would you search for this selection? (*b*) Explain your answer from a bonding point of view.

2.91 A certain application requires a material that is electrically nonconductive (insulator), extremely stiff, and lightweight. Which classes of materials would you search for this selection? (*b*) Explain your answer from a bonding point of view.

CHAPTER

3 Crystal and Amorphous Structure in Materials

(*a*) (*b*) (*c*) (*d*)

((*a*) © *Paul Silverman/Fundamental Photographs.*)
((*b*) © *The McGraw-Hill Companies, Inc./Doug Sherman, photographer.*)
((*c*) and (*d*) © *Dr. Parvinder Sethi.*)

Solids may be categorized broadly into crystalline and amorphous solids. Crystalline solids, due to orderly structure of their atoms, molecules, or ions, possess well-defined shapes. Metals are crystalline and are composed of well-defined crystals or grains. The grains are small and are not clearly observable due to the opaque nature of metals. In minerals, mostly translucent to transparent in nature, the well-defined crystalline shapes are clearly observable. The following images show the crystalline nature of minerals such as (*a*) celestite ($SrSo_4$) with a sky blue or celestial color, (*b*) pyrite (FeS_2), also called the "fool's gold" due to its brassy yellow color, (*c*) amethyst (SiO_2), a purple variety of quartz, and (*d*) halite (NaCl), better known as rock salt. In contrast, amorphous solids have poor or no long-range order and do not solidify with the symmetry and regularity of crystalline solids. ■

LEARNING OBJECTIVES

By the end of this chapter, students will be able to. . .

1. Describe what crystalline and noncrystalline (amorphous) materials are.
2. Learn how atoms and ions in solids are arranged in space and identify the basic building blocks of solids.
3. Describe the difference between atomic structure and crystal structure for solid material.
4. Distinguish between crystal structure and crystal system.
5. Explain why plastics cannot be 100 percent crystalline in structure.
6. Explain polymorphism or allotropy in materials.
7. Compute the densities for metals having body-centered and face-centered cubic structures.
8. Describe how to use the X-ray diffraction method for material characterization.
9. Write the designation for atom position, direction indices, and Miller indices for cubic crystals. Specify what are the three densely packed structures for most metals. Determine Miller-Bravais indices for hexagonal-closed packed structure. Be able to draw directions and planes in cubic and hexagonal crystals.

3.1 THE SPACE LATTICE AND UNIT CELLS

Animation Tutorial

The physical structure of solid materials of engineering importance depends mainly on the arrangements of the atoms, ions, or molecules that make up the solid and the bonding forces between them. If the atoms or ions of a solid are arranged in a pattern that repeats itself in three dimensions, they form a solid that has *long-range order* (LRO) and is referred to as a *crystalline solid* or *crystalline material.* Examples of crystalline materials are metals, alloys, and some ceramic materials. In contrast to crystalline materials, there are some materials whose atoms and ions are not arranged in a long-range, periodic, and repeatable manner and possess only *short-range order* (SRO). This means that order exists only in the immediate neighborhood of an atom or a molecule. As an example, liquid water has short-range order in its molecules in which one oxygen atom is covalently bonded to two hydrogen atoms. But this order disappears, as each molecule is bonded to other molecules through weak secondary bonds in a random manner. Materials with only short-range order are classified as *amorphous* (without form) or noncrystalline. A more detailed definition and some examples of amorphous materials are given in Sec. 3.12.

Atomic arrangements in crystalline solids can be described by referring the atoms to the points of intersection of a network of lines in three dimensions. Such

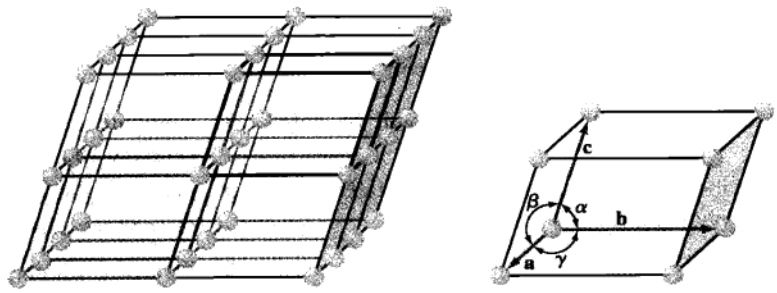

Figure 3.1
(*a*) Space lattice of ideal crystalline solid. (*b*) Unit cell showing lattice constants.

a network is called a **space lattice** (Fig. 3.1*a*), and it can be described as an infinite three-dimensional array of points. Each point in the space lattice has identical surroundings. In an ideal **crystal,** the grouping of **lattice points** about any given point are identical with the grouping about any other lattice point in the crystal lattice. Each space lattice can thus be described by specifying the atom positions in a repeating **unit cell,** such as the one heavily outlined in Fig. 3.1*a*. The unit cell may be considered the smallest subdivision of the lattice that maintains the characteristics of the overall crystal. A group of atoms organized in a certain arrangement relative to each other and associated with lattice points constitues the **motif** or basis. The crystal structure may then be defined as the collection of lattice and basis. It is important to note that atoms do not necessarily coincide with lattice points. The size and shape of the unit cell can be described by three lattice vectors **a, b,** and **c,** originating from one corner of the unit cell (Fig. 3.1*b*). The axial lengths a, b, and c and the interaxial angles α, β, and γ are the *lattice constants* of the unit cell.

3.2 CRYSTAL SYSTEMS AND BRAVAIS LATTICES


Tutorial

By assigning specific values for axial lengths and interaxial angles, unit cells of different types can be constructed. Crystallographers have shown that only seven different types of unit cells are necessary to create all space lattices. These crystal systems are listed in Table 3.1.

Many of the seven crystal systems have variations of the basic unit cell. A.J. Bravais[1] showed that 14 standard unit cells could describe all possible lattice networks. These Bravais lattices are illustrated in Fig. 3.2. There are four basic types of unit cells: (1) simple, (2) body-centered, (3) face-centered, and (4) base-centered.

[1]August Bravais (1811–1863). French crystallographer who derived the 14 possible arrangements of points in space.

Table 3.1 Classification of space lattices by crystal system

Crystal system	Axial lengths and interaxial angles	Space lattice
Cubic	Three equal axes at right angles $a = b = c, \alpha = \beta = \gamma = 90°$	Simple cubic Body-centered cubic Face-centered cubic
Tetragonal	Three axes at right angles, two equal $a = b \neq c, \alpha = \beta = \gamma = 90°$	Simple tetragonal Body-centered tetragonal
Orthorhombic	Three unequal axes at right angles $a \neq b \neq c, \alpha = \beta = \gamma = 90°$	Simple orthorhombic Body-centered orthorhombic Base-centered orthorhombic Face-centered orthorhombic
Rhombohedral	Three equal axes, equally inclined $a = b = c, \alpha = \beta = \gamma \neq 90°$	Simple rhombohedral
Hexagonal	Two equal axes at 120°, third axis at right angles $a = b \neq c, \alpha = \beta = 90°, \gamma = 120°$	Simple hexagonal
Monoclinic	Three unequal axes, one pair not at right angles $a \neq b \neq c, \alpha = \gamma = 90° \neq \beta$	Simple monoclinic Base-centered monoclinic
Triclinic	Three unequal axes, unequally inclined and none at right angles $a \neq b \neq c, \alpha \neq \beta \neq \gamma \neq 90°$	Simple triclinic

In the cubic system there are three types of unit cells: simple cubic, body-centered cubic, and face-centered cubic. In the orthorhombic system all four types are represented. In the tetragonal system there are only two: simple and body-centered. The face-centered tetragonal unit cell appears to be missing but can be constructed from four body-centered tetragonal unit cells. The monoclinic system has simple and base-centered unit cells, and the rhombohedral, hexagonal, and triclinic systems have only one simple type of unit cell.

3.3 PRINCIPAL METALLIC CRYSTAL STRUCTURES

In this chapter, the principal crystal structures of elemental metals will be discussed in detail. In Chap. 11, the principal ionic and covalent crystal structures that occur in ceramic materials will be treated.

Most elemental metals (about 90 percent) crystallize upon solidification into three densely packed crystal structures: **body-centered cubic (BCC)** (Fig. 3.3*a*), **face-centered cubic (FCC)** (Fig. 3.3*b*), and **hexagonal close-packed (HCP)** (Fig. 3.3*c*). The HCP structure is a denser modification of the simple hexagonal crystal structure shown in Fig. 3.2. Most metals crystallize in these dense-packed structures because energy is released as the atoms come closer together and bond more tightly with each other. Thus, the densely packed structures are in lower and more stable energy arrangements.

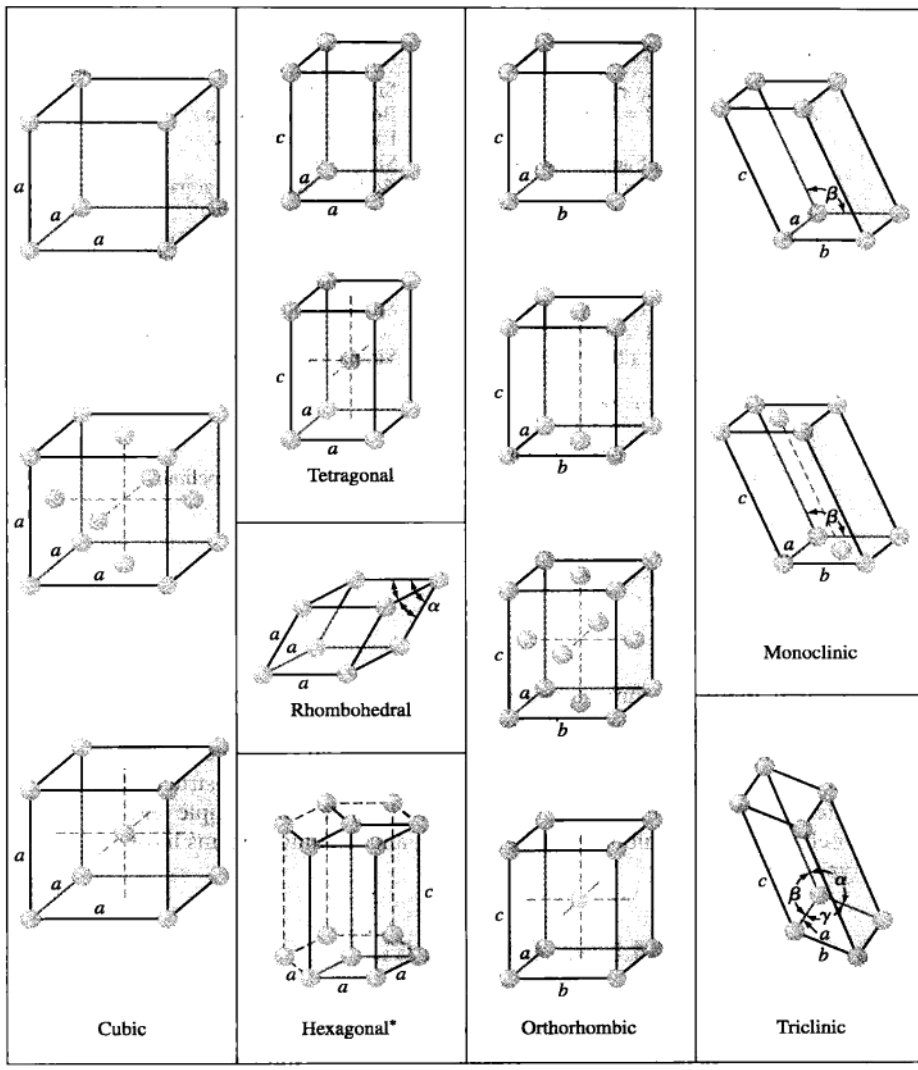

Tutorial
Animation
MatVis

Figure 3.2
The 14 Bravais conventional unit cells grouped according to crystal system. The dots indicate lattice points that, when located on faces or at corners, are shared by other identical lattice unit cells.
(From W.G. Moffatt, G.W. Pearsall, and J.Wulff, The Structure and Properties of Materials, vol. 1: "Structure", Wiley, 1964, p. 47.)
**The unit cell is represented by solid lines.*

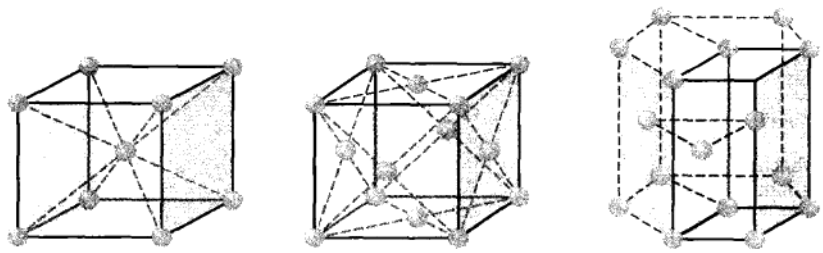

(a) (b) (c)

Figure 3.3
Principal metal crystal structure and unit cells: (*a*) body-centered cubic, (*b*) face-centered cubic, (*c*) hexagonal close-packed crystal structure (the unit cell is shown by solid lines).

The extremely small size of the unit cells of crystalline metals that are shown in Fig. 3.3 should be emphasized. The cube side of the unit cell of body-centered cubic iron, for example, at room temperature is equal to 0.287×10^{-9} m, or 0.287 nanometer (nm).[2] Therefore, if unit cells of pure iron are lined up side by side, in 1 mm there will be

$$1 \text{ mm} \times \frac{1 \text{ unit cell}}{0.287 \text{ nm} \times 10^{-6} \text{ mm/nm}} = 3.48 \times 10^{6} \text{ unit cells!}$$

Let us now examine in detail the arrangement of the atoms in the three principal crystal structure unit cells. Although an approximation, we shall consider atoms in these crystal structures to be hard spheres. The distance between the atoms (interatomic distance) in crystal structures can be determined experimentally by X-ray diffraction analysis.[3] For example, the interatomic distance between two aluminum atoms in a piece of pure aluminum at 20°C is 0.2862 nm. The radius of the aluminum atom in the aluminum metal is assumed to be half the interatomic distance, or 0.143 nm. The atomic radii of selected metals are listed in Tables 3.2 to 3.4.

3.3.1 Body-Centered Cubic (BCC) Crystal Structure

Animation Tutorial

First, consider the atomic-site unit cell for the BCC crystal structure shown in Fig. 3.4*a*. In this unit cell, the solid spheres represent the centers where atoms are located and clearly indicate their relative positions. If we represent the atoms in this cell as hard spheres, then the unit cell appears as shown in Fig. 3.4*b*. In this unit cell, we see that the central atom is surrounded by eight nearest neighbors and is said to have a coordination number of 8.

[2] 1 nanometer = 10^{-9} meter.

[3] Some of the principles of X-ray diffraction analysis will be studied in Sec. 3.11.

Table 3.2 Selected metals that have the BCC crystal structure at room temperature (20°C) and their lattice constants and atomic radii

Metal	Lattice constant a (nm)	Atomic radius R^* (nm)
Chromium	0.289	0.125
Iron	0.287	0.124
Molybdenum	0.315	0.136
Potassium	0.533	0.231
Sodium	0.429	0.186
Tantalum	0.330	0.143
Tungsten	0.316	0.137
Vanadium	0.304	0.132

*Calculated from lattice constants by using Eq. (3.1), $R = \sqrt{3}a/4$.

Tutorial

Table 3.3 Selected metals that have the FCC crystal structure at room temperature (20°C) and their lattice constants and atomic radii

Metal	Lattice constant a (nm)	Atomic radius R^* (nm)
Aluminum	0.405	0.143
Copper	0.3615	0.128
Gold	0.408	0.144
Lead	0.495	0.175
Nickel	0.352	0.125
Platinum	0.393	0.139
Silver	0.409	0.144

*Calculated from lattice constants by using Eq. (3.3), $R = \sqrt{2}a/4$.

Table 3.4 Selected metals that have the HCP crystal structure at room temperature (20°C) and their lattice constants, atomic radii, and c/a ratios

Metal	Lattice constants (nm)		Atomic radius R (nm)	c/a ratio	% deviation from ideality
	a	c			
Cadmium	0.2973	0.5618	0.149	1.890	+15.7
Zinc	0.2665	0.4947	0.133	1.856	+13.6
Ideal HCP				1.633	0
Magnesium	0.3209	0.5209	0.160	1.623	−0.66
Cobalt	0.2507	0.4069	0.125	1.623	−0.66
Zirconium	0.3231	0.5148	0.160	1.593	−2.45
Titanium	0.2950	0.4683	0.147	1.587	−2.81
Beryllium	0.2286	0.3584	0.113	1.568	−3.98

If we isolate a single hard-sphere unit cell, we obtain the model shown in Fig. 3.4*c*. Each of these cells has the equivalent of two atoms per unit cell. One complete atom is located at the center of the unit cell, and an eighth of a sphere is located at each corner of the cell, making the equivalent of another atom. Thus, there is a total of 1 (at the center) + 8 × $\frac{1}{8}$ (at the corners) = 2 atoms per unit cell. The atoms in the BCC unit cell contact each other across the cube diagonal, as indicated in

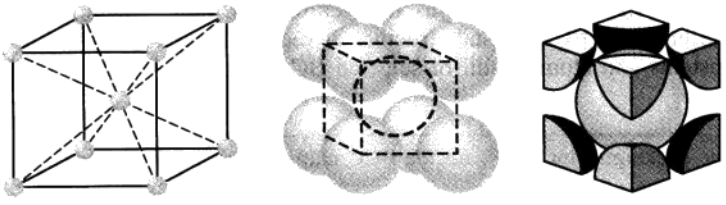

(a) (b) (c)

Figure 3.4
BCC unit cells: (*a*) atomic-site unit cell, (*b*) hard-sphere unit cell, and (*c*) isolated unit cell.

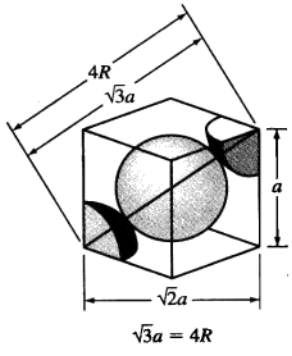

Figure 3.5
BCC unit cell showing relationship between the lattice constant *a* and the atomic radius *R*.

Tutorial
Animatio
MatVis

Fig. 3.5, so that the relationship between the length of the cube side a and the atomic radius R is

$$\sqrt{3}a = 4R \quad \text{or} \quad a = \frac{4R}{\sqrt{3}} \tag{3.1}$$

EXAMPLE PROBLEM 3.1

Iron at 20°C is BCC with atoms of atomic radius 0.124 nm. Calculate the lattice constant a for the cube edge of the iron unit cell.

■ **Solution**

From Fig. 3.5 it is seen that the atoms in the BCC unit cell touch across the cube diagonals. Thus, if a is the length of the cube edge, then

$$\sqrt{3}a = 4R \tag{3.1}$$

where R is the radius of the iron atom. Therefore

$$a = \frac{4R}{\sqrt{3}} = \frac{4(0.124\ \text{nm})}{\sqrt{3}} = 0.2864\ \text{nm} \blacktriangleleft$$

If the atoms in the BCC unit cell are considered to be spherical, an **atomic packing factor** (APF) can be calculated by using the equation

$$\text{APF} = \frac{\text{volume of atoms in unit cell}}{\text{volume of unit cell}} \tag{3.2}$$

Using this equation, the APF for the BCC unit cell (Fig. 3.4*c*) is calculated to be 68 percent (see Example Problem 3.2). That is, 68 percent of the volume of the BCC unit cell is occupied by atoms and the remaining 32 percent is empty space. The BCC crystal structure is *not* a close-packed structure since the atoms could be packed closer together. Many metals such as iron, chromium, tungsten, molybdenum, and vanadium have the BCC crystal structure at room temperature. Table 3.2 lists the lattice constants and atomic radii of selected BCC metals.

EXAMPLE PROBLEM 3.2

Calculate the atomic packing factor (APF) for the BCC unit cell, assuming the atoms to be hard spheres.

■ **Solution**

$$\text{APF} = \frac{\text{volume of atoms in BCC unit cell}}{\text{volume of BCC unit cell}} \tag{3.2}$$

Tutorial

Since there are two atoms per BCC unit cell, the volume of atoms in the unit cell of radius R is

$$V_{\text{atoms}} = (2)(\tfrac{4}{3}\pi R^3) = 8.373R^3$$

The volume of the BCC unit cell is

$$V_{\text{unit cell}} = a^3$$

where a is the lattice constant. The relationship between a and R is obtained from Fig. 3.5, which shows that the atoms in the BCC unit cell touch each other across the cubic diagonal. Thus

$$\sqrt{3}a = 4R \quad \text{or} \quad a = \frac{4R}{\sqrt{3}} \tag{3.1}$$

Thus,

$$V_{\text{unit cell}} = a^3 = 12.32R^3$$

The atomic packing factor for the BCC unit cell is, therefore,

$$\text{APF} = \frac{V_{\text{atoms}}/\text{unit cell}}{V_{\text{unit cell}}} = \frac{8.373R^3}{12.32R^3} = 0.68 \blacktriangleleft$$

3.3.2 Face-Centered Cubic (FCC) Crystal Structure

Consider next the FCC lattice-point unit cell of Fig. 3.6*a*. In this unit cell, there is one lattice point at each corner of the cube and one at the center of each cube face. The hard-sphere model of Fig. 3.6*b* indicates that the atoms in the FCC crystal structure are packed as close together as possible. The APF for this close-packed structure is 0.74 as compared to 0.68 for the BCC structure, which is not close-packed.

The FCC unit cell as shown in Fig. 3.6*c* has the equivalent of four atoms per unit cell. The eight corner octants account for one atom ($8 \times \frac{1}{8} = 1$), and the six

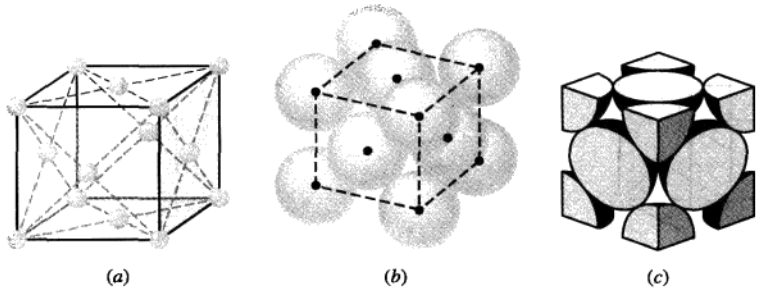

Figure 3.6
FCC unit cells: (*a*) atomic-site unit cell, (*b*) hard-sphere unit cell, and (*c*) isolated unit cell.

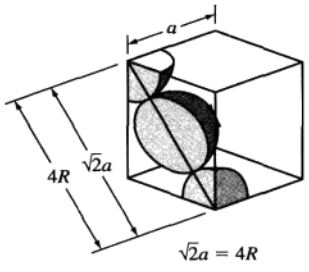

Figure 3.7
FCC unit cell showing relationship between the lattice constant *a* and atomic radius *R*. Since the atoms touch across the face diagonals, $\sqrt{2}a = 4R$.

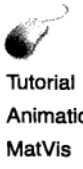

half-atoms on the cube faces contribute another three atoms, making a total of four atoms per unit cell. The atoms in the FCC unit cell contact each other across the cubic face diagonal, as indicated in Fig. 3.7, so that the relationship between the length of the cube side a and the atomic radius R is

$$\sqrt{2}a = 4R \quad \text{or} \quad a = \frac{4R}{\sqrt{2}} \tag{3.3}$$

The APF for the FCC crystal structure is 0.74, which is greater than the 0.68 factor for the BCC structure. The APF of 0.74 is for the closest packing possible of "spherical atoms." Many metals such as aluminum, copper, lead, nickel, and iron at elevated temperatures (912°C to 1394°C crystallize with the FCC crystal structure. Table 3.3 lists the lattice constants and atomic radii for some selected FCC metals.

3.3.3 Hexagonal Close-Packed (HCP) Crystal Structure

The third common metallic crystal structure is the HCP structure shown in Fig. 3.8*a* and *b*. Metals do not crystallize into the simple hexagonal crystal structure shown in Fig. 3.2 because the APF is too low. The atoms can attain a lower energy and a more stable condition by forming the HCP structure of Fig. 3.8*b*. The APF of the HCP crystal structure is 0.74, the same as that for the FCC crystal structure since in both structures the atoms are packed as tightly as possible. In both the HCP and FCC crystal structures, each atom is surrounded by 12 other atoms, and thus both structures have a coordination number of 12. The differences in the atomic packing in FCC and HCP crystal structures will be discussed in Sec. 3.8.

The isolated HCP unit cell, also called the *primitive cell*, is shown in Fig. 3.8*c*. The atoms at locations marked "1" on Fig. 3.8*c* contribute $\frac{1}{6}$ of an atom to the unit cell. The atoms at locations marked "2" contribute $\frac{1}{12}$ of an atom to the unit cell.

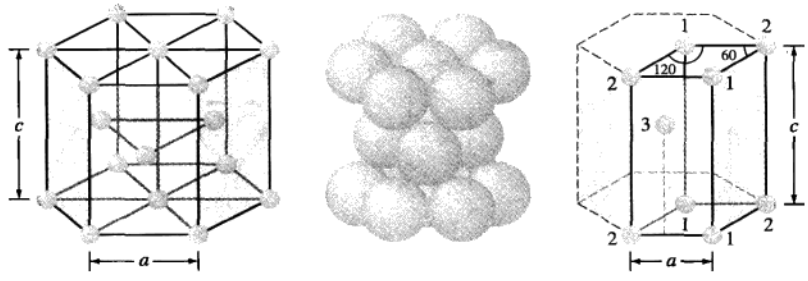

Tutorial
MatVis

Figure 3.8
HCP crystal structure: (*a*) schematic of the crystal structure, (*b*) hard-sphere model, and (*c*) isolated unit cell schematic.
(From F.M. Miller, Chemistry: Structure and Dynamics, McGraw-Hill, 1984, p. 296. Reproduced with permission of The McGraw-Hill Companies.)

Thus, the atoms at the eight corners of the unit cell collectively contribute one atom ($4(\frac{1}{8}) + 4(\frac{1}{12}) = 1$). The atom at location "3" is centered inside the unit cell but extends slightly beyond the boundary of the cell. The total number of atoms inside an HCP unit cell is therefore 2 (1 at corners and 1 at center). In some text books the HCP unit cell is represented by Fig. 3.8*a* and is called the "larger cell." In such a case one finds 6 atoms per unit cell. This is mostly for convenience and the true unit cell is presented in Fig. 3.8*c* by the solid lines. When presenting the topics of crystal directions and planes we will also use the larger cell for convenience, in addition to the primitive cell.

The ratio of the height c of the hexagonal prism of the HCP crystal structure to its basal side a is called the *c/a ratio* (Fig. 3.8*a*). The *c/a ratio* for an ideal HCP crystal structure consisting of uniform spheres packed as tightly together as possible is 1.633. Table 3.4 lists some important HCP metals and their c/a ratios. Of the metals listed, cadmium and zinc have c/a ratios higher than ideality, which indicates that the atoms in these structures are slightly elongated along the c axis of the HCP unit cell. The metals magnesium, cobalt, zirconium, titanium, and beryllium have c/a ratios less than the ideal ratio. Therefore, in these metals the atoms are slightly compressed in the direction along the c axis. Thus, for the HCP metals listed in Table 3.4, there is a certain amount of deviation from the ideal hard-sphere model.

EXAMPLE PROBLEM 3.3

a. Calculate the volume of the zinc crystal structure unit cell by using the following data: pure zinc has the HCP crystal structure with lattice constants $a = 0.2665$ nm and $c = 0.4947$ nm.
b. Find the volume of the larger cell.

■ Solution

The volume of the zinc HCP unit cell can be obtained by determining the area of the base of the unit cell and then multiplying this by its height (Fig. EP3.3).

a. The area of the base of the unit cell is area *ABDC* of Fig. EP3.3*a* and *b*. This total area consists of the areas of six equilateral triangles of area *ABC* of Fig. EP3.3*b*. From Fig. EP3.3*c*,

$$\text{Area of triangle } ABC = \tfrac{1}{2}(\text{base})(\text{height})$$
$$= \tfrac{1}{2}(a)(a \sin 60°) = \tfrac{1}{2}a^2 \sin 60°$$

From Fig. EP3.3*b*,

$$\text{Total area of HCP base, area } ABDC = (2)(\tfrac{1}{2}a^2 \sin 60°)$$
$$= a^2 \sin 60°$$

From Fig. EP3.3*a*,

$$\text{Volume of zinc HCP unit cell} = (a^2 \sin 60°)(c)$$
$$= (0.2665 \text{ nm})^2(0.8660)(0.4947 \text{ nm})$$
$$= 0.0304 \text{ nm}^3 \blacktriangleleft$$

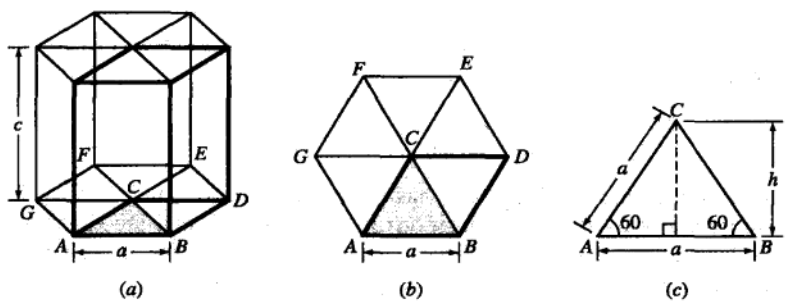

(*a*) (*b*) (*c*)

Figure EP3.3
Diagrams for calculating the volume of an HCP unit cell. (*a*) HCP unit cell. (*b*) Base of HCP unit cell. (*c*) Triangle *ABC* removed from base of unit cell.

b. From Fig. EP3.3*a*,

$$\text{Volume of the "large" zinc HCP cell} = 3(\text{volume of the unit cell or primitive cell})$$
$$= 3(0.0304) = 0.0913 \text{ nm}^3$$

3.4 ATOM POSITIONS IN CUBIC UNIT CELLS

To locate atom positions in cubic unit cells, we use rectangular x, y, and z axes. In crystallography, the positive x axis is usually the directin coming out of the paper, the positive y axis is the direction to the right of the paper, and the positive z axis is the direction to the top (Fig. 3.9). Negative directions are opposite to those just described.

Atom positions in unit cells are located by using unit distances along the x, y, and z axes, as indicated in Fig. 3.9*a*. For example, the position coordinates for the

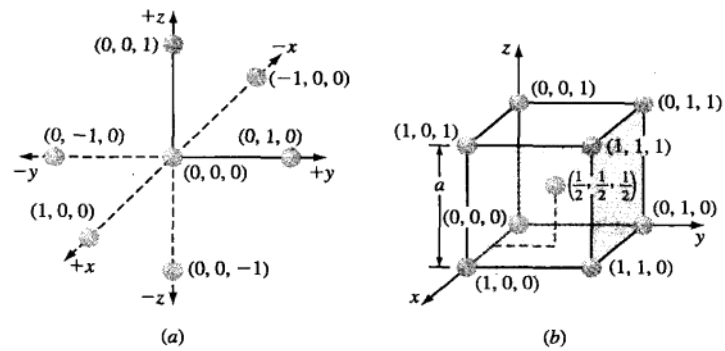

Tutorial

Figure 3.9
(*a*) Rectangular *x*, *y*, and *z* axes for locating atom positions in cubic unit cells. (*b*) Atom positions in a BCC unit cell.

atoms in the BCC unit cell are shown in Fig. 3.9*b*. The atom positions for the eight corner atoms of the BCC unit cell are

(0, 0, 0) (1, 0, 0) (0, 1, 0) (0, 0, 1)
(1, 1, 1) (1, 1, 0) (1, 0, 1) (0, 1, 1)

The center atom in the BCC unit cell has the position coordinates $(\frac{1}{2}, \frac{1}{2}, \frac{1}{2})$. For simplicity sometimes only two atom positions in the BCC unit cell are specified which are (0, 0, 0) and $(\frac{1}{2}, \frac{1}{2}, \frac{1}{2})$. The remaining atom positions of the BCC unit cell are assumed to be understood. In the same way, the atom positions in the FCC unit cell can be located.

3.5 DIRECTIONS IN CUBIC UNIT CELLS

Often it is necessary to refer to specific directions in crystal lattices. This is especially important for metals and alloys with properties that vary with crystallographic orientation. *For cubic crystals the crystallographic* **direction indices** *are the vector components of the direction resolved along each of the coordinate axes and reduced to the smallest integers.*

To diagrammatically indicate a direction in a cubic unit cell, we draw a direction vector from an origin, which is usually a corner of the cubic cell, until it emerges from the cube surface (Fig. 3.10). The position coordinates of the unit cell where the direction vector emerges from the cube surface after being converted to integers are the direction indices. The direction indices are enclosed by square brackets with no separating commas.

For example, the position coordinates of the direction vector *OR* in Fig. 3.10*a* where it emerges from the cube surface are (1, 0, 0), and so the direction indices for the direction vector *OR* are [100]. The position coordinates of the direction vector

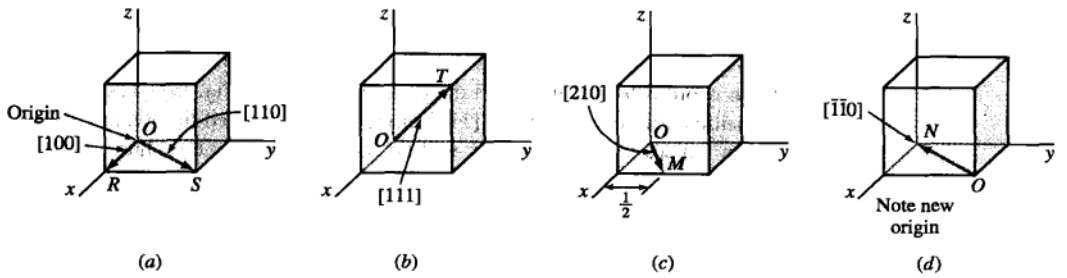

Figure 3.10
Some directions in cubic unit cells.

Tutorial

OS (Fig. 3.10*a*) are (1, 1, 0), and so the direction indices for *OS* are [110]. The position coordinates for the direction vector *OT* (Fig. 3.10*b*) are (1, 1, 1), and so the direction indices of *OT* are [111].

The position coordinates of the direction vector *OM* (Fig. 3.10*c*) are $(1, \frac{1}{2}, 0)$, and since the direction vectors must be integers, these position coordinates must be multiplied by 2 to obtain integers. Thus, the direction indices of *OM* become $2(1, \frac{1}{2}, 0) = [210]$. The position coordinates of the vector *ON* (Fig. 3.10*d*) are $(-1, -1, 0)$. A negative direction index is written with a bar over the index. Thus, the direction indices for the vector *ON* are $[\bar{1}\,\bar{1}0]$. Note that to draw the direction *ON* inside the cube, the origin of the direction vector had to be moved to the front lower-right corner of the unit cube (Fig. 3.10*d*). Further examples of cubic direction vectors are given in Example Problem 3.4.

The letters *u*, *v*, *w* are used in a general sense for the direction indices in the *x*, *y*, and *z* directions, respectively, and are written as [*uvw*]. It is also important to note that *all parallel direction vectors have the same direction indices.*

Directions are said to be *crystallographically equivalent* if the atom spacing along each direction is the same. For example, the following cubic edge directions are crystallographic equivalent directions:

$$[100],\ [010],\ [001],\ [0\bar{1}0],\ [00\bar{1}],\ [\bar{1}00] \equiv \langle 100 \rangle$$

Equivalent directions are called *indices of a family* or *form*. The notation ⟨100⟩ is used to indicate cubic edge directions collectively. Other directions of a form are the cubic body diagonals ⟨111⟩ and the cubic face diagonals ⟨110⟩.

EXAMPLE PROBLEM 3.4

Draw the following direction vectors in cubic unit cells:

a. [100] and [110]
b. [112]
c. $[\bar{1}10]$
d. $[\bar{3}2\bar{1}]$

■ **Solution**

a. The position coordinates for the [100] direction are (1, 0, 0) (Fig. EP3.4*a*). The position coordinates for the [110] direction are (1, 1, 0) (Fig. EP3.4*a*).

b. The position coordinates for the [112] direction are obtained by dividing the direction indices by 2 so that they will lie within the unit cube. Thus, they are $(\frac{1}{2}, \frac{1}{2}, 1)$ (Fig. EP3.4*b*).

c. The position coordinates for the $[\bar{1}10]$ direction are $(-1, 1, 0)$ (Fig. EP3.4*c*). Note that the origin for the direction vector must be moved to the lower-left front corner of the cube.

d. The position coordinates for the $[\bar{3}2\bar{1}]$ direction are obtained by first dividing all the indices by 3, the largest index. This gives $-1, \frac{2}{3}, -\frac{1}{3}$ for the position coordinates of the exit point of the direction $[\bar{3}2\bar{1}]$, which are shown in Fig. 3.4*d*.

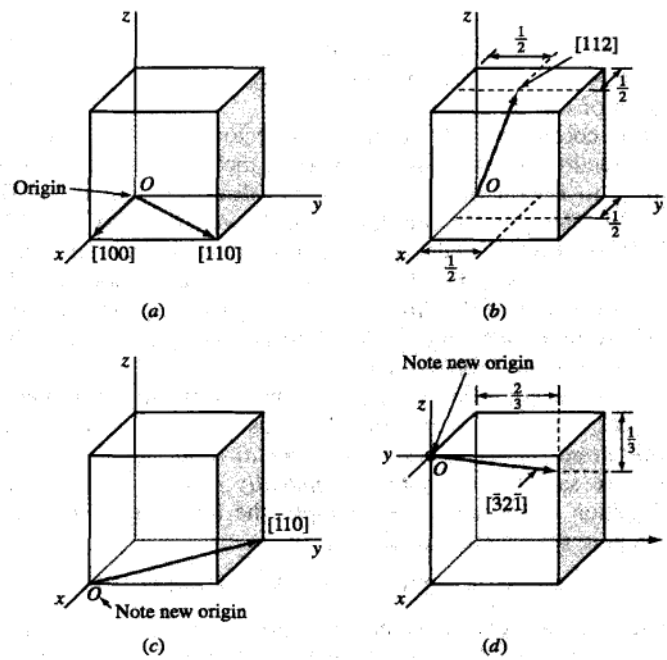

Figure EP3.4
Direction vectors in cubic unit cells.

Tutorial

EXAMPLE PROBLEM 3.5

Determine the direction indices of the cubic direction shown in Fig. EP3.5*a*.

■ **Solution**

Parallel directions have the same direction indices, and so we move the direction vector in a parallel manner until its tail reaches the nearest corner of the cube, still keeping the vector

within the cube. Thus, in this case, the upper-left front corner becomes the new origin for the direction vector (Fig. EP3.5*b*). We can now determine the position coordinates where the direction vector leaves the unit cube. These are $x = -1$, $y = +1$, and $z = -\frac{1}{6}$. The position coordinates of the direction where it leaves the unit cube are thus $(-1, +1, -\frac{1}{6})$. The direction indices for this direction are, after clearing the fraction $6x$, $(-1, +1, -\frac{1}{6})$, or $[\bar{6}6\bar{1}]$.

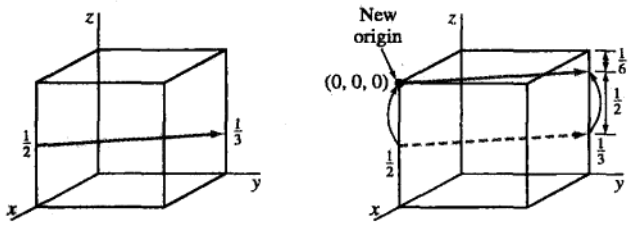

(*a*) (*b*)

Figure EP3.5

Tutorial

EXAMPLE PROBLEM 3.6

Determine the direction indices of the cubic direction between the position coordinates $(\frac{3}{4}, 0, \frac{1}{4})$ and $(\frac{1}{4}, \frac{1}{2}, \frac{1}{2})$.

■ Solution

First we locate the origin and termination points of the direction vector in a unit cube, as shown in Fig. EP3.6. The fraction vector components for this direction are

$$x = -(\tfrac{3}{4} - \tfrac{1}{4}) = -\tfrac{1}{2}$$
$$y = (\tfrac{1}{2} - 0) = \tfrac{1}{2}$$
$$z = (\tfrac{1}{2} - \tfrac{1}{4}) = \tfrac{1}{4}$$

Thus, the vector direction has fractional vector components of $-\frac{1}{2}, \frac{1}{2}, \frac{1}{4}$. The direction indices will be in the same ratio as their fractional components. By multiplying the fraction vector components by 4, we obtain $[\bar{2}21]$ for the direction indices of this vector direction.

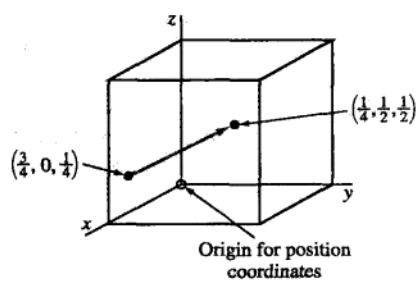

Figure EP3.6

3.6 MILLER INDICES FOR CRYSTALLOGRAPHIC PLANES IN CUBIC UNIT CELLS

Sometimes it is necessary to refer to specific lattice planes of atoms within a crystal structure, or it may be of interest to know the crystallographic orientation of a plane or group of planes in a crystal lattice. To identify crystal planes in cubic crystal structures, the *Miller notation system*[4] is used. The **Miller indices of a crystal plane** are defined as the *reciprocals of the fractional intercepts (with fractions cleared) that the plane makes with the crystallographic x, y, and z axes of the three nonparallel edges of the cubic unit cell.* The cube edges of the unit cell represent unit lengths, and the intercepts of the lattice planes are measured in terms of these unit lengths.

The procedure for determining the Miller indices for a cubic crystal plane is as follows:


Tutorial

1. Choose a plane that does *not* pass through the origin at (0, 0, 0).
2. Determine the intercepts of the plane in terms of the crystallographic x, y, and z axes for a unit cube. These intercepts may be fractions.
3. Form the reciprocals of these intercepts.
4. Clear fractions and determine the *smallest* set of whole numbers that are in the same ratio as the intercepts. These whole numbers are the Miller indices of the crystallographic plane and are enclosed in parentheses without the use of commas. The notation (*hkl*) is used to indicate Miller indices in a general sense, where h, k, and l are the Miller indices of a cubic crystal plane for the x, y, and z axes, respectively.

Figure 3.11 shows three of the most important crystallographic planes of cubic crystal structures. Let us first consider the shaded crystal plane in Fig. 3.11*a*, which has the intercepts 1, ∞, ∞ for the x, y, and z axes, respectively. We take the reciprocals of these intercepts to obtain the Miller indices, which are therefore 1, 0, 0. Since these numbers do not involve fractions, the Miller indices for this plane are (100), which is read as the one-zero-zero plane. Next let us consider the second plane shown in Fig. 3.11*b*. The intercepts of this plane are 1, 1, ∞. Since the reciprocals of these numbers are 1, 1, 0, which do not involve fractions, the Miller indices of this plane are (110). Finally, the third plane (Fig. 3.11*c*) has the intercepts 1, 1, 1, which give the Miller indices (111) for this plane.

Consider now the cubic crystal plane shown in Fig. 3.12 that has the intercepts $\frac{1}{3}$, $\frac{2}{3}$, 1. The reciprocals of these intercepts are 3, $\frac{3}{2}$, 1. Since fractional intercepts are not allowed, these fractional intercepts must be multiplied by 2 to clear the $\frac{3}{2}$ fraction. Thus, the reciprocal intercepts become 6, 3, 2 and the Miller

[4]William Hallowes Miller (1801–1880). English crystallographer who published a "Treatise on Crystallography" in 1839, using crystallographic reference axes that were parallel to the crystal edges and using reciprocal indices.

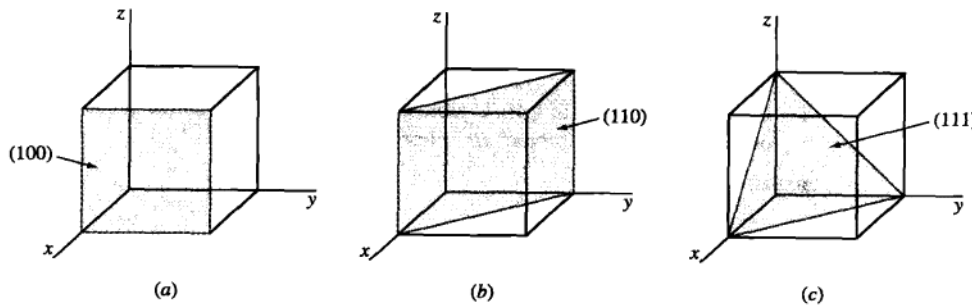

Figure 3.11
Miller indices of some important cubic crystal planes: (*a*) (100), (*b*) (110), and (*c*) (111).

Tutorial
MatVis

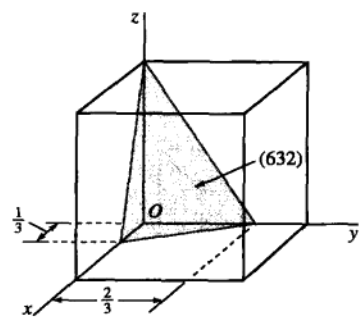

Figure 3.12
Cubic crystal plane (632), which has fractional intercepts.

indices are (632). Further examples of cubic crystal planes are shown in Example Problem 3.7.

If the crystal plane being considered passes through the origin so that one or more intercepts are zero, the plane must be moved to an equivalent position in the same unit cell and the plane must remain parallel to the original plane. This is possible because all equispaced parallel planes are indicated by the same Miller indices.

If sets of equivalent lattice planes are related by the symmetry of the crystal system, they are called *planes of a family or form,* and the indices of one plane of the family are enclosed in braces as {*hkl*} to represent the indices of a family of symmetrical planes. For example, the Miller indices of the cubic surface planes (100), (010), and (001) are designated collectively as a family or form by the notation {100}.

EXAMPLE PROBLEM 3.7

Draw the following crystallographic planes in cubic unit cells:

a. (101) b. $(1\bar{1}0)$ c. (221)

d. Draw a (110) plane in a BCC atomic-site unit cell, and list the position coordinates of the atoms whose centers are intersected by this plane.

■ **Solutions**

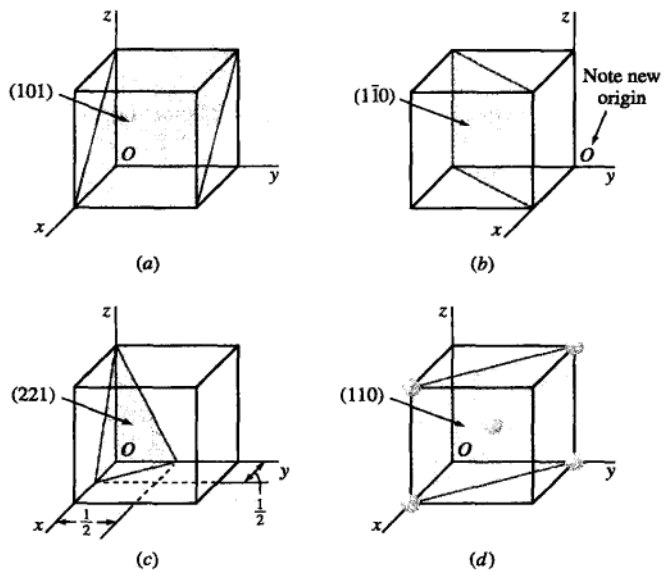

Figure EP3.7
Various important cubic crystal planes.

MatVis

a. First determine the reciprocals of the Miller indices of the (101) plane. These are 1, ∞, 1. The (101) plane must pass through a unit cube at intercepts $x = 1$ and $z = 1$ and be parallel to the y axis (Fig. EP3.7*a*).

b. First determine the reciprocals of the Miller indices of the $(1\bar{1}0)$ plane. These are $1, -1, \infty$. The $(1\bar{1}0)$ plane must pass through a unit cube at intercepts $x = 1$ and $y = -1$ and be parallel to the z axis. Note that the origin of axes must be moved to the lower-right back side of the cube (Fig. EP3.7*b*).

c. First determine the reciprocals of the Miller indices of the (221) plane. These are $\frac{1}{2}, \frac{1}{2}, 1$ The (221) plane must pass through a unit cube at intercepts $x = \frac{1}{2}$, $y = \frac{1}{2}$, and $z = 1$ (Fig. EP3.7*c*).

d. Atom positions whose centers are intersected by the (110) plane are (1, 0, 0), (0, 1, 0), (1, 0, 1), (0, 1, 1), and $(\frac{1}{2}, \frac{1}{2}, \frac{1}{2})$. These positions are indicated by the solid circles (Fig. EP3.7*d*).

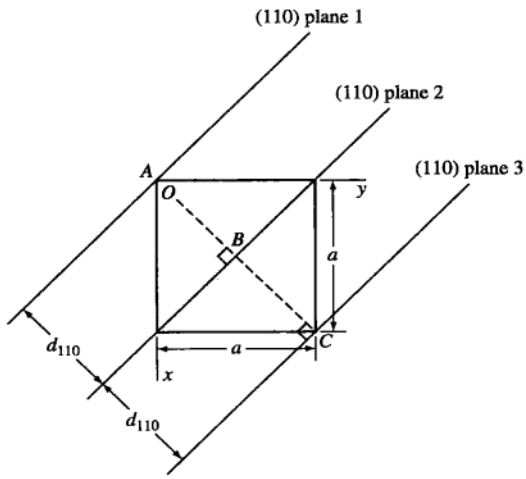

Figure 3.13
Top view of cubic unit cell showing the distance between (110) crystal planes, d_{110}.

An important relationship for the cubic system, and *only the cubic system,* is that the direction indices of a direction *perpendicular* to a crystal plane are the same as the Miller indices of that plane. For example, the [100] direction is perpendicular to the (100) crystal plane.

In cubic crystal structures the *interplanar spacing* between two closest parallel planes with the same Miller indices is designated d_{hkl}, where h, k, and l are the Miller indices of the planes. This spacing represents the distance from a selected origin containing one plane and another parallel plane with the same indices that is closest to it. For example, the distance between (110) planes 1 and 2, d_{110}, in Fig. 3.13 is AB. Also, the distance between (110) planes 2 and 3 is d_{110} and is length BC in Fig. 3.13. From simple geometry, it can be shown that for cubic crystal structures

$$d_{hkl} = \frac{a}{\sqrt{h^2 + k^2 + l^2}} \tag{3.4}$$

where d_{hkl} = interplanar spacing between parallel closest planes with Miller indices h, k, and l
a = lattice constant (edge of unit cube)
h, k, l = Miller indices of cubic planes being considered

EXAMPLE PROBLEM 3.8

Determine the Miller indices of the cubic crystallographic plane shown in Fig. EP3.8*a*.

■ **Solution**

First, transpose the plane parallel to the z axis $\frac{1}{4}$ unit to the right along the y axis as shown in Fig. EP3.8*b* so that the plane intersects the x axis at a unit distance from the new origin

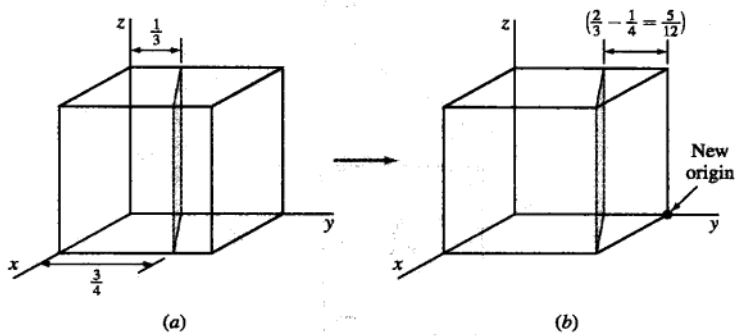

Figure EP3.8

located at the lower-right back corner of the cube. The new intercepts of the transposed plane with the coordinate axes are now $(+1, -\frac{5}{12}, \infty)$. Next, we take the reciprocals of these intercepts to give $(1, -\frac{12}{5}, 0)$. Finally, we clear the $\frac{12}{5}$ fraction to obtain $(5\bar{1}\bar{2}0)$ for the Miller indices of this plane.

EXAMPLE PROBLEM 3.9

Determine the Miller indices of the cubic crystal plane that intersects the position coordinates $(1, \frac{1}{4}, 0)$, $(1, 1, \frac{1}{2})$, $(\frac{3}{4}, 1, \frac{1}{4})$, and all coordinate axes.

■ Solution

First, we locate the three position coordinates as indicated in Fig. EP3.9 at *A*, *B*, and *C*. Next, we join *A* and *B*, extend *AB* to *D*, and then join *A* and *C*. Finally, we join *A* to *C* to complete plane *ACD*. The origin for this plane in the cube can be chosen at *E*, which gives axial intercepts for plane *ACD* at $x = -\frac{1}{2}$, $y = -\frac{3}{4}$, and $z = \frac{1}{2}$. The reciprocals of these axial intercepts are -2, $-\frac{4}{3}$, and 2. Multiplying these intercepts by 3 clears the fraction, giving Miller indices for the plane of $(\bar{6}\bar{4}6)$.

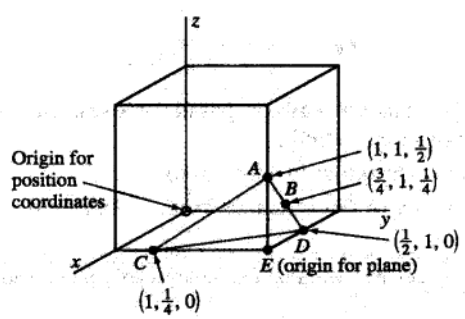

Figure EP3.9

EXAMPLE PROBLEM 3.10

Copper has an FCC crystal structure and a unit cell with a lattice constant of 0.361 nm. What is its interplanar spacing d_{220}?

■ **Solution**

$$d_{hkl} = \frac{a}{\sqrt{h^2 + k^2 + l^2}} = \frac{0.361 \text{ nm}}{\sqrt{(2)^2 + (2)^2 + (0)^2}} = 0.128 \text{ nm} \blacktriangleleft$$

3.7 CRYSTALLOGRAPHIC PLANES AND DIRECTIONS IN HEXAGONAL CRYSTAL STRUCTURE

3.7.1 Indices for Crystal Planes in HCP Unit Cells

Crystal planes in HCP unit cells are commonly identified by using four indices instead of three. The HCP crystal plane indices, called *Miller-Bravais indices,* are denoted by the letters h, k, i, and l and are enclosed in parentheses as ($hkil$). These four-digit hexagonal indices are based on a coordinate system with four axes, as shown in Fig. 3.14 in an HCP unit cell. There are three basal axes, a_1, a_2, and a_3, which make 120° with each other. The fourth axis or c axis is the vertical axis located at the center of the unit cell. The a unit of measurement along the a_1, a_2, and a_3 axes is the distance between the atoms along these axes and is indicated in Fig. 3.14. In the discussion of HCP planes and directions, we will use both the "unit cell" and the "larger cell" for the presentation of concepts. The unit of measurement along the c axis is the height of the unit cell. The reciprocals of the intercepts that a crystal plane makes with the a_1, a_2, and a_3 axes give the h, k, and i indices, while the reciprocal of the intercept with the c axis gives the l index.

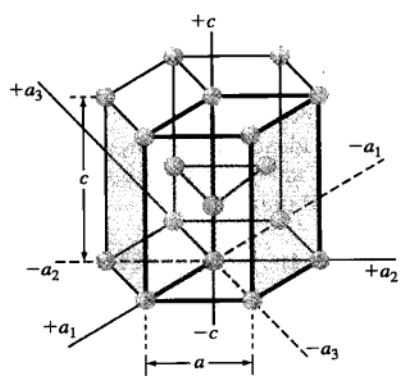

Figure 3.14
The four coordinate axes (a_1, a_2, a_3, and c) of the HCP crystal structure.

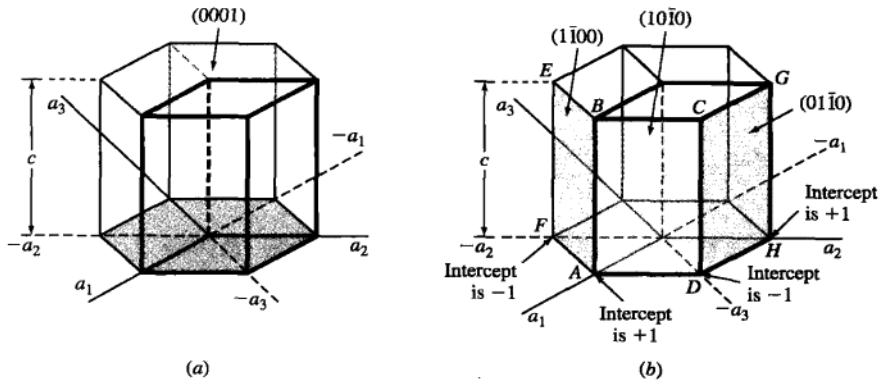

MatVis

Figure 3.15
Miller-Bravais indices of hexagonal crystal planes: (*a*) basal planes and (*b*) prism planes.

Basal Planes The basal planes of the HCP unit cell are very important planes for this unit cell and are indicated in Fig. 3.15*a*. Since the basal plane on the top of the HCP unit cell in Fig. 3.15*a* is parallel to the a_1, a_2, and a_3 axes, the intercepts of this plane with these axes will all be infinite. Thus, $a_1 = \infty$, $a_2 = \infty$, and $a_3 = \infty$. The c axis, however, is unity since the top basal plane intersects the c axis at unit distance. Taking the reciprocals of these intercepts gives the Miller-Bravais indices for the HCP basal plane. Thus $h = 0$, $k = 0$, $i = 0$, and $l = 1$. The HCP basal plane is, therefore, a zero-zero-zero-one or (0001) plane.

Prism Planes Using the same method, the intercepts of the front prism plane (*ABCD*) of Fig. 3.15*b* are $a_1 = +1$, $a_2 = \infty$, $a_3 = -1$, and $c = \infty$. Taking the reciprocals of these intercepts gives $h = 1$, $k = 0$, $i = -1$, and $l = 0$, or the $(10\bar{1}0)$ plane. Similarly, the *ABEF* prism plane of Fig. 3.15*b* has the indices $(1\bar{1}00)$ and the *DCGH* plane the indices $(01\bar{1}0)$. All HCP prism planes can be identified collectively as the $\{10\bar{1}0\}$ family of planes.

Sometimes HCP planes are identified only by three indices (*hkl*) since $h + k = -i$. However, the (*hkil*) indices are used more commonly because they reveal the hexagonal symmetry of the HCP unit cell.

3.7.2 Direction Indices in HCP Unit Cells[5]

Directions in HCP unit cells are also usually indicated by four indices u, v, t, and w enclosed by square brackets as $[uvtw]$. The u, v, and t indices are lattice vectors

[5]The topic of direction indices for hexagonal unit cells is not normally presented in an introductory course in materials but is included here for advanced students.

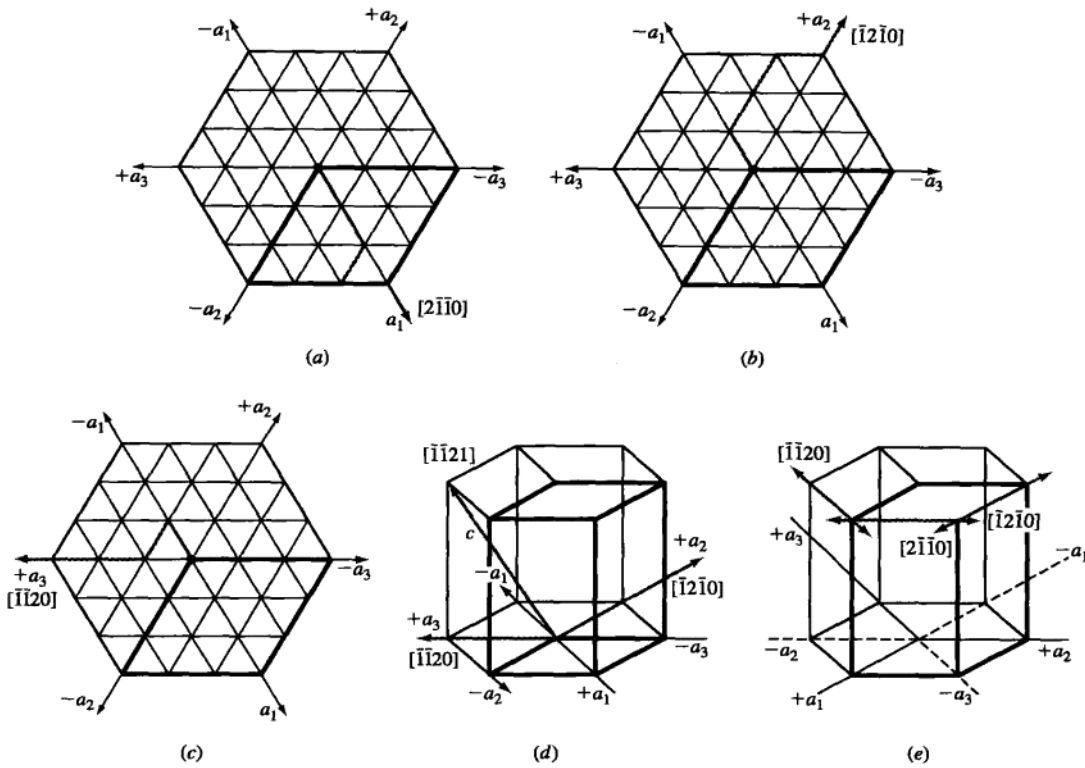

Figure 3.16
Miller-Bravais hexagonal crystal structure direction indices for principal directions: (*a*) $+a_1$ axis direction on basal plane, (*b*) $+a_2$ axis direction on basal plane, (*c*) $+a_3$ direction axis on basal plane, and (*d*) $+a_3$ direction axis incorporating *c* axis. (*e*) Positive and negative Miller-Bravais directions are indicated in simple hexagonal crystal structure on upper basal plane.

in the a_1, a_2, and a_3 directions, respectively (Fig. 3.16), and the w index is a lattice vector in the c direction. To maintain uniformity for both HCP indices for planes and directions, it has been agreed that $u + v = -t$ for directions.

Let us now determine the Miller-Bravais hexagonal indices for the directions a_1, a_2, and a_3, which are the positive basal axes of the hexagonal unit cell. The a_1 direction indices are given in Fig. 3.16*a*, the a_2 direction indices in Fig. 3.16*b*, and the a_3 direction indices in Fig. 3.16*c*. If we need to indicate a c direction also for the a_3 direction, this is shown in Fig. 3.16*d*. Figure 3.16*e* summarizes the positive and negative directions on the upper basal plane of the simple hexagonal crystal structure.

3.8 COMPARISON OF FCC, HCP, AND BCC CRYSTAL STRUCTURES

3.8.1 FCC and HCP Crystal Structures

As previously pointed out, both the HCP and FCC crystal structures are close-packed structures. That is, their atoms, which are considered approximate "spheres," are packed together as closely as possible so that an atomic packing factor of 0.74 is attained.[6] The (111) planes of the FCC crystal structure shown in Fig. 3.17*a* have the identical packing arrangement as the (0001) planes of the HCP crystal structure shown in Fig. 3.17*b*. However, the three-dimensional FCC and HCP crystal structures are not identical because there is a difference in the stacking arrangement of their atomic planes, which can best be described by considering the stacking of hard spheres representing atoms. As a useful analogy, one can imagine the stacking of planes of equal-sized marbles on top of each other, minimizing the space between the marbles.

Consider first a plane of close-packed atoms designated the *A* plane, as shown in Fig. 3.18. Note that there are two different types of empty spaces or voids between

[6]As pointed out in Sec. 3.3, the atoms in the HCP structure deviate to varying degrees from ideality. In some HCP metals, the atoms are elongated along the *c* axis, and in other cases, they are compressed along the *c* axis (see Table 3.4).

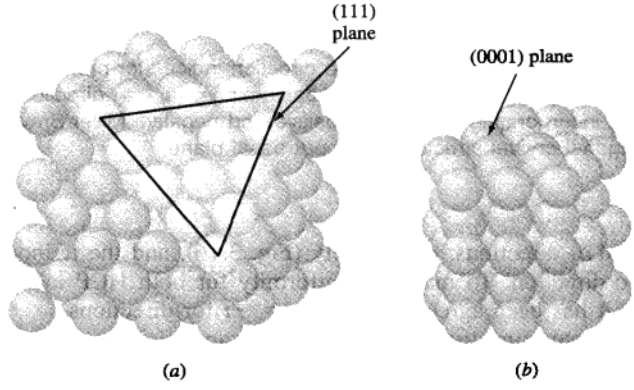

Figure 3.17
Comparison of the (*a*) FCC crystal structure showing a close-packed (111) plane and (*b*) a HCP crystal structure showing the close-packed (0001) plane.
(From W.G. Moffatt, G.W. Pearsall, and J. Wulff, The Structure and Properties of Materials, vol. 1: "Structure", Wiley, 1964, p. 51.)

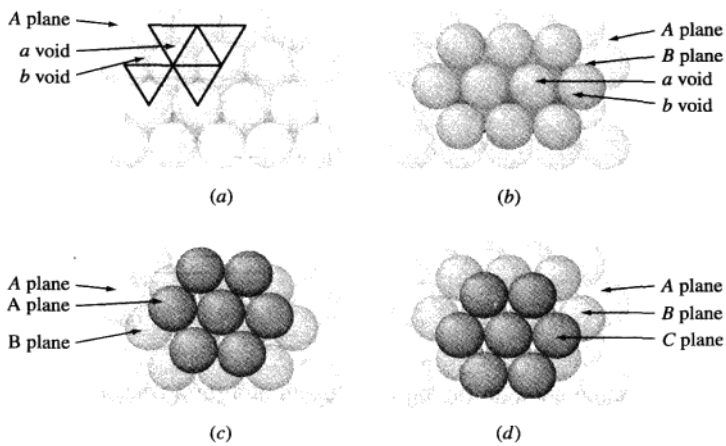

Figure 3.18
Formation of the HCP and FCC crystal structures by the stacking of atomic planes. (*a*) *A* plane showing the *a* and *b* voids. (*b*) *B* plane placed in *a* voids of plane *A*. (*c*) Third plane placed in *b* voids of *B* plane, making another *A* plane and forming the HCP crystal structure. (*d*) Third plane placed in the *a* voids of *B* plane, making a new *C* plane and forming the FCC crystal structure.
(Ander, P.; Sonnessa, A.J., Principles of Chemistry, 1st ed., © 1965, Reprinted by permission of Pearson Education, Inc., Upper Saddle River, NJ.)


Animation

the atoms. The voids pointing to the top of the page are designated *a* voids and those pointing to the bottom of the page, *b* voids. A second plane of atoms can be placed over the *a* or *b* voids, and the same three-dimensional structure will be produced. Let us place plane *B* over the *a* voids, as shown in Fig. 3.18*b*. Now if a third plane of atoms is placed over plane *B* to form a closest-packed structure, it is possible to form two different close-packed structures. One possibility is to place the atoms of the third plane in the *b* voids of the *B* plane. Then the atoms of this third plane will lie directly over those of the *A* plane and thus can be designated another *A* plane (Fig. 3.18*c*). If subsequent planes of atoms are placed in this same alternating stacking arrangement, then the stacking sequence of the three-dimensional structure produced can be denoted by *ABABAB*. . . . Such a stacking sequence leads to the HCP crystal structure (Fig. 3.17*b*).

The second possibility for forming a simple close-packed structure is to place the third plane in the *a* voids of plane *B* (Fig. 3.18*d*). This third plane is designated the *C* plane since its atoms do not lie directly above those of the *B* plane or the *A* plane. The stacking sequence in this close-packed structure is thus designated *ABCABCABC*. . . and leads to the FCC structure shown in Fig. 3.17*a*.

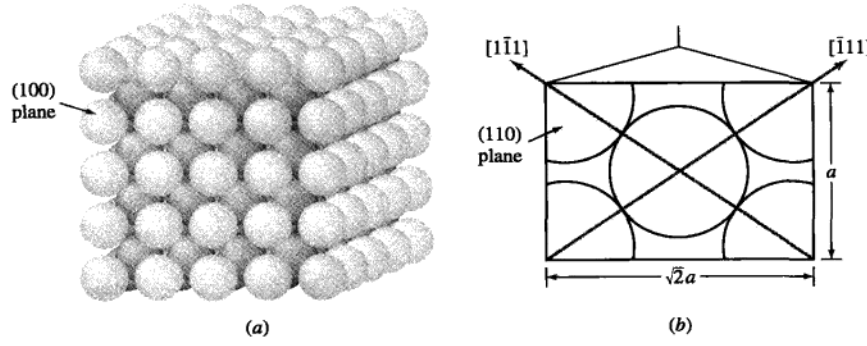

Figure 3.19
BCC crystal structure showing (*a*) the (100) plane and (*b*) a section of the (110) plane. Note that this is not a close-packed structure but that the diagonals have close-packed directions.
(From W.G. Moffatt, G.W. Pearsall, and J. Wulff, The Structure and Properties of Materials, vol. 1: "Structure", Wiley, 1964, p. 51.)

3.8.2 BCC Crystal Structure

The BCC structure is not a close-packed structure and hence does not have close-packed planes like the {111} planes in the FCC structure and the {0001} planes in the HCP structure. The most densely packed planes in the BCC structure are the {110} family of planes of which the (110) plane is shown in Fig. 3.19*b*. However, the atoms in the BCC structure do have close-packed directions along the cube diagonals, which are the ⟨111⟩ directions.

3.9 VOLUME, PLANAR, AND LINEAR DENSITY UNIT-CELL CALCULATIONS

3.9.1 Volume Density

Using the hard-sphere atomic model for the crystal structure unit cell of a metal and a value for the atomic radius of the metal obtained from X-ray diffraction analysis, a value for the **volume density** of a metal can be obtained by using the equation

$$\text{Volume density of metal} = \rho_v = \frac{\text{mass/unit cell}}{\text{volume/unit cell}} \tag{3.5}$$

In Example Problem 3.11 a value of 8.98 Mg/m^3 (8.98 g/cm^3) is obtained for the density of copper. The handbook experimental value for the density of copper is 8.96 Mg/m^3 (8.96 g/cm^3). The slightly lower density of the experimental value could be attributed to the absence of atoms at some atomic sites (vacancies), line defects,

and mismatch where grains meet (grain boundaries). These crystalline defects are discussed in Chap. 4. Another cause of the discrepancy could also be due to the atoms not being perfect spheres.

EXAMPLE PROBLEM 3.11

Copper has an FCC crystal structure and an atomic radius of 0.1278 nm. Assuming the atoms to be hard spheres that touch each other along the face diagonals of the FCC unit cell as shown in Fig. 3.7, calculate a theoretical value for the density of copper in megagrams per cubic meter. The atomic mass of copper is 63.54 g/mol.

■ **Solution**

For the FCC unit cell, $1\ \bar{2}a = 4R$, where a is the lattice constant of the unit cell and R is the atomic radius of the copper atom. Thus,

$$a = \frac{4R}{\sqrt{2}} = \frac{(4)(0.1278\ \text{nm})}{\sqrt{2}} = 0.361\ \text{nm}$$

$$\text{Volume density of copper} = \rho_v = \frac{\text{mass/unit cell}}{\text{volume/unit cell}} \tag{3.5}$$

In the FCC unit cell, there are four atoms/unit cell. Each copper atom has a mass of (63.54 g/mol)/(6.02×10^{23} atoms/mol). Thus, the mass m of Cu atoms in the FCC unit cell is

$$m = \frac{(4\ \text{atoms})(63.54\ \text{g/mol})}{6.02 \times 10^{23}\ \text{atoms/mol}}\left(\frac{10^{-6}\ \text{Mg}}{\text{g}}\right) = 4.22 \times 10^{-28}\ \text{Mg}$$

The volume V of the Cu unit cell is

$$V = a^3 = \left(0.361\ \text{nm} \times \frac{10^{-9}\ \text{m}}{\text{nm}}\right)^3 = 4.70 \times 10^{-29}\ \text{m}^3$$

Thus, the density of copper is

$$\rho_v = \frac{m}{V} = \frac{4.22 \times 10^{-28}\ \text{Mg}}{4.70 \times 10^{-29}\ \text{m}^3} = 8.98\ \text{Mg/m}^3 \quad (8.98\ \text{g/cm}^3) \blacktriangleleft$$

3.9.2 Planar Atomic Density

Sometimes it is important to determine the atomic densities on various crystal planes. To do this a quantity called the **planar atomic density** is calculated by using the relationship

$$\text{Planar atomic density} = \rho_p = \frac{\text{equiv. no. of atoms whose centers are intersected by selected area}}{\text{selected area}} \tag{3.6}$$

For convenience the area of a plane that intersects a unit cell is usually used in these calculations, as shown, for example, in Fig. 3.20 for the (110) plane in a BCC unit

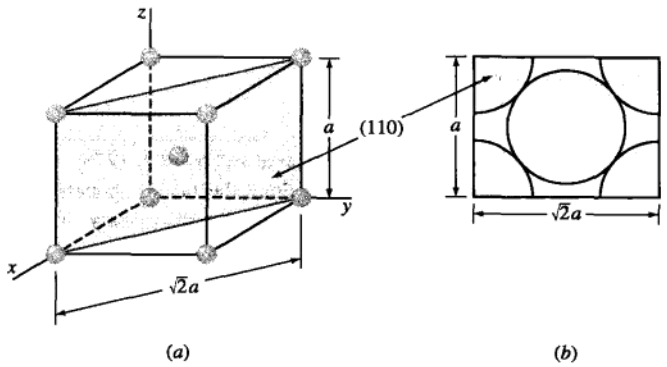

Figure 3.20
(*a*) A BCC atomic-site unit cell showing a shaded (110) plane.
(*b*) Areas of atoms in BCC unit cell cut by the (110) plane.

cell. In order for an atom area to be counted in this calculation, the plane of interest must intersect the center of an atom. In Example Problem 3.12 the (110) plane intersects the centers of five atoms, but the equivalent of only two atoms is counted since only one-quarter of each of the four corner atoms is included in the area inside the unit cell.

EXAMPLE PROBLEM 3.12

Calculate the planar atomic density ρ_p on the (110) plane of the α iron BCC lattice in atoms per square millimeter. The lattice constant of α iron is 0.287 nm.

■ **Solution**

$$\rho_p = \frac{\text{equiv. no. of atoms whose centers are intersected by selected area}}{\text{selected area}} \tag{3.6}$$

The equivalent number of atoms intersected by the (110) plane in terms of the surface area inside the BCC unit cell is shown in Fig. 3.22 and is

$$1 \text{ atom at center} + 4 \times \tfrac{1}{4} \text{ atoms at four corners of plane} = 2 \text{ atoms}$$

The area intersected by the (110) plane inside the unit cell (selected area) is

$$(\sqrt{2}a)(a) = \sqrt{2}a^2$$

Thus, the planar atomic density is

$$\rho_p = \frac{2 \text{ atoms}}{\sqrt{2}(0.287 \text{ nm})^2} = \frac{17.2 \text{ atoms}}{\text{nm}^2}$$

$$= \frac{17.2 \text{ atoms}}{\text{nm}^2} \times \frac{10^{12} \text{ nm}^2}{\text{mm}^2}$$

$$= 1.72 \times 10^{13} \text{ atoms/mm}^2 \blacktriangleleft$$

3.9.3 Linear Atomic Density

Sometimes it is important to determine the atomic densities in various directions in crystal structures. To do this a quantity called the **linear atomic density** is calculated by using the relationship

$$\text{Linear atomic density} = \rho_l = \frac{\text{no. of atomic diam. intersected by selected length of line in direction of interest}}{\text{selected length of line}} \tag{3.7}$$

Example Problem 3.13 shows how the linear atomic density can be calculated in the [110] direction in a pure copper crystal lattice.

EXAMPLE PROBLEM 3.13

Calculate the linear atomic density ρ_l in the [110] direction in the copper crystal lattice in atoms per millimeter. Copper is FCC and has a lattice constant of 0.361 nm.

■ Solution

The atoms whose centers the [110] direction intersects are shown in Fig. EP3.13. We shall select the length of the line to be the length of the face diagonal of the FCC unit cell, which is $\sqrt{2}a$. The number of atomic diameters intersected by this length of line are $\frac{1}{2} + 1 + \frac{1}{2} = 2$ atoms. Thus using Eq. 3.7, the linear atomic density is

$$\rho_l = \frac{2 \text{ atoms}}{\sqrt{2}a} = \frac{2 \text{ atoms}}{\sqrt{2}(0.361 \text{ nm})} = \frac{3.92 \text{ atoms}}{\text{nm}}$$

$$= \frac{3.92 \text{ atoms}}{\text{nm}} \times \frac{10^6 \text{ nm}}{\text{mm}}$$

$$= 3.92 \times 10^6 \text{ atoms/mm} \blacktriangleleft$$

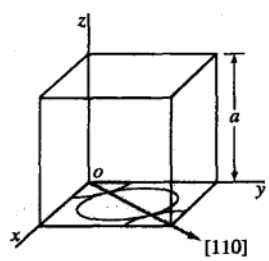

Figure EP3.13
Diagram for calculating the atomic linear density in the [110] direction in an FCC unit cell.

3.10 POLYMORPHISM OR ALLOTROPY

Many elements and compounds exist in more than one crystalline form under different conditions of temperature and pressure. This phenomenon is termed **polymorphism,** or *allotropy*. Many industrially important metals such as iron, titanium, and cobalt undergo allotropic transformations at elevated temperatures at atmospheric pressure. Table 3.5 lists some selected metals that show allotropic transformations and the structure changes that occur.

Iron exists in both BCC and FCC crystal structures over the temperature range from room temperature to its melting point at 1539°C as shown in Fig. 3.21. Alpha (α) iron exists from −273°C to 912°C and has the BCC crystal structure. Gamma (γ)

Table 3.5 Allotropic crystalline forms of some metals

Metal	Crystal structure at room temperature	At other temperatures
Ca	FCC	BCC (> 447°C)
Co	HCP	FCC (> 427°C)
Hf	HCP	BCC (> 1742°C)
Fe	BCC	FCC (912–1394°C) BCC (> 1394°C)
Li	BCC	HCP (< −193°C)
Na	BCC	HCP (< −233°C)
Tl	HCP	BCC (> 234°C)
Ti	HCP	BCC (> 883°C)
Y	HCP	BCC (> 1481°C)
Zr	HCP	BCC (> 872°C)

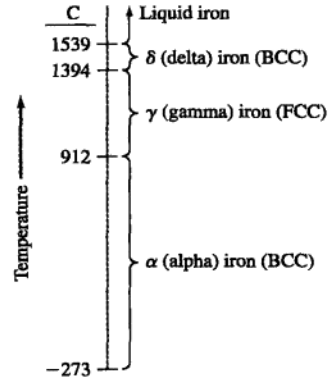

Figure 3.21
Allotropic crystalline forms of iron over temperature ranges at atmospheric pressure

iron exists from 912°C to 1394°C and has the FCC crystal structure. Delta (δ) iron exists from 1394°C to 1539°C which is the melting point of iron. The crystal structure of δ iron is also BCC but with a larger lattice constant than α iron.

EXAMPLE PROBLEM 3.14

Calculate the theoretical volume change accompanying a polymorphic transformation in a pure metal from the FCC to BCC crystal structure. Assume the hard-sphere atomic model and that there is no change in atomic volume before and after the transformation.

■ **Solution**

In the FCC crystal structure unit cell, the atoms are in contact along the face diagonal of the unit cell, as shown in Fig. 3.7. Hence,

$$\sqrt{2}a = 4R \quad \text{or} \quad a = \frac{4R}{\sqrt{2}} \tag{3.3}$$

In the BCC crystal structure unit cell, the atoms are in contact along the body diagonal of the unit cell as shown in Fig. 3.5. Hence,

$$\sqrt{3}a = 4R \quad \text{or} \quad a = \frac{4R}{\sqrt{3}} \tag{3.1}$$

The volume per atom for the FCC crystal lattice, since it has four atoms per unit cell, is

$$V_{FCC} = \frac{a^3}{4} = \left(\frac{4R}{\sqrt{2}}\right)^3\left(\frac{1}{4}\right) = 5.66R^3$$

The volume per atom for the BCC crystal lattice, since it has two atoms per unit cell, is

$$V_{BCC} = \frac{a^3}{2} = \left(\frac{4R}{\sqrt{3}}\right)^3\left(\frac{1}{2}\right) = 6.16R^3$$

The change in volume associated with the transformation from the FCC to BCC crystal structure, assuming no change in atomic radius, is

$$\frac{\Delta V}{V_{FCC}} = \frac{V_{BCC} - V_{FCC}}{V_{FCC}}$$

$$= \left(\frac{6.16R^3 - 5.66R^3}{5.66R^3}\right)100\% = +8.8\% \blacktriangleleft$$

3.11 CRYSTAL STRUCTURE ANALYSIS

Our present knowledge of crystal structures has been obtained mainly by X-ray diffraction techniques that use X-rays whose wavelength are the same as the distance between crystal lattice planes. However, before discussing the manner in

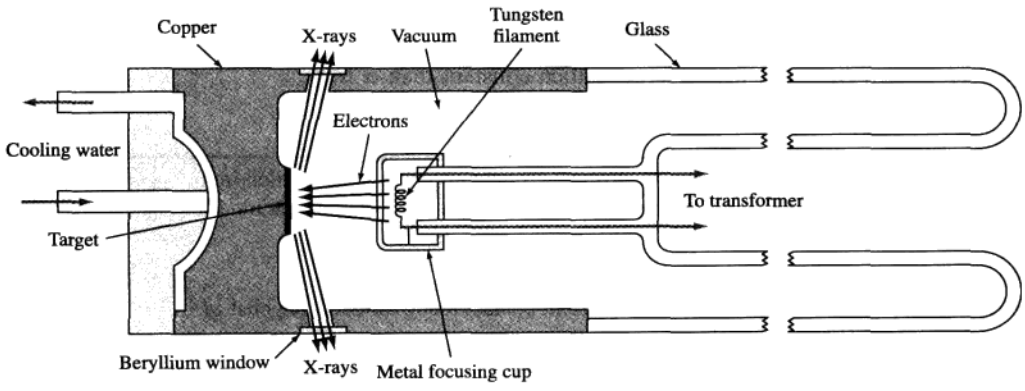

Figure 3.22
Schematic diagram of the cross section of a sealed-off filament X-ray tube.
(From B. D. Cullity, Elements of X-Ray Diffraction 2nd ed., Addison-Wesley, 1978, p. 23. Reprinted by permission of Elizabeth M. Cullity.)

which X-rays are diffracted in crystals, let us consider how X-rays are produced for experimental purposes.

3.11.1 X-Ray Sources

X-rays used for diffraction are electromagnetic waves with wavelengths in the range 0.05 to 0.25 nm (0.5 to 2.5 Å). By comparison, the wavelength of visible light is of the order of 600 nm (6000 Å). In order to produce X-rays for diffraction purposes, a voltage of about 35 kV is necessary and is applied between a cathode and an anode target metal, both of which are contained in a vacuum, as shown in Fig. 3.22. When the tungsten filament of the cathode is heated, electrons are released by thermionic emission and accelerated through the vacuum by the large voltage difference between the cathode and anode, thereby gaining kinetic energy. When the electrons strike the target metal (e.g., molybdenum), X-rays are given off. However, most of the kinetic energy (about 98 percent) is converted into heat, so the target metal must be cooled externally.

The X-ray spectrum emitted at 35 kV using a molybdenum target is shown in Fig. 3.23. The spectrum shows continuous X-ray radiation in the wavelength range from about 0.2 to 1.4 Å (0.02 to 0.14 nm) and two spikes of characteristic radiation that are designated the K_α and K_β lines. The wavelengths of the K_α and K_β lines are characteristic for an element. For molybdenum, the K_α line occurs at a wavelength of about 0.7 Å (0.07 nm). The origin of the characteristic radiation is explained as follows. First, K electrons (electrons in the $n = 1$ shell) are knocked out of the atom by highly energetic electrons bombarding the target, leaving excited atoms. Next, some electrons in higher shells (that is, $n = 2$ or 3) drop down to lower energy levels to replace the lost K electrons, emitting energy of a

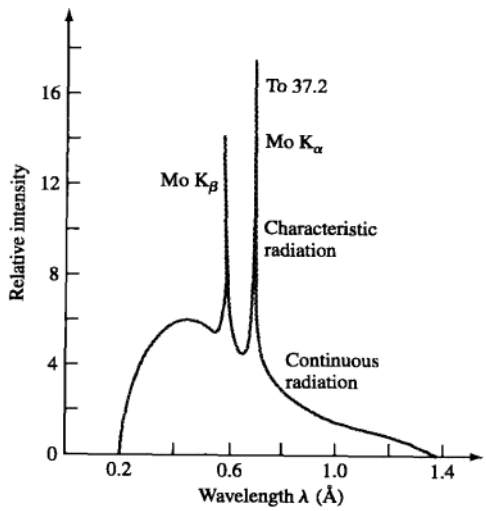

Figure 3.23
X-ray emission spectrum produced when molybdenum metal is used as the target metal in an X-ray tube operating at 35 kV.

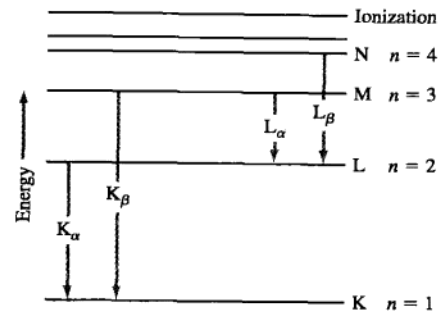

Figure 3.24
Energy levels of electrons in molybdenum showing the origin of K_α and K_β radiation.

characteristic wavelength. The transition of electrons from the L ($n = 2$) shell to the K ($n = 1$) shell creates energy of the wavelength of the K_α line, as indicated in Fig. 3.24.

3.11.2 X-Ray Diffraction

Since the wavelengths of some X-rays are about equal to the distance between planes of atoms in crystalline solids, reinforced diffraction peaks of radiation of varying intensities can be produced when a beam of X-rays strikes a crystalline solid. However, before considering the application of X-ray diffraction techniques to crystal structure analysis, let us examine the geometric conditions necessary to produce diffracted or reinforced beams of reflected X-rays.

Consider a monochromatic (single-wavelength) beam of X-rays to be incident on a crystal, as shown in Fig. 3.25. For simplification, let us allow the crystal planes of atomic scattering centers to be replaced by crystal planes that act as mirrors in reflecting the incident X-ray beam. In Fig. 3.25, the horizontal lines represent a set of parallel crystal planes with Miller indices (*hkl*). When an incident beam of monochromatic X-rays of wavelength λ strikes this set of planes at an angle such that the wave patterns of the beam leaving the various planes are *not in phase, no reinforced beam will be produced* (Fig. 3.25*a*). Thus, destructive interference occurs. If the reflected wave patterns of the beam leaving the various planes are in phase, then reinforcement of the beam or constructive interference occurs (Fig. 3.25*b*).

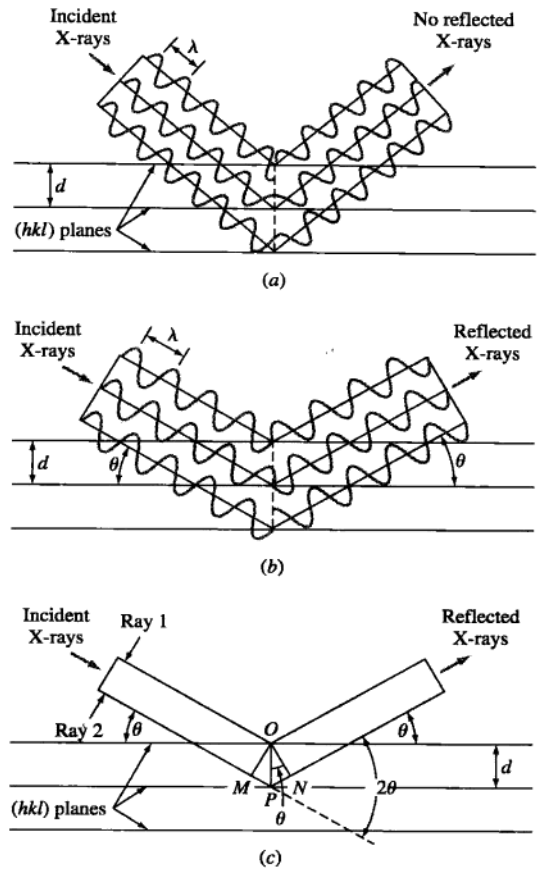

Figure 3.25
The reflection of an X-ray beam by the (*hkl*) planes of a crystal. (*a*) No reflected beam is produced at an arbitrary angle of incidence. (*b*) At the Bragg angle θ, the reflected rays are in phase and reinforce one another. (*c*) Similar to (*b*) except that the wave representation has been omitted.
(From p. 201 in A.G. Guy and J.J. Hren, Elements of Physical Metallurgy 3rd ed., Addison-Wesley, 1974.)

Let us now consider incident X-rays 1 and 2 as indicated in Fig. 3.25*c*. For these rays to be in phase, the extra distance of travel of ray 2 is equal to $MP + PN$, which must be an integral number of wavelengths λ. Thus,

$$n\lambda = MP + PN \tag{3.8}$$

where $n = 1, 2, 3, \ldots$ and is called the *order of the diffraction*. Since both *MP* and *PN* equal $d_{hkl} \sin \theta$, where d_{hkl} is the interplanar spacing of the crystal planes of indices (*hkl*), the condition for constructive interference (i.e., the production of a diffraction peak of intense radiation) must be

$$n\lambda = 2d_{hkl} \sin \theta \tag{3.9}$$

This equation, known as *Bragg's law*,[7] gives the relationship among the angular positions of the reinforced diffracted beams in terms of the wavelength λ of the incoming X-ray radiation and of the interplanar spacings d_{hkl} of the crystal planes. In most cases, the first order of diffraction where $n = 1$ is used, and so for this case, Bragg's law takes the form

$$\lambda = 2d_{hkl} \sin \theta \tag{3.10}$$

EXAMPLE PROBLEM 3.15

A sample of BCC iron was placed in an X-ray diffractometer using incoming X-rays with a wavelength $\lambda = 0.1541$ nm. Diffraction from the {110} planes was obtained at $2\theta = 44.704°$. Calculate a value for the lattice constant a of BCC iron. (Assume first-order diffraction with $n = 1$.)

■ **Solution**

$$2\theta = 44.704° \qquad \theta = 22.35°$$

$$\lambda = 2d_{hkl} \sin \theta \tag{3.10}$$

$$d_{110} = \frac{\lambda}{2 \sin \theta} = \frac{0.1541 \text{ nm}}{2(\sin 22.35°)}$$

$$= \frac{0.1541 \text{ nm}}{2(0.3803)} = 0.2026 \text{ nm}$$

Rearranging Eq. 3.4 gives

$$a = d_{hkl}\sqrt{h^2 + k^2 + l^2}$$

Thus,

$$a(\text{Fe}) = d_{110}\sqrt{1^2 + 1^2 + 0^2}$$

$$= (0.2026 \text{ nm})(1.414) = 0.287 \text{ nm} \blacktriangleleft$$

3.11.3 X-Ray Diffraction Analysis of Crystal Structures

The Powder Method of X-Ray Diffraction Analysis The most commonly used X-ray diffraction technique is the *powder method*. In this technique, a powdered specimen is utilized so that there will be a random orientation of many crystals to ensure that some of the particles will be oriented in the X-ray beam to satisfy the diffraction

[7]William Henry Bragg (1862–1942). English physicist who worked on X-ray crystallography.

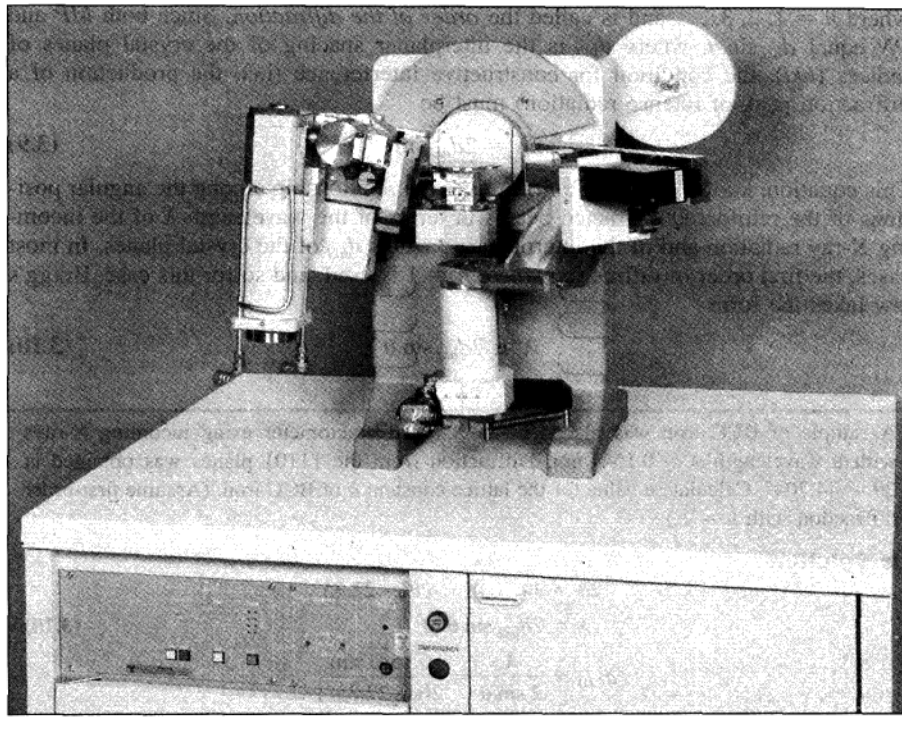

Figure 3.26
An X-ray diffractometer (with X-radiation shields removed).
(*Courtesy of Rigaku.*)

conditions of Bragg's law. Modern X-ray crystal analysis uses an X-ray diffractometer that has a radiation counter to detect the angle and intensity of the diffracted beam (Fig. 3.26). A recorder automatically plots the intensity of the diffracted beam as the counter moves on a goniometer[8] circle (Fig. 3.27) that is in synchronization with the specimen over a range of 2θ values. Figure 3.28 shows an X-ray diffraction recorder chart for the intensity of the diffracted beam versus the diffraction angles 2θ for a powdered pure-metal specimen. In this way, both the angles of the diffracted beams and their intensities can be recorded at one time. Sometimes a powder camera with an enclosed filmstrip is used instead of the diffractometer, but this method is much slower and in most cases less convenient.

Diffraction Conditions for Cubic Unit Cells X-ray diffraction techniques enable the structures of crystalline solids to be determined. The interpretation of X-ray

[8]A goniometer is an instrument for measuring angles.

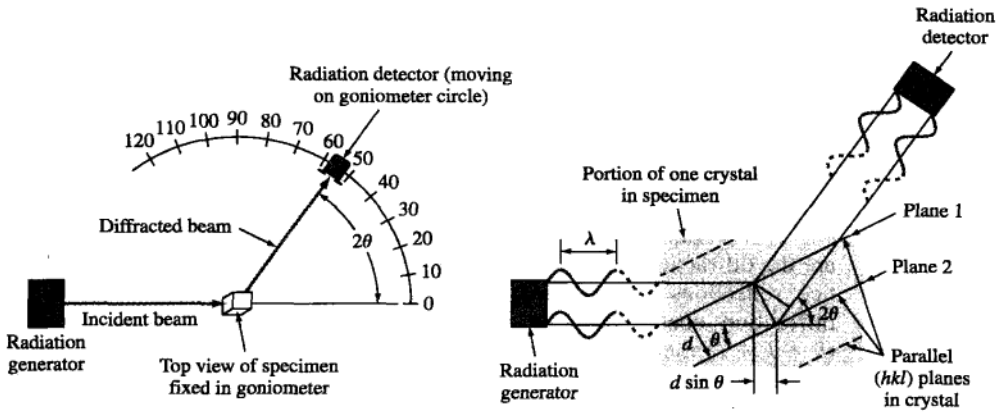

Figure 3.27
Schematic illustration of the diffractometer method of crystal analysis and of the conditions necessary for diffraction.
(From A.G. Guy, Essentials of Materials Science, McGraw-Hill, 1976.)

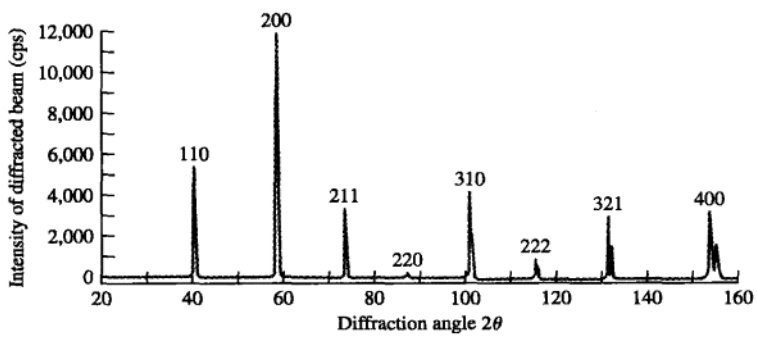

Figure 3.28
Record of the diffraction angles for a tungsten sample obtained by the use of a diffractometer with copper radiation.
(From p. 208 in A.G. Guy and J.J. Hren, Elements of Physical Metallurgy 3rd ed., Addison-Wesley, 1974.)

diffraction data for most crystalline substances is complex and beyond the scope of this book, and so only the simple case of diffraction in pure cubic metals will be considered. The analysis of X-ray diffraction data for cubic unit cells can be simplified by combining Eq. 3.4,

$$d_{hkl} = \frac{a}{\sqrt{h^2 + k^2 + l^2}}$$

with the Bragg equation $\lambda = 2d \sin\theta$, giving

$$\lambda = \frac{2a \sin\theta}{\sqrt{h^2 + k^2 + l^2}} \tag{3.11}$$

This equation can be used along with X-ray diffraction data to determine if a cubic crystal structure is body-centered or face-centered cubic. The rest of this subsection will describe how this is done.

To use Eq. 3.11 for diffraction analysis, we must know which crystal planes are the diffracting planes for each type of crystal structure. For the simple cubic lattice, reflections from all (*hkl*) planes are possible. However, for the BCC structure, diffraction occurs only on planes whose Miller indices when added together $(h + k + l)$ total to an even number (Table 3.6). Thus, for the BCC crystal structure, the principal diffracting planes are {110}, {200}, {211}, etc., which are listed in Table 3.7. In the case of the FCC crystal structure, the principal diffracting planes are those whose Miller indices are either all even or all odd (zero is considered even). Thus, for the FCC crystal structure, the diffracting planes are {111}, {200}, {220}, etc., which are listed in Table 3.7.

Interpreting Experimental X-Ray Diffraction Data for Metals with Cubic Crystal Structures We can use X-ray diffractometer data to determine crystal structures. A simple case to illustrate how this analysis can be used is to distinguish between the

Table 3.6 Rules for determining the diffracting {*hkl*} planes in cubic crystals

Bravais lattice	Reflections present	Reflections absent
BCC	$(h + k + l)$ = even	$(h + k + l)$ = odd
FCC	(h, k, l) all odd or all even	(h, k, l) not all odd or all even

Table 3.7 Miller indices of the diffracting planes for BCC and FCC lattices

Cubic planes {*hkl*}	$h^2 + k^2 + l^2$	Sum $\Sigma[h^2 + k^2 + l^2]$	Cubic diffracting planes {*hkl*}	
			FCC	BCC
{100}	$1^2 + 0^2 + 0^2$	1		
{110}	$1^2 + 1^2 + 0^2$	2	...	110
{111}	$1^2 + 1^2 + 1^2$	3	111	
{200}	$2^2 + 0^2 + 0^2$	4	200	200
{210}	$2^2 + 1^2 + 0^2$	5		
{211}	$2^2 + 1^2 + 1^2$	6	...	211
...		7		
{220}	$2^2 + 2^2 + 0^2$	8	220	220
{221}	$2^2 + 2^2 + 1^2$	9		
{310}	$3^2 + 1^2 + 0^2$	10	...	310

BCC and FCC crystal structures of a cubic metal. Let us assume that we have a metal with either a BCC or an FCC crystal structure and that we can identify the principal diffracting planes and their corresponding 2θ values, as indicated for the metal tungsten in Fig. 3.3.

By squaring both sides of Eq. 3.11 and solving for $\sin^2\theta$, we obtain

$$\sin^2\theta = \frac{\lambda^2(h^2 + k^2 + l^2)}{4a^2} \tag{3.12}$$

From X-ray diffraction data, we can obtain experimental values of 2θ for a series of principal diffracting $\{hkl\}$ planes. Since the wavelength of the incoming radiation and the lattice constant a are both constants, we can eliminate these quantities by forming the ratio of two $\sin^2\theta$ values as

$$\frac{\sin^2\theta_A}{\sin^2\theta_B} = \frac{h_A^2 + k_A^2 + l_A^2}{h_B^2 + k_B^2 + l_B^2} \tag{3.13}$$

where θ_A and θ_B are two diffracting angles associated with the principal diffracting planes $\{h_Ak_Al_A\}$ and $\{h_Bk_Bl_B\}$, respectively.

Using Eq. 3.13 and the Miller indices of the first two sets of principal diffracting planes listed in Table 3.7 for BCC and FCC crystal structures, we can determine values for the $\sin^2\theta$ ratios for both BCC and FCC structures.

For the BCC crystal structure, the first two sets of principal diffracting planes are the {110} and {200} planes (Table 3.7). Substitution of the Miller $\{hkl\}$ indices of these planes into Eq. 3.13 gives

$$\frac{\sin^2\theta_A}{\sin^2\theta_B} = \frac{1^2 + 1^2 + 0^2}{2^2 + 0^2 + 0^2} = 0.5 \tag{3.14}$$

Thus, if the crystal structure of the unknown cubic metal is BCC, the ratio of the $\sin^2\theta$ values that correspond to the first two principal diffracting planes will be 0.5.

For the FCC crystal structure the first two sets of principal diffracting planes are the {111} and {200} planes (Table 3.7). Substitution of the Miller $\{hkl\}$ indices of these planes into Eq. 3.13 gives

$$\frac{\sin^2\theta_A}{\sin^2\theta_B} = \frac{1^2 + 1^2 + 1^2}{2^2 + 0^2 + 0^2} = 0.75 \tag{3.15}$$

Thus, if the crystal structure of the unknown cubic metal is FCC, the ratio of the $\sin^2\theta$ values that correspond to the first two principal diffracting planes will be 0.75.

Example Problem 3.16 uses Eq. 3.13 and experimental X-ray diffraction data for the 2θ values for the principal diffracting planes to determine whether an unknown cubic metal is BCC or FCC. X-ray diffraction analysis is usually much more complicated than Example Problem 3.16, but the principles used are the same. Both experimental and theoretical X-ray diffraction analysis has been and continues to be used for the determination of the crystal structure of materials.

EXAMPLE PROBLEM 3.16

An X-ray diffractometer recorder chart for an element that has either the BCC or the FCC crystal structure shows diffraction peaks at the following 2θ angles: 40, 58, 73, 86.8, 100.4, and 114.7. The wavelength of the incoming X-ray used was 0.154 nm.

a. Determine the cubic structure of the element.
b. Determine the lattice constant of the element.
c. Identify the element.

■ Solution

a. *Determination of the crystal structure of the element.* First, the $\sin^2\theta$ values are calculated from the 2θ diffraction angles.

2θ(deg)	θ(deg)	$\sin\theta$	$\sin^2\theta$
40	20	0.3420	0.1170
58	29	0.4848	0.2350
73	36.5	0.5948	0.3538
86.8	43.4	0.6871	0.4721
100.4	50.2	0.7683	0.5903
114.7	57.35	0.8420	0.7090

Next, the ratio of the $\sin^2\theta$ values of the first and second angles is calculated:

$$\frac{\sin^2\theta}{\sin^2\theta} = \frac{0.117}{0.235} = 0.498 \approx 0.5$$

The crystal structure is BCC since this ratio is ≈ 0.5. If the ratio had been ≈ 0.75, the structure would have been FCC.

b. *Determination of the lattice constant.* Rearranging Eq. 3.12 and solving for a^2 gives

$$a^2 = \frac{\lambda^2}{4}\frac{h^2 + k^2 + l^2}{\sin^2\theta} \tag{3.16}$$

or

$$a = \frac{\lambda}{2}\sqrt{\frac{h^2 + k^2 + l^2}{\sin^2\theta}} \tag{3.17}$$

Substituting into Eq. 3.17 $h = 1$, $k = 1$, and $l = 0$ for the h, k, l Miller indices of the first set of principal diffracting planes for the BCC crystal structure, which are the {110} planes, the corresponding value for $\sin^2\theta$, which is 0.117, and 0.154 nm for λ, the incoming radiation, gives

$$a = \frac{0.154\text{ nm}}{2}\sqrt{\frac{1^2 + 1^2 + 0^2}{0.117}} = 0.318\text{ nm} \blacktriangleleft$$

c. *Identification of the element.* The element is tungsten since this element has a lattice constant of 0.316 nm and is BCC.

3.12 AMORPHOUS MATERIALS

As discussed previously, some materials are called amorphous or noncrystalline because they lack long-range order in their atomic structure. It should be noted that in general materials have a tendency to achieve a crystalline state because that is the most stable state and corresponds to the lowest energy level. However, atoms in amorphous materials are bonded in a disordered manner because of factors that inhibit the formation of a periodic arrangement. Atoms in amorphous materials, therefore, occupy random spatial positions as opposed to specific positions in crystalline solids. For clarity, various degrees of order (or disorder) are shown in Fig. 3.29.

Most polymers, glasses, and some metals are members of the amorphous class of materials. In polymers, the secondary bonds among molecules do not allow for the formation of parallel and tightly packed chains during solidification. As a result, polymers such as polyvinylchloride consist of long, twisted molecular chains that are entangled to form a solid with amorphous structure, similar to Fig. 3.32*c*. In some polymers such as polyethylene, the molecules are more efficiently and tightly packed in some regions of the material and produce a higher degree of regional long-range order. As a result, these polymers are often classified as *semicrystalline.* A more detailed discussion of semicrystalline polymers will be given in Chap. 10.

Inorganic glass based on glass-forming oxide, silica (SiO_2), is generally characterized as a ceramic material (ceramic glass) and is another example of a material with an amorphous structure. In this type of glass, the fundamental subunit in the molecules is the SiO_4^{4-} tetrahedron. The ideal crystalline structure of this glass is shown in Fig. 3.29*a*. The schematic shows the Si–O tetrahedrons joined corner to corner to form long-range order. In its viscous liquid state, the molecules have limited mobility, and, in general, crystallization occurs slowly. Therefore, a modest cooling rate suppresses the formation of the crystal structure and instead the tetrahedra join corner to corner to form a network lacking in long-range order (Fig. 3.29*b*).

In addition to polymers and glasses, some metals also have the ability to form amorphous structures (*metallic glass*) under strict and often difficult to achieve conditions. Unlike glasses, metals have very small and mobile building blocks under molten

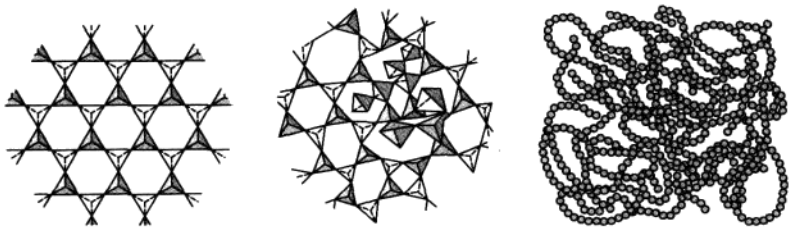

Figure 3.29
A schematic showing various degrees of order in materials: (*a*) long-range order in crystalline silica, (*b*) silica glass without long-range order, and (*c*) amorphous structure in polymers.

conditions. As a result, it is difficult to prevent metals from crystallizing. However, alloys such as 78%Fe–9%Si–13%B that contain a high percentage of semimetals, Si and B, may form metallic glasses through rapid solidification at cooling rates in excess of 10^8 °C/s. At such high cooling rates, the atoms simply do not have enough time to form a crystalline structure and instead form a metal with an amorphous structure, that is, they are highly disordered. In theory, any crystalline material can form a noncrystalline structure if solidified rapidly enough from a molten state.

Amorphous materials, because of their structure, possess properties that are superior. For instance, metallic glasses possess higher strength, better corrosion characteristics, and magnetic properties when compared to their crystalline counterparts. Finally, it is important to note that amorphous materials do not show sharp diffraction patterns when analyzed using X-ray diffraction techniques. This is due to a lack of order and periodicity in the atomic structure. In future chapters, the role of structure of the material on its properties will be explained in detail.

3.13 SUMMARY

Atomic arrangements in crystalline solids can be described by a network of lines called a *space lattice.* Each space lattice can be described by specifying the atom positions in a repeating *unit cell.* The crystal structure consists of space lattice and *motif* or *basis.* Crystalline materials possess long-range atomic order such as most metals. But some materials such as many polymers and glasses possess only short-range order. Such materials are called semicrystalline or amorphous. There are seven crystal systems based on the geometry of the axial lengths and interaxial angles of the unit cells. These seven systems have a total of 14 sublattices (unit cells) based on the internal arrangements of atomic sites within the unit cells.

In metals, the most common crystal structure unit cells are: *body-centered cubic* (BCC), *face-centered cubic* (FCC), and *hexagonal close-packed* (HCP) (which is a dense variation of the simple hexagonal structure).

Crystal directions in cubic crystals are the vector components of the directions resolved along each of the component axes and reduced to smallest integers. They are indicated as [*uvw*]. Families of directions are indexed by the direction indices enclosed by pointed brackets as ⟨*uvw*⟩. *Crystal planes* in cubic crystals are indexed by the reciprocals of the axial intercepts of the plane (followed by the elimination of fractions) as (*hkl*). Cubic crystal planes of a form (family) are indexed with braces as {*hkl*}. Crystal planes in hexagonal crystals are commonly indexed by four indices *h*, *k*, *i*, and *l* enclosed in parentheses as (*hkil*). These indices are the reciprocals of the intercepts of the plane on the a_1, a_2, a_3, and *c* axes of the hexagonal crystal structure unit cell. Crystal directions in hexagonal crystals are the vector components of the direction resolved along each of the four coordinate axes and reduced to smallest integers as [*uvtw*].

Using the hard-sphere model for atoms, calculations can be made for the volume, planar, and linear density of atoms in unit cells. Planes in which atoms are packed as tightly as possible are called *close-packed planes,* and directions in which atoms are in closest contact are called *close-packed directions.* Atomic packing factors for different crystal structures can also be determined by assuming the hard-sphere atomic model. Some metals have different crystal structures at different ranges of temperature and pressure, a phenomenon called *polymorphism.*

Crystal structures of crystalline solids can be determined by using X-ray diffraction analysis techniques. X-rays are diffracted in crystals when the *Bragg's law* ($n\lambda = 2d \sin\theta$) conditions are satisfied. By using the X-ray diffractometer and the *powder method*, the crystal structure of many crystalline solids can be determined.

3.14 DEFINITIONS

Sec. 3.1

Amorphous: lacking in long range atomic order.

Crystal: a solid composed of atoms, ions, or molecules arranged in a pattern that is repeated in three dimensions.

Crystal structure: a regular three-dimensional pattern of atoms or ions in space.

Space lattice: a three-dimensional array of points each of which has identical surroundings.

Lattice point: one point in an array in which all the points have identical surroundings.

Unit cell: a convenient repeating unit of a space lattice. The axial lengths and axial angles are the lattice constants of the unit cell.

Motif: a group of atoms that or (basis) are organized relative to each other and are associated with corresponding lattice points.

Sec. 3.3

Body-centered cubic (BCC) unit cell: a unit cell with an atomic packing arrangement in which one atom is in contact with eight identical atoms located at the corners of an imaginary cube.

Face-centered cubic (FCC) unit cell: a unit cell with an atomic packing arrangement in which 12 atoms surround a central atom. The stacking sequence of layers of close-packed planes in the FCC crystal structure is *ABCABC*. . . .

Hexagonal close-packed (HCP) unit cell: a unit cell with an atomic packing arrangement in which 12 atoms surround a central identical atom. The stacking sequence of layers of close-packed planes in the HCP crystal structure is *ABABAB*. . . .

Atomic packing factor (APF): the volume of atoms in a selected unit cell divided by the volume of the unit cell.

Sec. 3.5

Indices of direction in a cubic crystal: a direction in a cubic unit cell is indicated by a vector drawn from the origin at one point in a unit cell through the surface of the unit cell; the position coordinates (x, y, and z) of the vector where it leaves the surface of the unit cell (with fractions cleared) are the indices of direction. These indices, designated u, v, and w are enclosed in brackets as $[uvw]$. Negative indices are indicated by a bar over the index.

Sec. 3.6

Indices for cubic crystal planes (Miller indices): the reciprocals of the intercepts (with fractions cleared) of a crystal plane with the x, y, and z axes of a unit cube are called the Miller indices of that plane. They are designated h, k, and l for the x, y, and z axes, respectively, and are enclosed in parentheses as (hkl). Note that the selected crystal plane must *not* pass through the origin of the x, y, and z axes.

Sec. 3.9

Volume density ρ_v: mass per unit volume; this quantity is usually expressed in Mg/m^3 or g/cm^3.

Planar density ρ_p: the equivalent number of atoms whose centers are intersected by a selected area divided by the selected area.

Linear density ρ_l: the number of atoms whose centers lie on a specific direction on a specific length of line in a unit cube.

Sec. 3.10

Polymorphism (as pertains to metals): the ability of a metal to exist in two or more crystal structures. For example, iron can have a BCC or an FCC crystal structure, depending on the temperature.

Sec. 3.12

Semicrystalline: materials with regions of crystalline structure dispersed in the surrounding, amorphous region, for instance, some polymers.

Metallic glass: metals with an amorphous atomic structure.

3.15 PROBLEMS

Answers to problems marked with an asterisk are given at the end of the book.

Knowledge and Comprehension Problems

3.1 Define the following terms: (*a*) crystalline solid, (*b*) long-range order, (*c*) short-range order, and (*d*) amorphous.

3.2 Define the following terms: (*a*) crystal structure, (*b*) space lattice, (*c*) lattice point, (*d*) unit cell, (*e*) motif, and (*f*) lattice constants.

3.3 What are the 14 Bravais unit cells?

3.4 What are the three most common metal crystal structures? List five metals that have each of these crystal structures.

3.5 For a BCC unit cell, (*a*) how many atoms are there inside the unit cell, (*b*) what is the coordination number for the atoms, (*c*) what is the relationship between the length of the side *a* of the BCC unit cell and the radius of its atoms, and (*d*) what is the atomic packing factor?

3.6 For an FCC unit cell, (*a*) how many atoms are there inside the unit cell, (*b*) what is the coordination number for the atoms, (*c*) what is the relationship between the length of the side *a* of the FCC unit cell and the radius of its atoms, and (*d*) what is the atomic packing factor?

3.7 For an HCP unit cell (consider the primitive cell), (*a*) how many atoms are there inside the unit cell, (*b*) what is the coordination number for the atoms, (*c*) what is the atomic packing factor, (*d*) what is the ideal *c/a* ratio for HCP metals, and (*e*) repeat a through c considering the "larger" cell.

3.8 How are atomic positions located in cubic unit cells?

***3.9** List the atom positions for the eight corner and six face-centered atoms of the FCC unit cell.

3.10 How are the indices for a crystallographic direction in a cubic unit cell determined?

3.11 What are the crystallographic directions of a family or form? What generalized notation is used to indicate them?

3.12 How are the Miller indices for a crystallographic plane in a cubic unit cell determined? What generalized notation is used to indicate them?

3.13 What is the notation used to indicate a family or form of cubic crystallographic planes?

3.14 How are crystallographic planes indicated in HCP unit cells?

3.15 What notation is used to describe HCP crystal planes?

3.16 What is the difference in the stacking arrangement of close-packed planes in (*a*) the HCP crystal structure and (*b*) the FCC crystal structure?

3.17 What are the closest-packed directions in (*a*) the BCC structure, (*b*) the FCC structure, and (*c*) the HCP structure?

3.18 Identify the close-packed planes in (*a*) the BCC structure, (*b*) the FCC structure, and (*c*) the HCP structure?

3.19 What is polymorphism with respect to metals?

3.20 What are X-rays, and how are they produced?

3.21 Draw a schematic diagram of an X-ray tube used for X-ray diffraction, and indicate on it the path of the electrons and X-rays.

3.22 What is the characteristic X-ray radiation? What is its origin?

3.23 Distinguish between destructive interference and constructive interference of reflected X-ray beams through crystals.

Tutorial

Application and Analysis Problems

3.24 Molybdenum at 20°C is BCC and has an atomic radius of 0.140 nm. Calculate a value for its lattice constant a in nanometers.

3.25 Lithium at 20°C is BCC and has a lattice constant of 0.35092 nm. Calculate a value for the atomic radius of a lithium atom in nanometers.

3.26 Gold is FCC and has a lattice constant of 0.40788 nm. Calculate a value for the atomic radius of a gold atom in nanometers.

3.27 Palladium is FCC and has an atomic radius of 0.137 nm. Calculate a value for its lattice constant a in nanometers.

3.28 Verify that the atomic packing factor for the FCC structure is 0.74.

***3.29** Calculate the volume in cubic nanometers of the titanium crystal structure unit cell (use the larger cell). Titanium is HCP at 20°C with $a = 0.29504$ nm and $c = 0.46833$ nm.

3.30 Consider a 0.05-mm thick, 500 mm^2 (about three times the area of a dime) piece of aluminum foil. How many units cells exist in the foil? If the density of aluminum is 2.7 g/cm^3, what is the mass of each cell?

3.31 Draw the following directions in a BCC unit cell, and list the position coordinates of the atoms whose centers are intersected by the direction vector:
(*a*) [100] (*b*) [110] (*c*) [111]

3.32 Draw direction vectors in unit cells for the following cubic directions:
(*a*) $[1\bar{1}\bar{1}]$ (*b*) $[1\bar{1}0]$ (*c*) $[\bar{1}2\bar{1}]$ (*d*) $[\bar{1}\bar{1}3]$

3.33 Draw direction vectors in unit cells for the following cubic directions:
(*a*) $[1\bar{1}\bar{2}]$ (*c*) $[\bar{3}31]$ (*e*) $[2\bar{1}2]$ (*g*) $[\bar{1}01]$ (*i*) [321] (*k*) $[1\bar{2}\bar{2}]$
(*b*) $[1\bar{2}3]$ (*d*) $[0\bar{2}1]$ (*f*) $[2\bar{3}3]$ (*h*) $[12\bar{1}]$ (*j*) $[10\bar{3}]$ (*l*) $[\bar{2}\bar{2}3]$

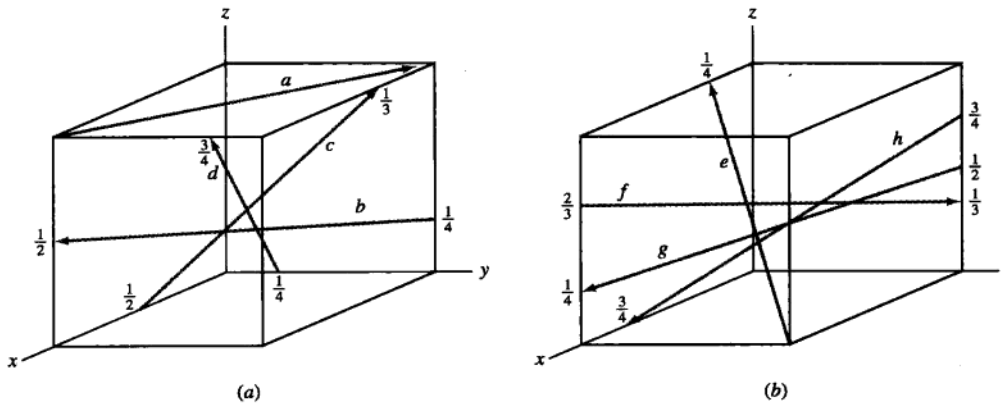

(a) (b)

Figure P3.34

3.34 What are the indices of the directions shown in the unit cubes of Fig. P3.34?

***3.35** A direction vector passes through a unit cube from the $(\frac{3}{4}, 0, \frac{1}{4})$ to the $(\frac{1}{2}, 1, 0)$ positions. What are its direction indices?

3.36 A direction vector passes through a unit cube from the $(1, 0, \frac{3}{4})$ to the $(\frac{1}{4}, 1, \frac{1}{4})$ positions. What are its direction indices?

***3.37** What are the directions of the $\langle 10\bar{3} \rangle$ family or form for a unit cube?

3.38 What are the directions of the $\langle 111 \rangle$ family or form for a unit cube?

3.39 What $\langle 110 \rangle$ type directions lie on the (111) plane of a cubic unit cell?

3.40 What $\langle 111 \rangle$ type directions lie on the (110) plane of a cubic unit cell?

3.41 Draw in unit cubes the crystal planes that have the following Miller indices:
(*a*) $(1\bar{1}\bar{1})$ (*c*) $(12\bar{1})$ (*e*) $(3\bar{2}1)$ (*g*) $(20\bar{1})$ (*i*) $(\bar{2}32)$ (*k*) $(3\bar{1}2)$
(*b*) $(10\bar{2})$ (*d*) $(21\bar{3})$ (*f*) $(30\bar{2})$ (*h*) $(\bar{2}1\bar{2})$ (*j*) $(13\bar{3})$ (*l*) $(\bar{3}3\bar{1})$

***3.42** What are the Miller indices of the cubic cyrsyallographic planes shown in Fig. P3.42?

3.43 What are the {100} family of planes of the cubic system?

3.44 Draw the following crystallographic planes in a BCC unit cell, and list the position of the atoms whose centers are intersected by each of the planes:
(*a*) (100) (*b*) (110) (*c*) (111)

Tutorial
MatVis

3.45 Draw the following crystallographic planes in an FCC unit cell, and list the position coordinates of the atoms whose centers are intersected by each of the planes:
(*a*) (100) (*b*) (110) (*c*) (111)

3.46 A cubic plane has the following axial intercepts: $a = \frac{1}{3}, b = -\frac{2}{3}, c = \frac{1}{2}$. What are the Miller indices of this plane?

3.47 A cubic plane has the following axial intercepts: $a = -\frac{1}{2}, b = -\frac{1}{2}, c = \frac{2}{3}$. What are the Miller indices of this plane?

***3.48** A cubic plane has the following axial intercepts:$a = 1, b = \frac{2}{3}, c = -\frac{1}{2}$. What are the Miller indices of this plane?

3.49 Determine the Miller indices of the cubic crystal plane that intersects the following position coordinates: $(1, 0, 0);(1, \frac{1}{2}, \frac{1}{4});(\frac{1}{2}, \frac{1}{2}, 0)$.

3.50 Determine the Miller indices of the cubic crystal plane that intersects the following position coordinates: $(\frac{1}{2}, 0, \frac{1}{2});(0, 0, 1);(1, 1, 1)$.

3.51 Determine the Miller indices of the cubic crystal plane that intersects the following position coordinates: $(1, \frac{1}{2}, 1);(\frac{1}{2}, 0, \frac{3}{4});(1, 0, \frac{1}{2})$.

3.52 Determine the Miller indices of the cubic crystal plane that intersects the following position coordinates: $(0, 0, \frac{1}{2});(1, 0, 0);(\frac{1}{2}, \frac{1}{4}, 0)$.

3.53 Rodium is FCC and has a lattice constant a of 0.38044 nm. Calculate the following interplanar spacings:

(*a*) d_{111} (*b*) d_{200} (*c*) d_{220}

***3.54** Tungsten is BCC and has a lattice constant a of 0.31648 nm. Calculate the following interplanar spacings:

(*a*) d_{110} (*b*) d_{220} (*c*) d_{310}

3.55 The d_{310} interplanar spacing in a BCC element is 0.1587 nm. (*a*) What is its lattice constant a? (*b*) What is the atomic radius of the element? (*c*) What could this element be?

***3.56** The d_{422} interplanar spacing in an FCC metal is 0.083397 nm. (*a*) What is its lattice constant a? (*b*) What is the atomic radius of the metal? (*c*) What could this metal be?

3.57 Draw the hexagonal crystal planes whose Miller-Bravais indices are:

(*a*) $(10\bar{1}1)$ (*d*) $(1\bar{2}12)$ (*g*) $(\bar{1}2\bar{1}2)$ (*j*) $(\bar{1}100)$

(*b*) $(01\bar{1}1)$ (*e*) $(2\bar{1}\bar{1}1)$ (*h*) $(2\bar{2}00)$ (*k*) $(\bar{2}111)$

(*c*) $(\bar{1}2\bar{1}0)$ (*f*) $(1\bar{1}01)$ (*i*) $(10\bar{1}2)$ (*l*) $(\bar{1}012)$

***3.58** Determine the Miller-Bravais indices of the hexagonal crystal planes in Fig. P3.58.

3.59 Determine the Miller-Bravais direction indices of the $-a_1$, $-a_2$, and $-a_3$ directions.

MatVis

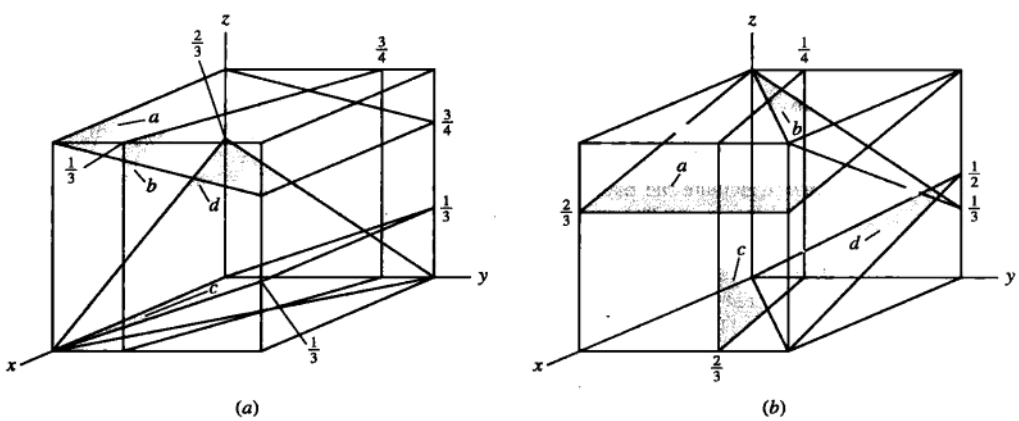

Figure P3.42

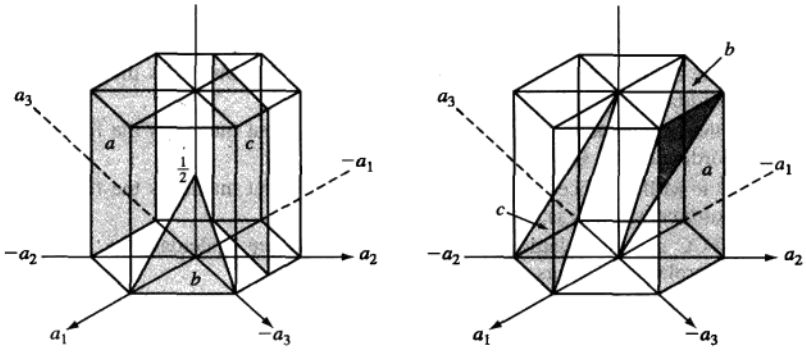

Figure P3.58

3.60 Determine the Miller-Bravais direction indices of the vectors originating at the center of the lower basal plane and ending at the endpoints of the upper basal plane as indicated in Fig. 3.16*d*.

3.61 Determine the Miller-Bravais direction indices of the basal plane of the vectors originating at the center of the lower basal plane and exiting at the midpoints between the principal planar axes.

***3.62** Determine the Miller-Bravais direction indices of the directions indicated in Fig. P3.62.

3.63 The lattice constant for BCC tantalum at 20°C is 0.33026 nm and its density is 16.6 g/cm^3. Calculate a value for its relative atomic mass.

3.64 Calculate a value for the density of FCC platinum in grams per cubic centimeter from its lattice constant a of 0.39239 nm and its atomic mass of 195.09 g/mol.

3.65 Calculate the planar atomic density in atoms per square millimeter for the following crystal planes in BCC chromium, which has a lattice constant of 0.28846 nm: (*a*) (100), (*b*) (110), (*c*) (111).

***3.66** Calculate the planar atomic density in atoms per square millimeter for the following crystal planes in FCC gold, which has a lattice constant of 0.40788 nm: (*a*) (100), (*b*) (110), (*c*) (111).

3.67 Calculate the planar atomic density in atoms per square millimeter for the (0001) plane in HCP beryllium, which has a lattice constant a = 0.22856 nm and a c constant of 0.35832 nm.

3.68 Calculate the linear atomic density in atoms per millimeter for the following directions in BCC vanadium, which has a lattice constant of 0.3039 nm: (*a*) [100], (*b*) [110], (*c*) [111].

***3.69** Calculate the linear atomic density in atoms per millimeter for the following directions in FCC iridium, which has a lattice constant of 0.38389 nm: (*a*) [100], (*b*) [110], (*c*) [111].

3.70 Titanium goes through a polymorphic change from BCC to HCP crystal structure upon cooling through 332°C. Calculate the percentage change in volume when the

crystal structure changes from BCC to HCP. The lattice constant a of the BCC unit cell at 882°C is 0.332 nm, and the HCP unit cell has $a = 0.2950$ nm and $c = 0.4683$ nm.

3.71 Pure iron goes through a polymorphic change from BCC to FCC upon heating through 912°C. Calculate the volume change associated with the change in crystal structure from BCC to FCC if at 912°C the BCC unit cell has a lattice constant $a = 0.293$ nm and the FCC unit cell $a = 0.363$ nm.

3.72 Derive Bragg's law by using the simple case of incident X-ray beams being diffracted by parallel planes in a crystal.

3.73 A sample of BCC metal was placed in an X-ray diffractometer using X-rays with a wavelength of $\lambda = 0.1541$ nm. Diffraction from the {221} planes was obtained at $2\theta = 88.838°$. Calculate a value for the lattice constant a for this BCC elemental metal. (Assume first-order diffraction, $n = 1$.)

3.74 X-rays of an unknown wavelength are diffracted by a gold sample. The 2θ angle was 64.582° for the {220} planes. What is the wavelength of the X-rays used? (The lattice constant of gold = 0.40788 nm; assume first-order diffraction, $n = 1$.)

3.75 An X-ray diffractometer recorder chart for an element that has either the BCC or the FCC crystal structure showed diffraction peaks at the following 2θ angles: 41.069°, 47.782°, 69.879°, and 84.396°. The wavelength of the incoming radiation was 0.15405 nm. (X-ray diffraction data courtesy of the International Centre for Diffraction Data.)

(*a*) Determine the crystal structure of the element.

(*b*) Determine the lattice constant of the element.

(*c*) Identify the element.

***3.76** An X-ray diffractometer recorder chart for an element that has either the BCC or the FCC crystal structure showed diffraction peaks at the following 2θ angles: 38.60°, 55.71°, 69.70°, 82.55°, 95.00°, and 107.67°. Wavelength λ of the incoming radiation was 0.15405 nm.

(*a*) Determine the crystal structure of the element.

(*b*) Determine the lattice constant of the element.

(*c*) Identify the element.

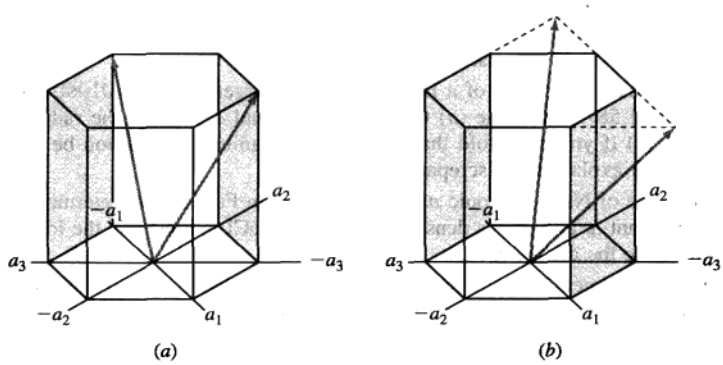

Figure P3.62

3.77 An X-ray diffractometer recorder chart for an element that has either the BCC or the FCC crystal structure showed diffraction peaks at the following 2θ angles: 36.191°, 51.974°, 64.982°, and 76.663°. The wavelength of the incoming radiation was 0.15405 nm.

(*a*) Determine the crystal structure of the element.

(*b*) Determine the lattice constant of the element.

(*c*) Identify the element.

3.78 An X-ray diffractometer recorder chart for an element that has either the BCC or the FCC crystal structure showed diffraction peaks at the following 2θ angles: 40.663°, 47.314°, 69.144°, and 83.448°. Wavelength λ of the incoming radiation was 0.15405 nm.

(*a*) Determine the crystal structure of the element.

(*b*) Determine the lattice constant of the element.

(*c*) Identify the element.

Synthesis and Evaluation Problems

3.79 Do you expect iron and silver to have the same (*a*) atomic packing factor, (*b*) volume of unit cell, (*c*) number of atoms per unit cell, and (*d*) coordination number?

3.80 Do you expect gold and silver to have the same (*a*) atomic packing factor, (*b*) volume of unit cell, (*c*) number of atoms per unit cell, and (*d*) coordination number? Verify your answers.

3.81 Do you expect titanium and silver to have the same (*a*) atomic packing factor, (*b*) volume of unit cell, (*c*) number of atoms per unit cell, and (*d*) coordination number? Verify your answers.

***3.82** Show using geometry that the ideal c/a ration of the hexagonal close-packed unit cell (when atoms are perfect spheres) is 1.633. Hint: draw the center atom in the top basal plane in contact with the three atoms in the center of the HCP cell; connect the centers of the three atoms inside the HCP cell to each other and to the atom at the center of one of the basal planes.

3.83 Assuming that the volume of a HCP metal cell (larger cell) is 0.09130 nm^3 and the *c/a* ratio is 1.856, determine (*a*) the values for *c* and *a*, and (*b*) the radius, R, of the atom. (*c*) If you were told that the metal is titanium, would you be surprised? How do you explain the discrepancy?

***3.84** Assuming that the volume of a HCP metal cell (larger cell) is 0.01060 nm^3 and the *c/a* ratio is 1.587, determine (*a*) the values for *c* and *a*, and (*b*) the radius, R, of the atom. (*c*) If you were told that the metal is titanium, would you be surprised? How do you explain the discrepancy?

3.85 The structure of NaCl (an ionic material) is given in Fig. 2.18b. Determine (*a*) its lattice constant *a*, and (*b*) its density. Hint: since NaCl is ionic use the ion radius data and note the atomic radii.

3.86 The unit cell structure of the ionic solid, CsI, is similar to that in Fig. 2.18*a*. Determine (*a*) its packing factor, and (*b*) compare this packing factor with that of BCC metals. Explain the difference, if any.

3.87 Iron (below 912°C) and tungsten are both BCC with significantly different atomic radii. However, they have the same atomic packing factor of 0.68. How do you explain this?

3.88 Verify that there are eight atoms inside a diamond cubic structure (see Fig. 2.23 *b* and *c*). Draw a 3D schematic of the atoms inside the cell.

***3.89** The lattice constant for the diamond cubic structure of diamond is 0.357 nm. Diamond is metastable, meaning that it will transform to graphite at elevated temperatures. If this transformation occurs, what % volume change will occur? (Density of graphite is 2.25 gr/cm^3)

3.90 Calculate the center-to-center distance between adjacent atoms of gold along the following directions: (*a*) [100], (*b*) [101], (*c*) [111], and (*d*) [102]. Speculate as to why such information may be important in understanding the behavior of the material.

***3.91** Calculate the center-to-center distance between adjacent atoms of tungsten along the following directions: (*a*) [100], (*b*) [101], (*c*) [111], and (*d*) [102]. Speculate as to why such information may be important in understanding the behavior of the material.

3.92 A plane in a cubic crystal intersects the x axis at 0.25, the y axis at 2, and is parallel to the z axis. What are the miller indices for this plane? Draw this plane in a single cube and show all key dimensions.

3.93 A plane in a cubic crystal intersects the x axis at 3, the y axis at 1, and the z axis at 1. What are the miller indices for this plane? Draw this plane in a single cube and show all key dimensions.

3.94 A plane in a hexagonal crystal intersects at the a_1 axis at -1, the a_2 axis at 1 and the c axis at infinity? What are the Miller indices for this plane? Draw this plane in a hexagonal unit cell and show all key dimensions.

3.95 A plane in a hexagonal crystal intersects at the a_1 axis at 1, the a_2 axis at 1 and the c axis at 0.5? What are the Miller indices for this plane? Draw this plane in a hexagonal unit cell and show all key dimensions.

***3.96** Without drawing any of the hexagonal planes given below, determine which of the planes is, in fact, not a plane. (*a*) $(\bar{1}010)$, (*b*) $(10\bar{1}0)$, and (*c*) $(\bar{1}\bar{1}10)$.

3.97 Name as many carbon allotropes as you can, and discuss their crystal structure.

3.98 A thin layer of aluminum nitride is sometimes deposited on Silicon wafers at high temperatures (1000°C). The coefficient of thermal expansion and the lattice constant of the silicon crystal is different than that of aluminum nitride. Will this cause a problem? Explain.

3.99 An unknown material is being analyzed using X-ray diffraction techniques. However, the diffraction patterns are extremely broad (no clear peaks are visible). (*a*) What does this tell you about the material? (*b*) What are some of the tests that you can perform to help identify the material or narrow the possibilities?

3.100 Explain, in general terms, why many polymers and some ceramic glasses have an amorphous or semicrystalline structure.

3.101 Explain how ultra-rapid cooling of some metal alloys produces metallic glass.

CHAPTER 4

Solidification and Crystalline Imperfections

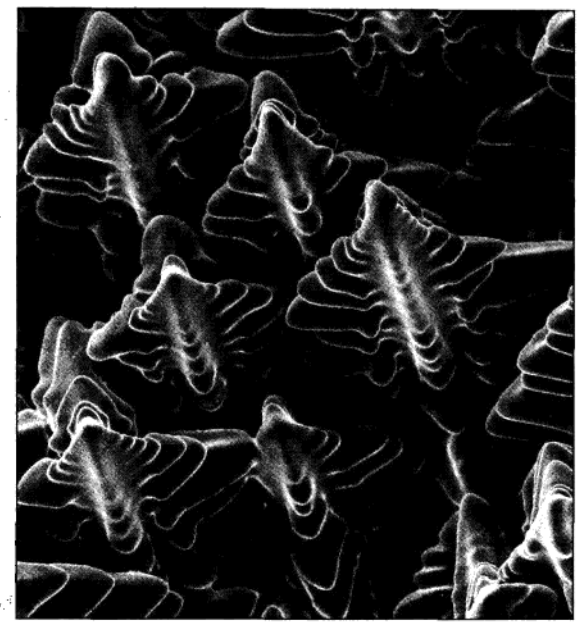

(Photo courtesy of Stan David and Lynn Boatner, Oak Ridge National Library.)

When molten alloys are cast, solidification starts at the walls of the mold as it is being cooled. The solidification of the alloy takes place not at a specific temperature but over a range of temperatures. While the alloy is in this range, it has a pasty form that consists of solid, tree-like structures called *dendrites* (meaning *tree-like*) and liquid metal. The size and shape of the dendrite depends on the cooling rate. The liquid metal existing among these three-dimensional dendritic structures eventually solidifies to form a completely solid structure that we refer to as the grain structure. The study of dendrites is important because they influence compositional variations, porosity, and segregation and therefore the properties of the cast metal. The figure shows the three-dimensional structure of dendrites. The figure shows a "forest" of dendrites formed during the solidification of a nickel-based superalloy.[1] ■

[1]http://mgnews.msfc.nasa.gov/IDGE/IDGE.html

LEARNING OBJECTIVES

By the end of this chapter, students will be able to . . .

1. Describe the process of the solidification of metals, distinguishing between homogeneous and heterogeneous nucleation.
2. Describe the two energies involved in the solidification process of a pure metal, and write the equation for the total free-energy change associated with the transformation of the liquid state to solid nucleus.
3. Distinguish between equiaxed and columnar grains and the advantage of the former over the latter.
4. Distinguish between single crystal and polycrystalline materials, and explain why single crystal and polycrystalline forms of the material have different mechanical properties.
5. Describe various forms of metallic solid solutions and explain the differences between solid solution and mixture alloys.
6. Classify various types of crystalline imperfections, and explain the role of defects on the mechanical and electrical properties of crystalline materials.
7. Determine the ASTM grain size number and average grain size diameter, and describe the importance of grain size and grain boundary density on the behavior of crystalline materials.
8. Learn how and why optical microscopy, SEM, TEM, HRTEM, AFM, and STM techniques are used to understand more about the internal and surface structures of materials at various magnifications.
9. Explain, in general terms, why alloys are preferred materials over pure metals for structural applications.

4.1 SOLIDIFICATION OF METALS

The solidification of metals and alloys is an important industrial process since most metals are melted and then cast into a semifinished or finished shape. Figure 4.1 shows a large, semicontinuously[2] cast aluminum ingot that will be further fabricated into aluminum alloy flat products. It illustrates the large scale on which the casting process (solidification) of metals is sometimes carried out.

In general, the solidification of a metal or alloy can be divided into the following steps:

1. The formation of stable **nuclei** in the melt (nucleation) (Fig. 4.2*a*)
2. The growth of nuclei into crystals (Fig. 4.2*b*) and the formation of a grain structure (Fig. 4.2*c*)

[2]A semicontinuously cast ingot is produced by solidifying molten metal (e.g., aluminum or copper alloys) in a mold that has a movable bottom block (see Fig. 4.8) that is slowly lowered as the metal is solidified. The prefix *semi-* is used since the maximum length of the ingot produced is determined by the depth of the pit into which the bottom block is lowered.

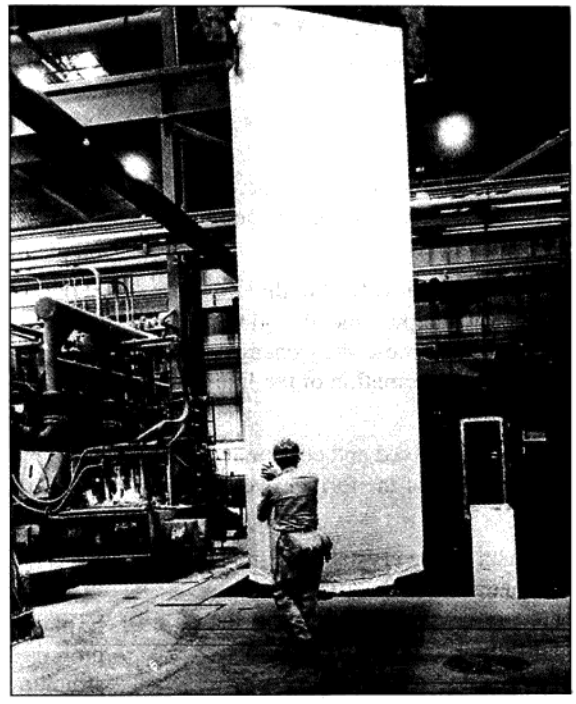

Animation

Figure 4.1
Large, semicontinuously cast aluminum alloy ingot being removed from casting pit. Ingots of this type are subsequently hot- and cold-rolled into plate or sheet.
(*Courtesy of Reynolds Metals Co.*)

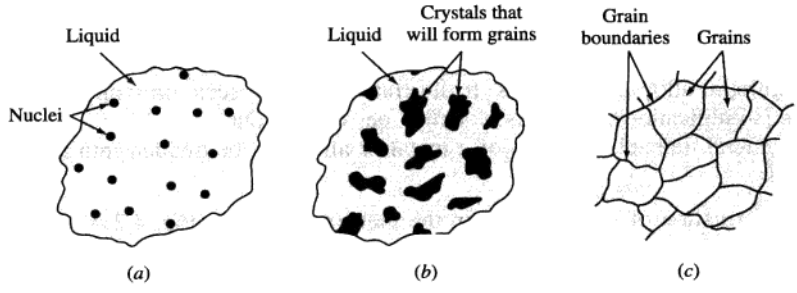

Virtual Lab

Figure 4.2
Schematic illustration showing the several stages in the solidification of metals: (*a*) formation of nuclei, (*b*) growth of nuclei into crystals, and (*c*) joining together of crystals to form grains and associated grain boundaries. Note that the grains are randomly oriented.

Figure 4.3
A grain grouping parted from an arc-cast titanium alloy ingot under the blows of a hammer. The grouping has preserved the true bonding facets of the individual grains of the original cast structure. (Magnification $\frac{1}{6}\times$.)
(After W. Rostoker and J.R. Dvorak, "Interpretation of Metallographic Structures," Academic, 1965, p. 7.)

The shapes of some real grains formed by the solidification of a titanium alloy are shown in Fig. 4.3. The shape that each grain acquires after solidification of the metal depends on many factors, of which thermal gradients are important. The grains shown in Fig. 4.3 are *equiaxed* since their growth is about equal in all directions.

4.1.1 The Formation of Stable Nuclei in Liquid Metals

The two main mechanisms by which the nucleation of solid particles in liquid metal occurs are homogeneous nucleation and heterogeneous nucleation.

Homogeneous Nucleation Homogeneous nucleation is considered first since it is the simplest case of nucleation. **Homogeneous nucleation** in a liquid melt occurs when the metal itself provides the atoms needed to form a nuclei. Let us consider the case of a pure metal solidifying. When a pure liquid metal is cooled below its equilibrium freezing temperature to a sufficient degree, many homogeneous nuclei are created by slow-moving atoms bonding together. Homogeneous nucleation usually requires a considerable amount of undercooling, which may be as much as several hundred degrees Celsius for some metals (see Table 4.1). For a nucleus to be stable so that it can grow into a crystal, it must reach a *critical size.* A cluster of atoms bonded together that is less than the critical size is called an **embryo,** and one that is larger than the critical size is called a *nucleus.* Because of their instability, embryos are continuously being formed and redissolved in the molten metal due to the agitation of the atoms.

Energies Involved in Homogeneous Nucleation In the homogeneous nucleation of a solidifying pure metal, two kinds of energy changes must be considered: (1) the *volume (or bulk) free energy* released by the liquid-to-solid transformation and (2) *the surface energy* required to form the new solid surfaces of the solidified particles.

Table 4.1 Values for the freezing temperature, heat of fusion, surface energy, and maximum undercooling for selected metals

Metal	Freezing temp. °C	Freezing temp. K	Heat of fusion (J/cm^3)	Surface energy (J/cm^2)	Maximum undercooling, observed (ΔT[°C])
Pb	327	600	280	33.3×10^{-7}	80
Al	660	933	1066	93×10^{-7}	130
Ag	962	1235	1097	126×10^{-7}	227
Cu	1083	1356	1826	177×10^{-7}	236
Ni	1453	1726	2660	255×10^{-7}	319
Fe	1535	1808	2098	204×10^{-7}	295
Pt	1772	2045	2160	240×10^{-7}	332

Source: B. Chalmers, "Solidification of Metals," Wiley, 1964.

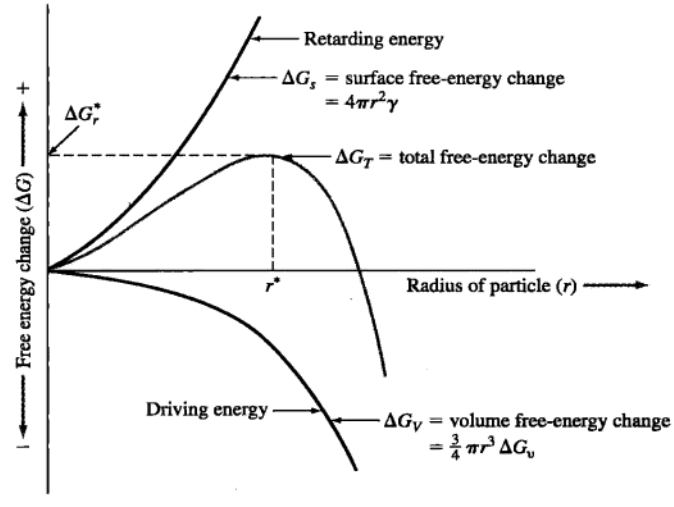

Figure 4.4
Free-energy change ΔG versus radius of embryo or nucleus created by the solidifying of a pure metal. If the radius of the particle is greater than r^*, a stable nucleus will continue to grow.

When a pure liquid metal such as lead is cooled below its equilibrium freezing temperature, the driving energy for the liquid-to-solid transformation is the difference in the volume (bulk) free energy ΔG_v of the liquid and that of the solid. If ΔG_v is the change in free energy between the liquid and solid per unit volume of metal, then the free-energy change for a *spherical nucleus* of radius r is $\frac{4}{3}\pi r^3 \Delta G_v$ since the volume of a sphere is $\frac{4}{3}\pi r^3$. The change in volume free energy versus radius of an

embryo or nucleus is shown schematically in Fig. 4.4 as the lower curve and is a negative quantity since energy is released by the liquid-to-solid transformation.

However, there is an opposing energy to the formation of embryos and nuclei, the energy required to form the surface of these particles. The energy needed to create a surface for these spherical particles, ΔG_s, is equal to the specific surface free energy of the particle, γ, times the area of the surface of the sphere, or $4\pi r^2\gamma$, where $4\pi r^2$ is the surface area of a sphere. This retarding energy ΔG_s for the formation of the solid particles is shown graphically in Fig. 4.4 by an upward curve in the positive upper half of the figure. The total free energy associated with the formation of an embryo or nucleus, which is the sum of the volume free-energy and surface free-energy changes, is shown in Fig. 4.4 as the middle curve. In equation form, the total free-energy change for the formation of a spherical embryo or nucleus of radius r formed in a freezing pure metal is

$$\Delta G_T = \tfrac{4}{3}\pi r^3 \Delta G_v + 4\pi r^2\gamma \tag{4.1}$$

where ΔG_T = total free-energy change
r = radius of embryo or nucleus
ΔG_v = volume free energy
γ = specific surface free energy

In nature, a system can change spontaneously from a higher- to a lower-energy state. In the case of the freezing of a pure metal, if the solid particles formed upon freezing have radii less than the **critical radius** r^*, the energy of the system will be lowered if they redissolve. These small embryos can, therefore, redissolve in the liquid metal. However, if the solid particles have radii greater than r^*, the energy of the system will be lowered when these particles (nuclei) grow into larger particles or crystals (Fig. 4.2*b*). When r reaches the critical radius r^*, ΔG_T has its maximum value of ΔG^* (Fig. 4.4).

A relationship among the size of the critical nucleus, surface free energy, and volume free energy for the solidification of a pure metal can be obtained by differentiating Eq. 4.1. The differential of the total free energy ΔG_T with respect to r is zero when $r = r^*$ since the total free energy versus radius of the embryo or nucleus plot is then at a maximum and the slope $d(\Delta G_T)/dr = 0$. Thus,

$$\frac{d(\Delta G_T)}{dr} = \frac{d}{dr}\left(\frac{4}{3}\pi r^3 \Delta G_v + 4\pi r^2\gamma\right)$$

$$\frac{12}{3}\pi r^{*2}\,\Delta G_V + 8\pi r^*\gamma = 0 \tag{4.1a}$$

$$r^* = -\frac{2\gamma}{\Delta G_v}.$$

Critical Radius versus Undercooling The greater the degree of undercooling ΔT below the equilibrium melting temperature of the metal, the greater the change in

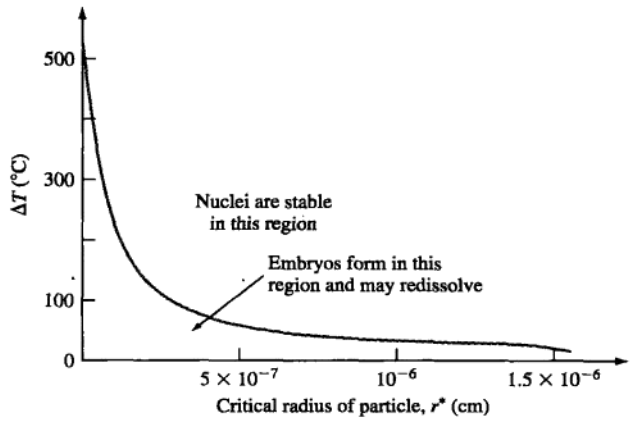

Figure 4.5
Critical radius of copper nuclei versus degree of undercooling ΔT.
(From B. Chalmers, Principles of Solidification, Wiley, 1964.)

volume free energy ΔG_V. However, the change in free energy due to the surface energy ΔG_s does not change much with temperature. Thus, the critical nucleus size is determined mainly by ΔG_V. Near the freezing temperature, the critical nucleus size must be infinite since ΔT approaches zero. As the amount of undercooling increases, the critical nucleus size decreases. Figure 4.5 shows the variation in critical nucleus size for copper as a function of undercooling. The maximum amount of undercooling for homogeneous nucleation in the pure metals listed in Table 4.1 is from 327°C to 1772°C. The critical-sized nucleus is related to the amount of undercooling by the relation

$$r^* = \frac{2\gamma T_m}{\Delta H_f \Delta T} \tag{4.2}$$

where r^* = critical radius of nucleus
γ = surface free energy
ΔH_f = latent heat of fusion
ΔT = amount of undercooling at which nucleus is formed

Example Problem 4.1 shows how a value for the number of atoms in a critical nucleus can be calculated from experimental data.

EXAMPLE PROBLEM 4.1

a. Calculate the critical radius (in centimeters) of a homogeneous nucleus that forms when pure liquid copper solidifies. Assume ΔT(undercooling) = $0.2T_m$. Use data from Table 4.1.
b. Calculate the number of atoms in the critical-sized nucleus at this undercooling.

■ **Solution**

a. Calculation of critical radius of nucleus:

$$r^* = \frac{2\gamma T_m}{\Delta H_f \Delta T} \tag{4.2}$$

$$\Delta T = 0.2T_m = 0.2(1083°C + 273) = (0.2 \times 1356\ K) = 271\ K$$

$$\gamma = 177 \times 10^{-7}\ J/cm^2 \quad \Delta H_f = 1826\ J/cm^3 \quad T_m = 1083°C = 1356\ K$$

$$r^* = \frac{2(177 \times 10^{-7}\ J/cm^2)(1356\ K)}{(1826\ J/cm^3)(271\ K)} = 9.70 \times 10^{-8}\ cm \blacktriangleleft$$

b. Calculation of number of atoms in critical-sized nucleus:

$$\text{Vol. of critical-sized nucleus} = \tfrac{4}{3}\pi r^{*3} = \tfrac{4}{3}\pi(9.70 \times 10^{-8}\ cm)^3$$

$$= 3.82 \times 10^{-21}\ cm^3$$

$$\text{Vol. of unit cell of Cu } (a = 0.361\ nm) = a^3 = (3.61 \times 10^{-8}\ cm)^3$$

$$= 4.70 \times 10^{-23}\ cm^3$$

Since there are four atoms per FCC unit cell,

$$\text{Volume/atom} = \frac{4.70 \times 10^{-23}\ cm^3}{4} = 1.175 \times 10^{-23}\ cm^3$$

Thus, the number of atoms per homogeneous critical nucleus is

$$\frac{\text{Volume of nucleus}}{\text{Volume/atom}} = \frac{3.82 \times 10^{-21}\ cm^3}{1.175 \times 10^{-23}\ cm^3} = 325\ \text{atoms} \blacktriangleleft$$

Heterogeneous Nucleation **Heterogeneous nucleation** is nucleation that occurs in a liquid on the surfaces of its container, insoluble impurities, and other structural material that lower the critical free energy required to form a stable nucleus. Since large amounts of undercooling do not occur during industrial casting operations and usually range between 0.1°C and 10°C, the nucleation must be heterogeneous and not homogeneous.

For heterogeneous nucleation to take place, the solid nucleating agent (impurity solid or container) must be wetted by the liquid metal. Also the liquid should solidify easily on the nucleating agent. Figure 4.6 shows a nucleating agent (substrate) that is wetted by the solidifying liquid, creating a low contact angle θ between the solid metal and the nucleating agent. Heterogeneous nucleation takes place on the nucleating agent because the surface energy to form a stable nucleus is lower on this material than in the pure liquid itself (homogeneous nucleation). Since the surface energy is lower for heterogeneous nucleation, the total free-energy change for the formation of a stable nucleus will be lower and the critical size of the nucleus will be smaller. Thus, a much smaller amount of undercooling is required to form a stable nucleus produced by heterogeneous nucleation.

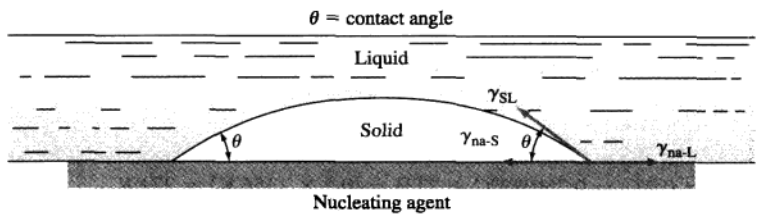

Figure 4.6
Heterogeneous nucleation of a solid on a nucleating agent. na = nucleating agent, SL = solid-liquid, S = solid, L = liquid; θ = contact angle.
(From J.H. Brophy, R.M. Rose and J. Wulff, The Structure and Properties of Materials, vol. II: "Thermodynamics of Structure," Wiley, 1964, p. 105.)

4.1.2 Growth of Crystals in Liquid Metal and Formation of a Grain Structure

After stable nuclei have been formed in a solidifying metal, these nuclei grow into crystals, as shown in Fig. 4.2*b*. In each solidifying crystal, the atoms are arranged in an essentially regular pattern, but the orientation of each crystal varies (Fig. 4.2*b*). When solidification of the metal is finally completed, the crystals join together in different orientations and form crystal boundaries at which changes in orientation take place over a distance of a few atoms (Fig. 4.2*c*). Solidified metal containing many crystals is said to be *polycrystalline.* The crystals in the solidified metal are called **grains,** and the surfaces between them, *grain boundaries.*

The number of nucleation sites available to the freezing metal will affect the grain structure of the solid metal produced. If relatively few nucleation sites are available during solidification, a coarse, or large-grain, structure will be produced. If many nucleation sites are available during solidification, a fine-grain structure will result. Almost all engineering metals and alloys are cast with a fine-grain structure since this is the most desirable type for strength and uniformity of finished metal products.

When a relatively pure metal is cast into a stationary mold without the use of *grain refiners,*[3] two major types of grain structures are usually produced:

1. Equiaxed grains
2. Columnar grains

If the nucleation and growth conditions in the liquid metal during solidification are such that the crystals can grow about equally in all directions, **equiaxed grains** will be produced. Equiaxed grains are commonly found adjacent to a cold mold wall, as shown in Fig. 4.7. Large amounts of undercooling near the wall create a relatively high concentration of nuclei during solidification, a condition necessary to produce the equiaxed gain structure.

[3]A grain refiner is a material added to a molten metal to attain finer grains in the final grain structure.

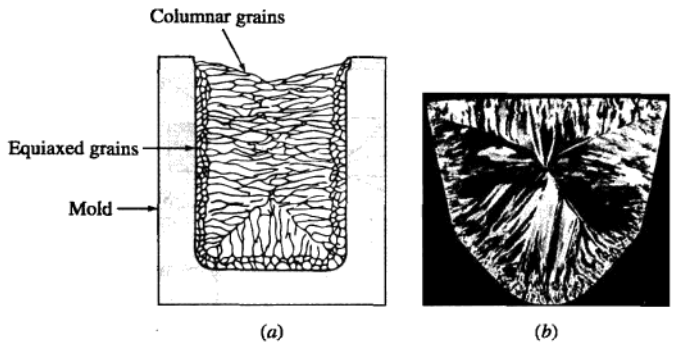

Figure 4.7
(*a*) Schematic drawing of a solidified metal grain structure produced by using a cold mold. (*b*) Transverse section through an ingot of aluminum alloy 1100 (99.0% Al) cast by the Properzi method (a wheel and belt method). Note the consistency with which columnar grains have grown perpendicular to each mold face.
(After "Metals Handbook," vol. 8, 8th ed., American Society for Metals, 1973, p. 164.)

Columnar grains are long, thin, coarse grains created when a metal solidifies rather slowly in the presence of a steep temperature gradient. Relatively few nuclei are available when columnar grains are produced. Equiaxed and columnar grains are shown in Fig. 4.7*a*. Note that in Fig. 4.7*b* the columnar grains have grown perpendicular to the mold faces since large thermal gradients were present in those directions.

4.1.3 Grain Structure of Industrial Castings

In industry, metals and alloys are cast into various shapes. If the metal is to be further fabricated after casting, large castings of simple shapes are produced first and then fabricated further into semifinished products. For example, in the aluminum industry, common shapes for further fabrication are sheet ingots (Fig. 4.1), which have rectangular cross sections, and extrusion[4] ingots, which have circular cross sections. For some applications, the molten metal is cast into essentially its final shape as, for example, an automobile piston (see Fig. 6.3).

The large aluminum alloy sheet ingot in Fig. 4.1 was cast by a direct-chill semicontinuous casting process. In this casting method, the molten metal is cast into a mold with a movable bottom block that is slowly lowered after the mold is filled

[4]*Extrusion* is the process of converting a metal ingot into lengths of uniform cross section by forcing solid plastic metal through a die or orifice of the desired cross-sectional outline.

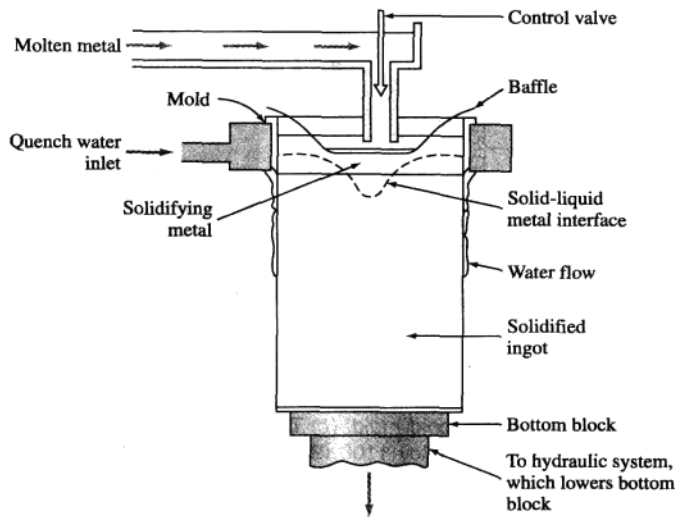

Figure 4.8
Schematic of an aluminum alloy ingot being cast in a direct-chill semicontinuous casting unit.

(Fig. 4.8). The mold is water-cooled by a water box, and water is also sprayed down the sides of the solidified surface of the ingot. In this way, large ingots about 15 ft long can be cast continuously, as shown in Fig. 4.1. In the steel industry, about 60 percent of the metal is cast into stationary molds, with the remaining 40 percent being continuously cast, as shown in Fig. 4.9.

To produce cast ingots with a fine grain size, grain refiners are usually added to the liquid metal before casting. For aluminum alloys, small amounts of grain refining elements such as titanium, boron, or zirconium are included in the liquid metal just before the casting operation so that a fine dispersion of heterogeneous nuclei will be available during solidification. Figure 4.10 shows the effect of using a grain refiner while casting 6-in.-diameter aluminum extrusion ingots. The ingot section cast without the grain refiner has large columnar grains (Fig. 4.10*a*), and the section cast with the grain refiner has a fine, equiaxed grain structure (Fig. 4.10*b*).

4.2 SOLIDIFICATION OF SINGLE CRYSTALS

Almost all engineering crystalline materials are composed of many crystals and are therefore **polycrystalline.** However, there are a few that consist of only one crystal and are therefore *single crystals.* For example, high-temperature creep-

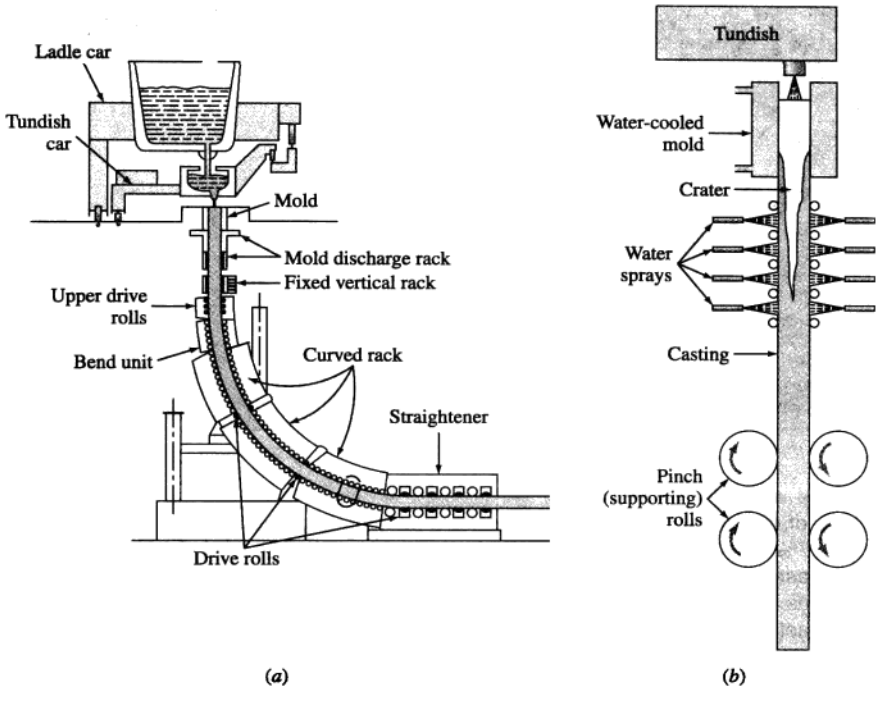

Figure 4.9
Continuous casting of steel ingots. (*a*) General setup and (*b*) close-up of the mold arrangement.
(*From Making, Shaping and Treating of Steel, 10th ed., Association of Iron and Steel Engineers, 1985.*)

resistant gas turbine blades are sometimes made of single crystals, as shown in Fig. 4.11*c*. Single-crystal turbine blades are more creep resistant at high temperatures than the same blades made with an equiaxed grain structure (Fig. 4.11*a*) or a columnar grain structure (Fig. 4.11*b*) because at high temperatures above about half the absolute melting temperature of a metal the grain boundaries become weaker than the grain bodies.

In growing single crystals, solidification must take place around a single nucleus so that no other crystals are nucleated and grow. To accomplish this, the interface temperature between the solid and liquid must be slightly lower than the melting point of the solid, and the liquid temperature must increase beyond the interface. To achieve this temperature gradient, the latent heat of solidification[5] must be conducted through

[5]The latent heat of solidification is the thermal energy released when a metal solidifies.

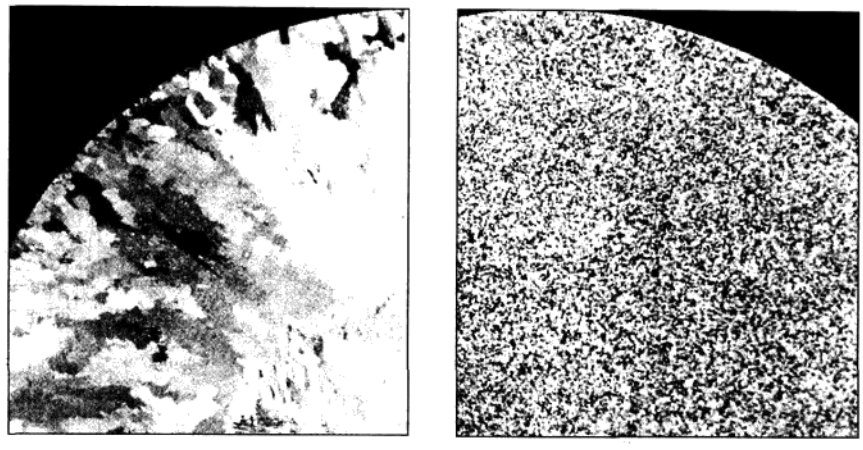

(*a*) (*b*)

Figure 4.10
Parts of transverse sections through two 6-in.-diameter ingots of alloy 6063 (Al–0.7% Mg–0.4% Si) that were direct-chill semicontinuous cast. (*a*) Ingot section was cast without the addition of a grain refiner; note columnar grains and colonies of featherlike crystals near the center of the section. (*b*) Ingot section was cast with the addition of a grain refiner and shows a fine, equiaxed grain structure. (Tucker's reagent; actual size.)
(*After "Metals Handbook," vol. 8, 8th ed., American Society for Metals, 1973, p. 164.*)

the solidifying solid crystal. The growth rate of the crystal must be slow so that the temperature at the liquid-solid interface is slightly below the melting point of the solidifying solid. Figure 4.12*a* illustrates how single-crystal turbine blades can be cast, and Fig. 4.12*b* and *c* show how competitive grain growth is reduced to a single grain by using a "pigtail" selector.

Another example of an industrial use of single crystals is the silicon single crystals that are sliced into wafers for solid-state electronic integrated circuit chips (see Fig. 14.1). Single crystals are necessary for this application since grain boundaries would disrupt the flow of electrons in devices made from semiconductor silicon. In industry, single crystals of silicon 8 to 12 in. (20 to 25 cm) in diameter have been grown for semiconducting device applications. One of the commonly used techniques to produce high-quality (minimization of defects) silicon single crystals is the Czochralski method. In this process, high-purity polycrystalline silicon is first melted in a nonreactive crucible and held at a temperature just above the melting point. A high-quality seed crystal of silicon of the desired orientation is lowered into the melt while it is rotated. Part of the surface of the seed crystal is melted in the liquid to remove the outer strained region and

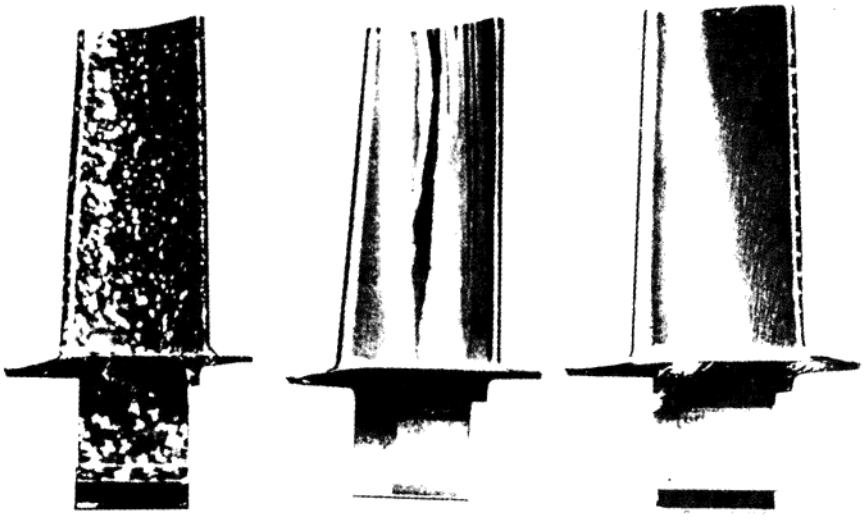

(*a*) (*b*) (*c*)

Figure 4.11
Different grain structures of gas turbine airfoil blades: (*a*) Polycrystal equiaxed, (*b*) polycrystal columnar, and (*c*) single crystal.
(*Courtesy of Pratt and Whitney Co.*)

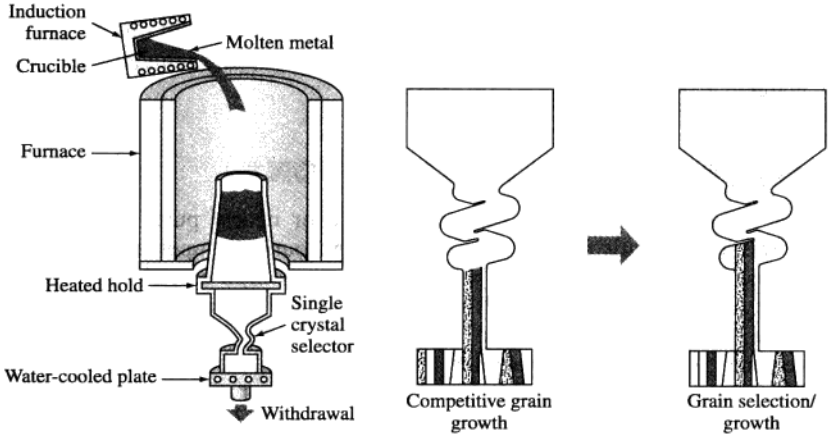

Figure 4.12
(*a*) A process schematic for producing a single-crystal gas turbine airfoil. (*b*) Starter section of casting for producing a single-crystal airfoil showing competitive growth during solidification below the single-crystal selector ("pigtail"). (*c*) Same as (*b*) but showing the survival of only one grain during solidification through the single-crystal selector.
(*After Pratt and Whitney Co.*)

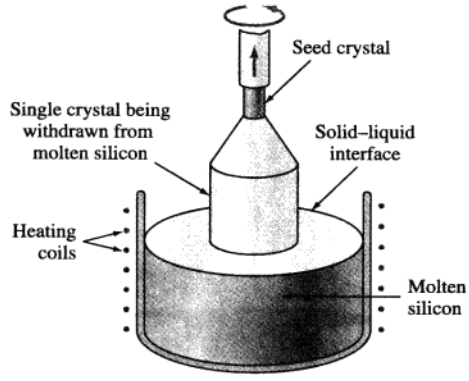

Figure 4.13
Formation of single crystal of silicon by the Czochralski process.

to produce a surface for the liquid to solidify on. The seed crystal continues to rotate and is slowly raised from the melt. As it is raised from the melt, silicon from the liquid in the crucible adheres and grows on the seed crystal, producing a much larger diameter single crystal of silicon (Fig. 4.13). With this process large single-crystal silicon ingots up to about 12 in. (≅30 cm) in diameter can and have been made.

4.3 METALLIC SOLID SOLUTIONS

Although very few metals are used in the pure or nearly pure state, a few are used in the nearly pure form. For example, high-purity copper of 99.99 percent purity is used for electronic wires because of its very high electrical conductivity. High-purity aluminum (99.99% Al) (called *superpure aluminum*) is used for decorative purposes because it can be finished with a very bright metallic surface. However, most engineering metals are combined with other metals or nonmetals to provide increased strength, higher corrosion resistance, or other desired properties.

A *metal alloy,* or simply an **alloy,** is a mixture of two or more metals or a metal (metals) and a nonmetal (nonmetals). Alloys can have structures that are relatively simple, such as that of cartridge brass, which is essentially a binary alloy (two metals) of 70 wt% Cu and 30 wt% Zn. On the other hand, alloys can be extremely complex, such as the nickel-base superalloy Inconel 718 used for jet engine parts, which has about 10 elements in its nominal composition.

The simplest type of alloy is that of the solid solution. A **solid solution** is a *solid* that consists of two or more elements atomically dispersed in a single-phase structure. In general there are two types of solid solutions: *substitutional* and *interstitial.*

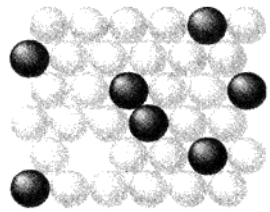

Figure 4.14
Substitutional solid solution. The dark circles represent one type of atom and the light another. The plane of atoms is a (111) plane in an FCC crystal lattice.

4.3.1 Substitutional Solid Solutions

In **substitutional solid solutions** formed by two elements, solute atoms can substitute for parent solvent atoms in a crystal lattice. Figure 4.14 shows a (111) plane in an FCC crystal lattice in which some solute atoms of one element have substituted for solvent atoms of the parent element. The crystal structure of the parent element or solvent is unchanged, but the lattice may be distorted by the presence of the solute atoms, particularly if there is a significant difference in atomic diameters of the solute and solvent atoms.

The fraction of atoms of one element that can dissolve in another can vary from a fraction of an atomic percent to 100 percent. The following conditions, known as *Hume–Rothery rules*, are favorable for extensive solid solubility of one element in another:

1. The diameters of the atoms of the elements must not differ by more than about 15 percent.
2. The crystal structures of the two elements must be the same.
3. There should be no appreciable difference in the electronegativities of the two elements so that compounds will not form.
4. The two elements should have the same valence.

If the atomic diameters of the two elements that form a solid solution differ, there will be a distortion of the crystal lattice. Since the atomic lattice can only sustain a limited amount of contraction or expansion, there is a limit in the difference in atomic diameters that atoms can have and still maintain a solid solution with the same kind of crystal structure. When the atomic diameters differ by more than about 15 percent, the "size factor" becomes unfavorable for extensive solid solubility.

EXAMPLE PROBLEM 4.2

Using the data in the following table, predict the relative degree of atomic solid solubility of the following elements in copper:

a. Zinc
b. Lead
c. Silicon
d. Nickel
e. Aluminum
f. Beryllium

Use the scale very high, 70%–100%; high, 30%–70%; moderate, 10%–30%; low, 1%–10%; and very low, <1%.

Element	Atom radius (nm)	Crystal structure	Electronegativity	Valence
Copper	0.128	FCC	1.8	+2
Zinc	0.133	HCP	1.7	+2
Lead	0.175	FCC	1.6	+2, +4
Silicon	0.117	Diamond cubic	1.8	+4
Nickel	0.125	FCC	1.8	+2
Aluminum	0.143	FCC	1.5	+3
Beryllium	0.114	HCP	1.5	+2

■ **Solution**

A sample calculation for the atomic radius difference for the Cu–Zn system is

$$\text{Atomic radius difference} = \frac{\text{final radius} - \text{initial radius}}{\text{initial radius}}(100\%)$$

$$= \frac{R_{Zn} - R_{Cu}}{R_{Cu}}(100\%) \qquad (4.3)$$

$$= \frac{0.133 - 0.128}{0.128}(100\%) = +3.9\%$$

System	Atomic radius difference (%)	Electronegativity difference	Predicted relative degree of solid solubility	Observed maximum solid solubility (at %)
Cu–Zn	+3.9	0.1	High	38.3
Cu–Pb	+36.7	0.2	Very low	0.1
Cu–Si	−8.6	0	Moderate	11.2
Cu–Ni	−2.3	0	Very high	100
Cu–Al	+11.7	0.3	Moderate	19.6
Cu–Be	−10.9	0.3	Moderate	16.4

The predictions can be made principally on the atomic radius difference. In the case of the Cu–Si system, the difference in the crystal structures is important. There is very little electronegativity difference for all these systems. The valences are all the same except for Al and Si. In the final analysis, the experimental data must be referred to.

If the solute and solvent atoms have the same crystal structure, then extensive solid solubility is favorable. If the two elements are to show complete solid solubility in all proportions, then both elements must have the same crystal structure. Also, there cannot be too great a difference in the electronegativities of the two elements forming solid solutions, or else the highly electropositive element will lose electrons, the highly electronegative element will acquire electrons, and compound formation will result. Finally, if the two solid elements have the same valence, solid solubility will be favored. If there is a shortage of electrons between the atoms, the binding between them will be upset, resulting in conditions unfavorable for solid solubility.

4.3.2 Interstitial Solid Solutions

In interstitial solutions the solute atoms fit into the spaces between the solvent or parent atoms. These spaces or voids are called *interstices*. **Interstitial solid solutions** can form when one atom is much larger than another. Examples of atoms that can form interstitial solid solutions due to their small size are hydrogen, carbon, nitrogen, and oxygen.

An important example of an interstitial solid solution is that formed by carbon in FCC γ iron that is stable between 912°C and 1394°C. The atomic radius of γ iron is 0.129 nm and that of carbon is 0.075 nm, and so there is an atomic radius difference of 42 percent. However, in spite of this difference, a maximum of 2.08 percent of the carbon can dissolve interstitially in iron at 1148°C. Figure 4.15 illustrates this schematically by showing distortion around the carbon atoms in the γ iron lattice.

The radius of the largest interstitial hole in FCC γ iron is 0.053 nm (see Example Problem 4.3), and since the atomic radius of the carbon atom is 0.075 nm, it is not surprising that the maximum solid solubility of carbon in γ iron is only 2.08 percent. The radius of the largest interstitial void in BCC α iron is only 0.036 nm, and as a result, just below 723°C, only 0.025 percent of the carbon can be dissolved interstitially.

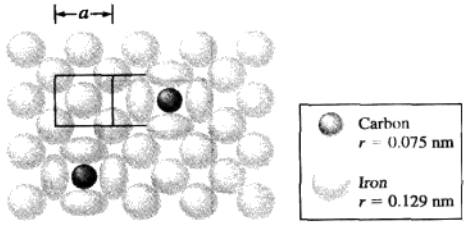

Figure 4.15
Schematic illustration of an interstitial solid solution of carbon in FCC γ iron just above 912°C showing a (100) plane. Note the distortion of the iron atoms (0.129 nm radius) around the carbon atoms (0.075 nm radius), fitting into voids of 0.053 nm radius.
(From p. 113 in L. H. Van Vlack, Elements of Materials Science and Engineering, 4th ed.)

EXAMPLE PROBLEM 4.3

Calculate the radius of the largest interstitial void in the FCC γ iron lattice. The atomic radius of the iron atom is 0.129 nm in the FCC lattice, and the largest interstitial voids occur at the $(\frac{1}{2}, 0, 0)$, $(0, \frac{1}{2}, 0)$, $(0, 0, \frac{1}{2})$, etc., -type positions.

■ Solution

Figure EP4.3 shows a (100) FCC lattice plane on the yz plane. Let the radius of an iron atom be R and that of the interstitial void at the position $(0, \frac{1}{2}, 0)$ be r. Then, from Fig. EP4.3,

$$2R + 2r = a \tag{4.4}$$

Also from Fig. 4.15*b*,

$$(2R)^2 = (\tfrac{1}{2}a)^2 + (\tfrac{1}{2}a)^2 = \tfrac{1}{2}a^2 \tag{4.5}$$

Solving for a gives

$$2R = \frac{1}{\sqrt{2}}a \quad \text{or} \quad a = 2\sqrt{2}R \tag{4.6}$$

Combining Eqs. 4.4 and 4.6 gives

$$2R + 2r = 2\sqrt{2}R$$
$$r = (\sqrt{2} - 1)R = 0.414R$$
$$= (0.414)(0.129 \text{ nm}) = 0.053 \text{ nm} \blacktriangleleft$$

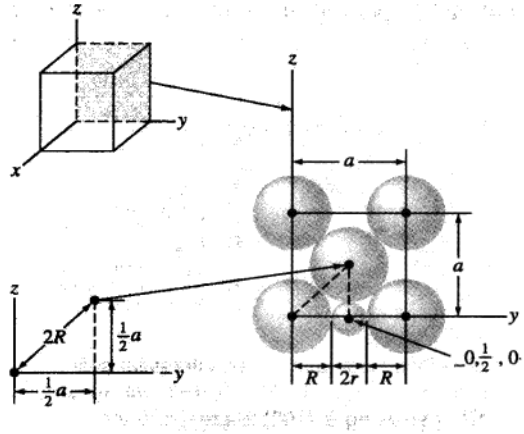

Figure EP4.3
(100) plane of the FCC lattice containing an interstitial atom at the $(0, \frac{1}{2}, 0)$ position coordinate.

4.4 CRYSTALLINE IMPERFECTIONS

In reality, crystals are never perfect and contain various types of imperfections and defects that affect many of their physical and mechanical properties, which in turn affect many important engineering properties of materials such as the cold formability of alloys, the electronic conductivity of semiconductors, the rate of migration of atoms in alloys, and the corrosion of metals.

Crystal lattice imperfections are classified according to their geometry and shape. The three main divisions are (1) zero-dimensional or point defects, (2) one-dimensional or line defects (dislocations), and (3) two-dimensional defects, that include external surfaces, grain boundaries, twins, low-angle boundaries, high-angle boundaries, twists, stacking faults, voids, and precipitates. Three-dimensional macroscopic or bulk defects could also be included. Examples of these defects are pores, cracks, and foreign inclusions.

4.4.1 Point Defects

The simplest point defect is the vacancy, an atom site from which an atom is missing (Fig. 4.16*a*). **Vacancies** may be produced during solidification as a result of local disturbances during the growth of crystals, or they may be created by atomic rearrangements in an existing crystal due to atomic mobility. In metals the equilibrium concentration of vacancies rarely exceeds about 1 in 10,000 atoms. Vacancies are equilibrium defects in metals, and their energy of formation is about 1 eV.

Additional vacancies in metals can be introduced by plastic deformation, rapid cooling from higher temperatures to lower ones to entrap the vacancies, and by bombardment with energetic particles such as neutrons. Nonequilibrium vacancies have a tendency to cluster, causing divacancies or trivacancies to form. Vacancies can move by exchanging positions with their neighbors. This process is important in the

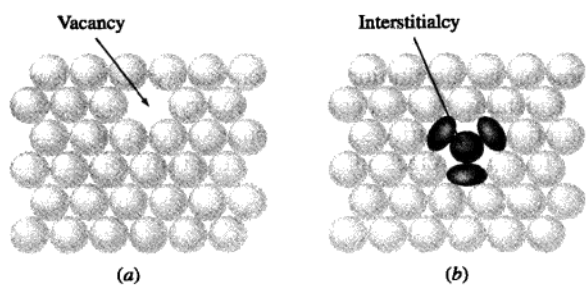

Figure 4.16
(*a*) Vacancy point defect. (*b*) Self-interstitial, or interstitialcy, point defect in a close-packed solid-metal lattice.

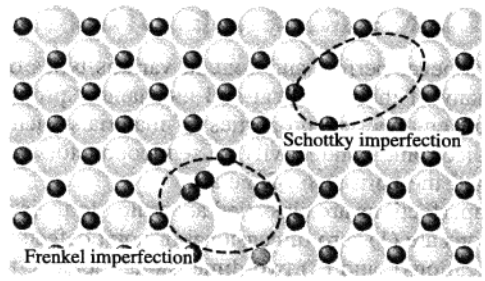

Figure 4.17
Two-dimensional representation of an ionic crystal illustrating a Schottky defect and a Frenkel defect.
(From Wulff et al., Structure and Properties of Materials, Vol. I: "Structure," Wiley, 1964, p. 78.)

migration or diffusion of atoms in the solid state, particularly at elevated temperatures where atomic mobility is greater.

Sometimes an atom in a crystal can occupy an interstitial site between surrounding atoms in normal atom sites (Fig. 4.16*b*). This type of point defect is called a **self-interstitial,** or **interstitialcy.** These defects do not generally occur naturally because of the structural distortion they cause, but they can be introduced into a structure by irradiation.

In ionic crystals point defects are more complex due to the necessity to maintain electrical neutrality. When two oppositely charged ions are missing from an ionic crystal, a cation-anion divacancy is created that is known as a **Schottky imperfection** (Fig. 4.17). If a positive cation moves into an interstitial site in an ionic crystal, a cation vacancy is created in the normal ion site. This vacancy-interstitialcy pair is called a **Frenkel[6] imperfection** (Fig. 4.17). The presence of these defects in ionic crystals increases their electrical conductivity.

Impurity atoms of the substitutional or interstitial type are also point defects and may be present in metallic or covalently bonded crystals. For example, very small amounts of substitutional impurity atoms in pure silicon can greatly affect its electrical conductivity for use in electronic devices. Impurity ions are also point defects in ionic crystals.

4.4.2 Line Defects (Dislocations)

Line imperfections, or **dislocations,** in crystalline solids are defects that cause lattice distortion centered around a line. Dislocations are created during the solid-

[6]Yakov Ilyich Frenkel (1894–1954). Russian physicist who studied defects in crystals. His name is associated with the vacancy-interstitialcy defect found in some ionic crystals.

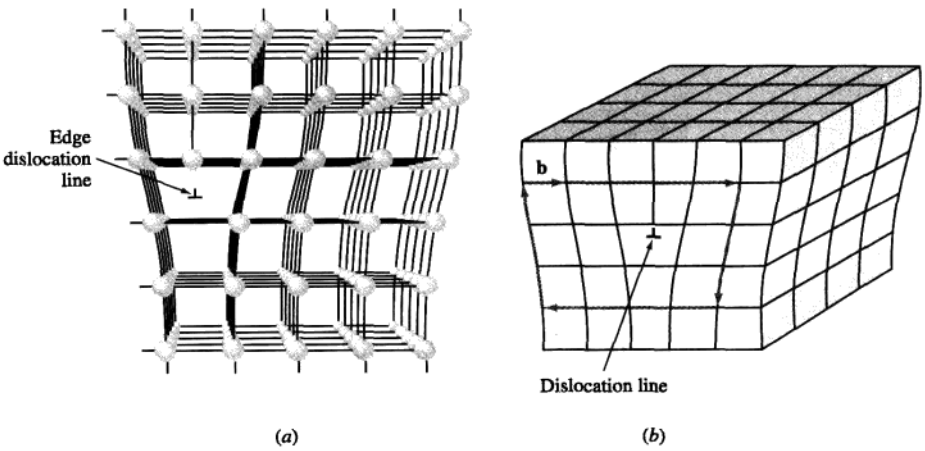

Figure 4.18
(*a*) Positive edge dislocation in a crystalline lattice. A linear defect occurs in the region just above the inverted "tee," ⊥, where an extra half plane of atoms has been wedged in.
(*After A.G. Guy, "Essentials of Materials Science," McGraw-Hill, 1976, p. 153.*)
(*b*) Edge dislocation that indicates the orientation of its Burgers or slip vector **b**.
(*Eisenstadt, M., Introduction to Mechanical Properties of Materials: An Ecological Approach, 1st ed., © 1971. Reprinted by permission of Pearson Education, Inc., Upper Saddle River, NJ.*)


Animation

ification of crystalline solids. They are also formed by the permanent or plastic deformation of crystalline solids, vacancy condensation, and atomic mismatch in solid solutions.

The two main types of dislocations are the *edge* and *screw types.* A combination of the two gives *mixed dislocations,* which have edge and screw components. An edge dislocation is created in a crystal by the insertion of an extra half plane of atoms, as shown in Fig. 4.18*a* just above the symbol ⊥. The inverted "tee," ⊥, indicates a positive edge dislocation, whereas the upright "tee," ⊤, indicates a negative edge dislocation.

The displacement distance of the atoms around the dislocation is called the *slip* or *Burgers vector* **b** and is *perpendicular* to the edge-dislocation line (Fig. 4.18*b*). Dislocations are nonequilibrium defects, and they store energy in the distorted region of the crystal lattice around the dislocation. The edge dislocation has a region of compressive strain at the extra half plane and a region of tensile strain below the extra half plane of atoms (Fig. 4.19*a*).

The screw dislocation can be formed in a perfect crystal by applying upward and downward shear stresses to regions of a perfect crystal that have been separated by a cutting plane, as shown in Fig. 4.20*a*. These shear stresses introduce a region of distorted crystal lattice in the form of a spiral ramp of distorted atoms or screw dislocation (Fig. 4.20*b*). The region of distorted crystal is not well

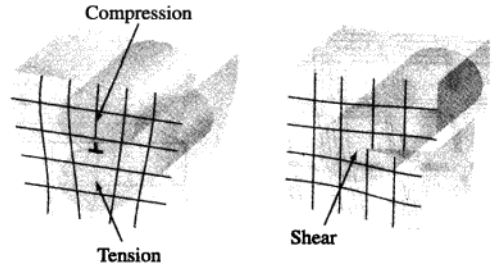

Figure 4.19
Strain fields surrounding (*a*) an edge dislocation and (*b*) a screw dislocation.
(From Wulff et al., Structure and Properties of Materials, Vol. III, H.W. Hayden, L.G. Moffatt, and J. Wulff, "Mechanical Behavior," Wiley, 1965, p. 69.)

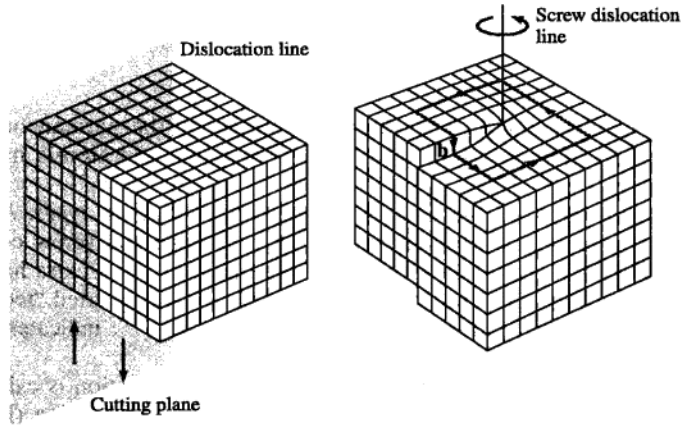

Figure 4.20
Formation of a screw dislocation. (*a*) A perfect crystal is sliced by a cutting plane, and up and down shear stresses are applied parallel to the cutting plane to form the screw dislocation in (*b*). (*b*) A screw dislocation is shown with its slip or Burgers vector **b** parallel to the dislocation line.
(Eisenstadt, M., Introduction to Mechanical Properties of Materials: An Ecological Approach, 1st ed., © 1971. Reprinted by permission of Pearson Education, Inc., Upper Saddle River, NJ.)

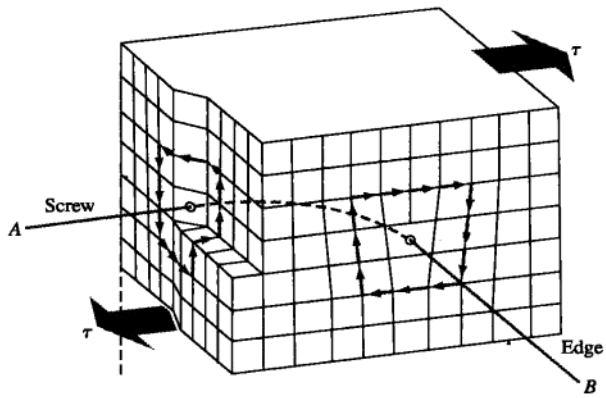

Figure 4.21
Mixed dislocation in a crystal. Dislocation line *AB* is pure screw type where it enters the crystal on left and pure edge type where it leaves the crystal on right.
(From Wulff et al., Structure and Properties of Materials, Vol. III, H.W. Hayden, L.G. Moffatt, and J. Wulff, "Mechanical Properties", Wiley, 1965, p. 65.)

defined and is at least several atoms in diameter. A region of shear strain is created around the screw dislocation in which energy is stored (Fig. 4.19*b*). The slip or Burgers vector of the screw dislocation is *parallel* to the dislocation line, as shown in Fig. 4.20*b*.

Most dislocations in crystals are of the mixed type, having edge and screw components. In the curved dislocation line *AB* in Fig. 4.21, the dislocation is of the pure screw type at the left where it enters the crystal and of the pure edge type on the right where it leaves the crystal. Within the crystal, the dislocation is of the mixed type, with edge and screw components.

4.4.3 Planar Defects

Planar defects include external surfaces, **grain boundaries, twins, low-angle boundaries, high-angle boundaries, twists,** and **stacking faults.** The free or external surface of any material is the most common type of planar defect. External surfaces are considered defects because the atoms on the surface are bonded to other atoms only on one side. Therefore, the surface atoms have a lower number of neighbors. As a result, these atoms have a higher state of energy when compared to the atoms positioned inside the crystal with an optimal number of neighbors. The higher energy associated with the atoms on the surface of a material makes the surface susceptible to erosion and reaction with elements in the environment. This point further illustrates the importance of defects in the behavior of materials.

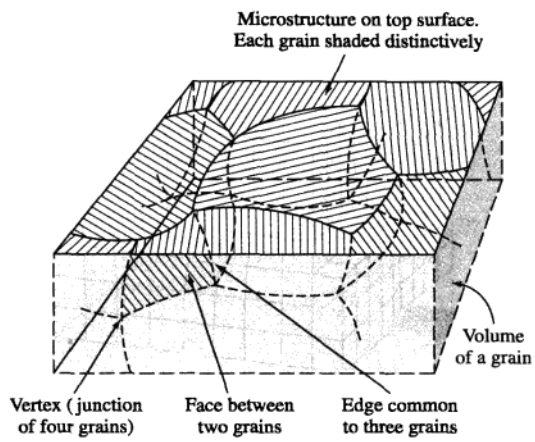

Figure 4.22
Sketch showing the relation of the two-dimensional microstructure of a crystalline material to the underlying three-dimensional network. Only portions of the total volume and total face of any one grain are shown.
(After A.G. Guy, "Essentials of Materials Science," McGraw-Hill, 1976.)

Grain boundaries are surface imperfections in polycrystalline materials that separate grains (crystals) of different orientations. In metals, grain boundaries are created during solidification when crystals formed from different nuclei grow simultaneously and meet each other (Fig. 4.2). The shape of the grain boundaries is determined by the restrictions imposed by the growth of neighboring grains. Grain-boundary surfaces of an approximately equiaxed grain structure are shown schematically in Fig. 4.22 and of real grains in Fig. 4.3.

The grain boundary itself is a narrow region between two grains of about two to five atomic diameters in width and is a region of atomic mismatch between adjacent grains. The atomic packing in grain boundaries is lower than within the grains because of the atomic mismatch. Grain boundaries also have some atoms in strained positions that raise the energy of the grain-boundary region.

The higher energy of the grain boundaries and their more open structure make them a more favorable region for the nucleation and growth of precipitates (see Sec. 9.5). The lower atomic packing of the grain boundaries also allows for more rapid diffusion of atoms in the grain boundary region. At ordinary temperatures, grain boundaries also restrict plastic flow by making it difficult for the movement of dislocations in the grain boundary region.

Figure 4.23
Twin boundaries in the grain structure of brass.
(*Figure from A.G. Guy, Essentials of Materials Science, McGraw-Hill, 1976.*)


Virtual Lab

Twins or *twin boundaries* are another example of a two-dimensional defect. A twin is defined as a region in which a mirror image of the structure exists across a plane or a boundary. Twin boundaries form when a material is permanently or plastically deformed (*deformation twin*). They can also appear during the recrystallization process in which atoms reposition themselves in a deformed crystal (*annealing twin*), but this happens only in some FCC alloys. A number of annealing twins formed in the microstructure of brass are shown in Fig. 4.23. As the name indicates, twin boundaries form in pairs. Similar to dislocations, twin boundaries tend to strengthen a material. A more detailed explanation of twin boundaries is given in Sec. 6.5.

When an array of edge dislocations are oriented in a crystal in a manner that seems to misorient or tilt two regions of a crystal (Fig. 4.24*a*), a two-dimensional defect called a *small-angle tilt boundary* is formed. A similar phenomenon can occur when a network of screw dislocations create a small-angle twist boundary (Fig 4.24*b*). The misorientation angle θ for a small-angle boundary is generally less than 10 degrees. As the density of dislocations in small-angle boundaries (tilt or twist) increases, the misorientation angle θ becomes larger. If θ exceeds 20 degrees, the boundary is no longer characterized as a small-angle boundary but

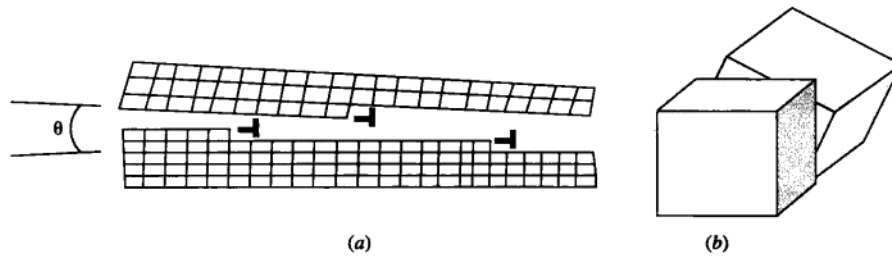

Figure 4.24
(*a*) Edge dislocations in an array forming a small-angle tilt boundary. (*b*) Schematic of a small-angle twist boundary.

is considered a general grain boundary. Similar to dislocations and twins, small-angle boundaries are regions of high energy due to local lattice distortions and tend to strengthen a metal.

In Sec. 3.8, we discussed formation of FCC and HCP crystal structures by the stacking of atomic planes. It was noted that the stacking sequence *ABABAB . . .* leads to the formation of an HCP crystal structure while the sequence *ABCABCABC . . .* leads to the FCC structure. Sometimes during the growth of a crystalline material, collapse of a vacancy cluster, or interaction of dislocations, one or more of the stacking planes may be missing, giving rise to another two-dimensional defect called a *stacking fault* or a *piling-up fault.* Stacking faults *ABCABAACBABC* and *ABAABBAB* are typical in FCC and HCP crystals, respectively. The bold-faced planes indicate the faults. Stacking faults also tend to strengthen the material.

It is important to note that, generally speaking, of the two-dimensional defects discussed here, grain boundaries are most effective in strengthening a metal; however stacking faults, twin boundaries, and small-angle boundaries often also serve a similar purpose. The reason why these defects tend to strengthen a metal will be discussed in more detail in Chap. 6.

4.4.4 Volume Defects

Volume or *three-dimensional defects* form when a cluster of point defects join to form a three-dimensional void or a pore. Conversely, a cluster of impurity atoms may join to form a three-dimensional precipitate. The size of a volume defect may range from a few nanometers to centimeters or sometimes larger. Such defects have a tremendous effect or influence on the behavior and performance of the material. Finally, the concept of a three-dimensional or volume defect may be extended to an amorphous region within a polycrystalline material. Such materials were briefly discussed in Chap. 3 and will be more extensively discussed in future chapters.

4.5 EXPERIMENTAL TECHNIQUES FOR IDENTIFICATION OF MICROSTRUCTURE AND DEFECTS

Material scientists and engineers use various instruments to study and understand the behavior of materials based on their microstructures, existing defects, microconstituents, and other features and characteristics specific to the internal structure. The instruments reveal information about the internal makeup and structure of the material at various length scales extending from the micro- to nanorange. In this range, the structure of grains, grain boundaries, various microphases, line defects, surface defects and their effect on material behavior may be studied by various instruments. In the following sections, we will discuss the use of optical metallography, scanning electron microscopy, transmission electron microscopy, high-resolution transmission electron microscopy, and scanning probe microscopy techniques to learn about the internal and surface features of materials.

4.5.1 Optical Metallography, ASTM Grain Size, and Grain Diameter Determination


Virtual Lab

Optical metallography techniques are used to study the features and internal makeup of materials at the micrometer level (magnification level of around 2000×). Qualitative and quantitative information pertaining to grains size, grain boundary, existence of various phases, internal damage, and some defects may be extracted using optical metallography techniques. In this technique, the surface of a small sample of a material such as a metal or a ceramic is first prepared through a detailed and rather lengthy procedure. The preparation process includes numerous surface grinding stages (usually four) that remove large scratches and thin plastically deformed layers from the surface of the specimen. The grinding stage is followed with a number of polishing stages (usually four) that remove fine scratches formed during the grinding stage. The quality of the surface is extremely important in the outcome of the process, and generally speaking, a smooth, mirror-like surface without scratches must be produced at the end of the polishing stage. These steps are necessary to minimize topographic contrast. The polished surface is then exposed to chemical etchants. The choice of the etchant and the etching time (the time interval in which the sample will remain in contact with the etchant) are two critical factors that depend on the specific material under study. The atoms at the grain boundary will be attacked at a much more rapid rate by the etchant than those atoms inside the grain. This is because the atoms at the grain boundary possess a higher state of energy because of the less efficient packing. As a result, the etchant produces tiny grooves along the boundaries of the grains. The prepared sample is then examined using a metallurgical microscope (inverted microscope) based on visible incident light. A schematic representation of the metallurgical microscope is given in Fig. 4.25. When exposed to incident light in an optical microscope, these grooves do not reflect the light as intensely as the remainder of

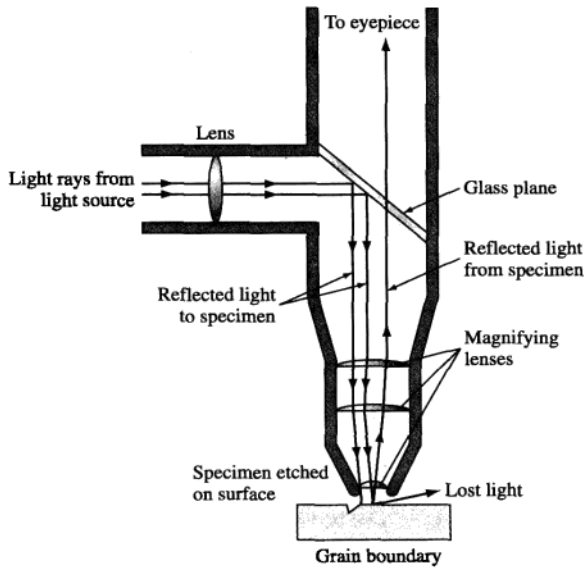

Virtual Lab

Figure 4.25
Schematic diagram illustrating how light is reflected from the surface of a polished and etched metal. The irregular surface of the etched-out grain boundary does not reflect light.
(After M. Eisenstadt, "Mechanical Properties of Materials," Macmillan, 1971, p. 126.)

the grain material (Fig. 4.26). Because of the reduced light reflection, the tiny grooves appear as dark lines to the observer, thus revealing the grain boundaries (Fig. 4.27). Additionally, impurities, other existing phases, and internal defects also react differently to the etchant and reveal themselves in photomicrographs taken from the sample surface. Overall, this technique provides a great deal of qualitative information about the material.

In addition to the qualitative information that is extracted from the photomicrographs, some limited quantitative information may also be extracted. Grain size and average grain diameter of the material may be determined using the photomicrographs obtained by this technique.

The grain size of polycrystalline metals is important since the amount of grain boundary surface has a significant effect on many properties of metals, especially strength. At lower temperatures (less than about one-half of their melting temperature), grain boundaries strengthen metals by restricting dislocation movement under stress. At elevated temperatures, grain boundary sliding may occur, and grain boundaries can become regions of weakness in polycrystalline metals.

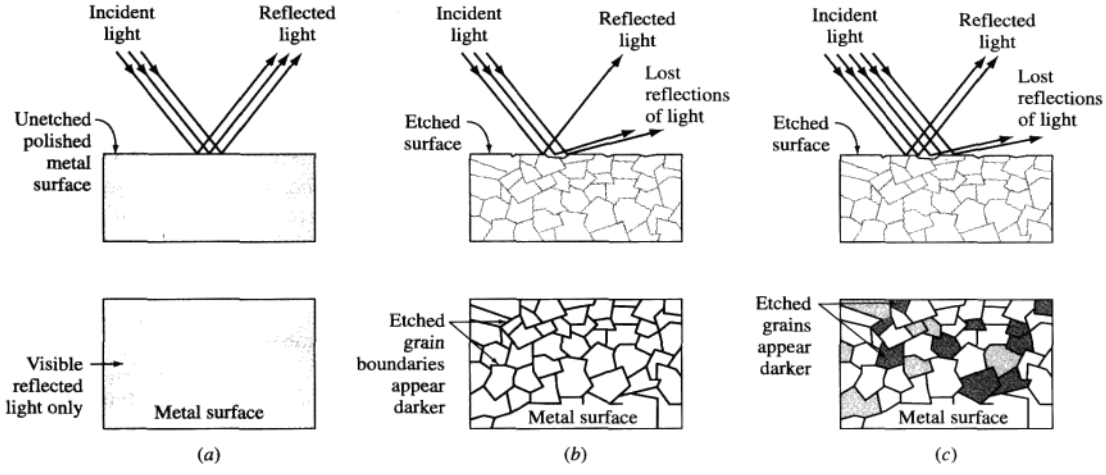

Figure 4.26
The effect of etching a polished surface of a steel metal sample on the microstructure observed in the optical microscope. (*a*) In the as-polished condition, no microstructural features are observed. (*b*) After etching a very low-carbon steel, only grain boundaries are chemically attacked severely, and so they appear as dark lines in the optical microstructure. (*c*) After etching a medium-carbon steel polished sample, dark (pearlite) and light (ferrite) regions are observed in the microstructure. The darker pearlite regions have been more severely attacked by the etchant and thus do not reflect much light.
(Eisenstadt, M., Introduction to Mechanical Properties of Materials: An Ecological Approach, 1st ed., © 1971. Reprinted by permission of Pearson Education, Inc., Upper Saddle River, NJ.)

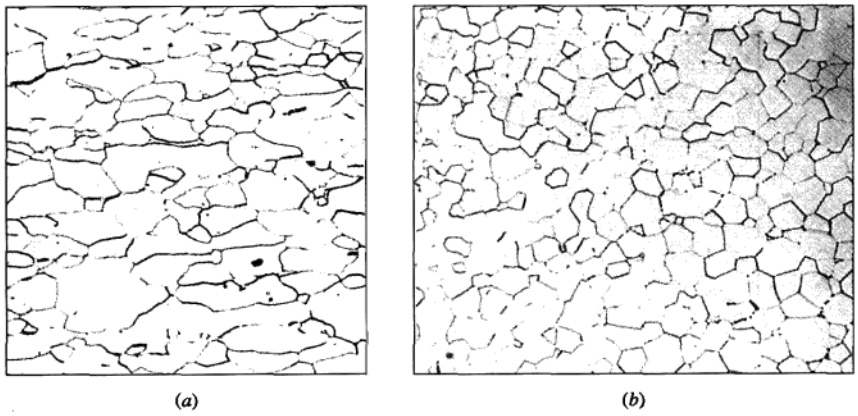

Figure 4.27
Grain boundaries on the surface of polished and etched samples as revealed in the optical microscope. (*a*) Low-carbon steel (magnification 100×).
(After "Metals Handbook," vol. 7, 8th ed., American Society for Metals, 1972, p. 4.)
(*b*) Magnesium oxide (magnification 225×).
(After R.E. Gardner and G.W. Robinson, J. Am. Ceram. Soc., 45:46 (1962).)

One method of measuring grain size is the *American Society for Testing and Materials* (ASTM) method, in which the **grain-size number** n is defined by

$$N = 2^{n-1} \tag{4.7}$$

Virtual Lab Tutorial

where N is the number of grains per square inch on a polished and etched material surface at a magnification of 100× and n is an integer referred to as the *ASTM grain-size number.* Grain-size numbers with the nominal number of grains per square inch at 100× and grains per square millimeter at 1× are listed in Table 4.2. Figure 4.28 shows some examples of nominal grain sizes for low-carbon sheet steel samples. Gen-

Table 4.2 ASTM grain sizes

	Nominal number of grains	
Grain-size no.	**Per sq mm at 1×**	**Per sq in. at 100×**
1	15.5	1.0
2	31.0	2.0
3	62.0	4.0
4	124	8.0
5	248	16.0
6	496	32.0
7	992	64.0
8	1980	128
9	3970	256
10	7940	512

Source: "Metals Handbook," vol. 7, 8th ed., American Society for Metals, 1972, p. 4.

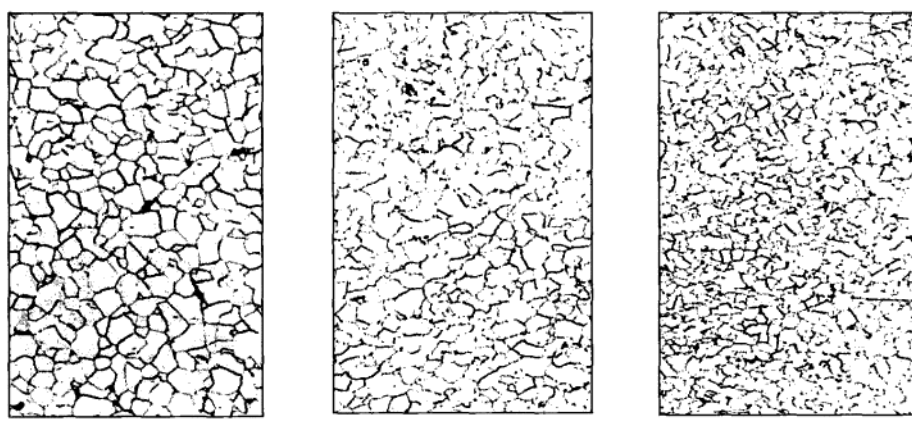

(*a*) (*b*) (*c*)

Figure 4.28
Several nominal ASTM grain sizes of low-carbon sheet steels: (*a*) no. 7, (*b*) no. 8, and (*c*) no. 9. (Etch: nital; magnification 100×.)
(*After "Metals Handbook," vol. 7, 8th ed., American Society for Metals, 1972, p. 4.*)

erally speaking, a material may be classified as coarse-grained when $n < 3$; medium-grained, $4 < n < 6$; fine-grained, $7 < n < 9$, and ultrafine-grained, $n > 10$.

A more direct approach of assessing the grain size of a material would be to determine the actual average grain diameter. This offers clear advantages to the ASTM grain-size number that in reality does not offer any direct information about the actual size of the grain. In this approach, once a photomicrograph is prepared at a specific magnification, a random line of known length is drawn on the photomicrograph. The number of grains intersected by this line is then determined, and the ratio of the number of grains to the actual length of the line is determined, n_L. The average grain diameter d is determined using the equation,

$$d = C/(n_L M) \tag{4.8}$$

where C is a constant ($C = 1.5$ for typical microstructures) and M is the magnification at which the photomicrograph is taken.

EXAMPLE PROBLEM 4.4

An ASTM grain size determination is being made from a photomicrograph of a metal at a magnification of 100×. What is the ASTM grain-size number of the metal if there are 64 grains per square inch?

Tutorial

■ **Solution**

$$N = 2^{n-1}$$

where N = no. of grains per square inch at 100×
n = ASTM grain-size number

Thus,

$$64 \text{ grains/in}^2 = 2^{n-1}$$
$$\log 64 = (n - 1)(\log 2)$$
$$1.806 = (n - 1)(0.301)$$
$$n = 7 \blacktriangleleft$$

EXAMPLE PROBLEM 4.5

If there are 60 grains per square inch on a photomicrograph of a metal at 200×, what is the ASTM grain-size number of the metal?

■ **Solution**

If there are 60 grains per square inch at 200×, then at 100× we will have

$$N = \left(\frac{200}{100}\right)^2 (60 \text{ grains/in}^2) = 240 = 2^{n-1}$$

$$\log 240 = (n - 1)(\log 2)$$
$$2.380 = (n - 1)(0.301)$$
$$n = 8.91 \blacktriangleleft$$

Note that the ratio of the magnification change must be squared since we are concerned with the number of grains per square inch.

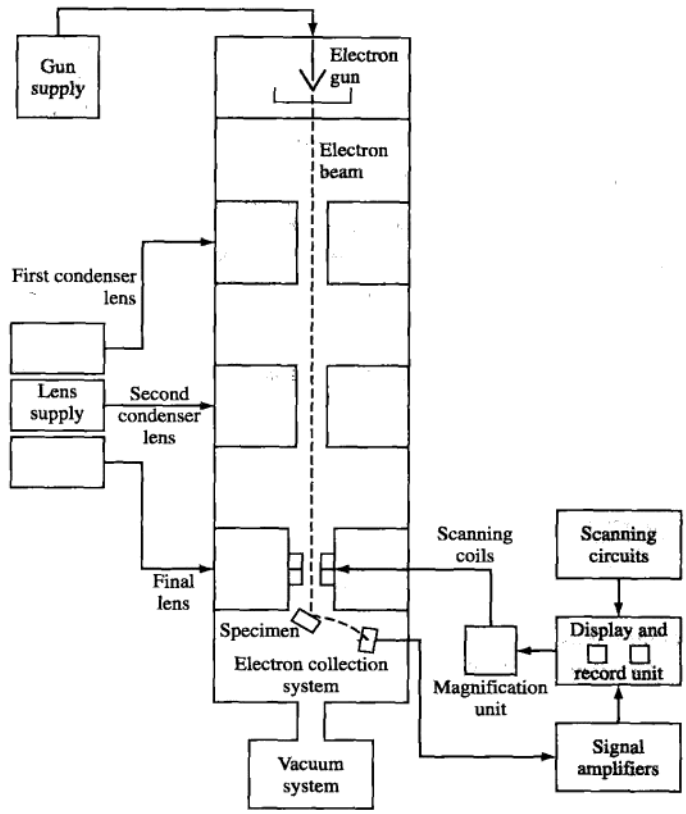

Figure 4.29
Schematic diagram of the basic design of a scanning electron microscope.
(After V.A. Phillips, "Modern Metallographic Techniques and Their Applications," Wiley, 1971, p. 425.)

4.5.2 Scanning Electron Microscopy (SEM)

Scanning electron microscope is an important tool in materials science and engineering; it is used for microscopic feature measurement, fracture characterization, microstructure studies, thin coating evaluations, surface contamination examination, and failure analysis of materials. As opposed to optical microscopy where the sample's surface is exposed to incident visible light, the SEM impinges a beam of electrons in a pinpointed spot on the surface of a target specimen and collects and displays the electronic signals given off by the target material. Figure 4.29 is a schematic illustration of the principles of operation of an SEM. Basically, an electron gun produces an electron beam in an evacuated column that is focused and directed so that it impinges on a small spot on the target. Scanning coils allow the beam to scan a small area of the surface of the sample. Low-angle backscattered electrons

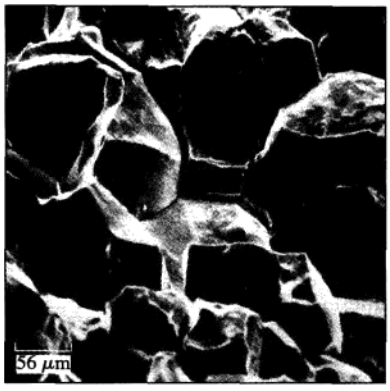

Figure 4.30
Scanning electron fractograph of intergranular corrosion fracture near a circumferential weld in a thick-wall tube made of type 304 stainless steel. (Magnification 180×.)
(After "Metals Handbook," vol. 9: "Fractography and Atlas of Fractographs," 8th ed., American Society for Metals, 1974, p. 77. ASM International.)

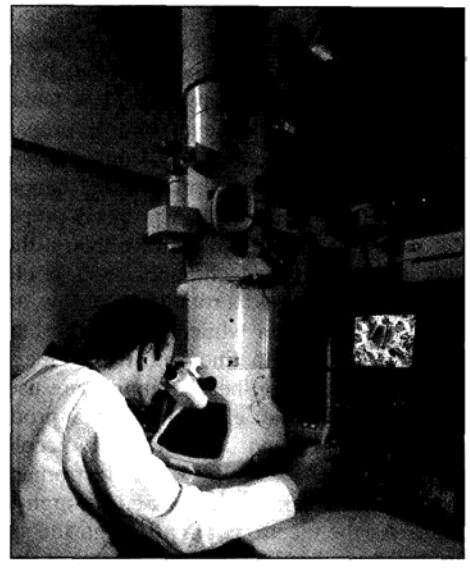

Figure 4.31
Man looking into an electron microscope.
(© Getty Images/RF.)

interact with the protuberances of the surface and generate secondary[7] backscattered electrons to produce an electronic signal, which in turn produces an image having a depth of field of up to about 300 times that of the optical microscope (about 10 μm at 10,000 diameters magnification). The resolution of many SEM instruments is about 5 nm, with a wide range of magnification (about 15 to 100,000×).

The SEM is particularly useful in materials analysis for the examination of fractured surfaces of metals. Figure 4.30 shows an SEM fractograph of an intergranular corrosion fracture. Notice how clearly the metal grain surfaces are delineated and the depth of perception. SEM fractographs are used to determine whether a fractured surface is intergranular (along the grain boundary) transgranular (across the grain), or a mixture of both. The samples to be analyzed using standard SEM are often coated with gold or other heavy metals to achieve better resolution and signal quality. This is especially important if the sample is made of a nonconducting material. Qualitative and quantitative information relating to the makeup of the sample may also be obtained when the SEM is equipped with an x-ray spectrometer.

4.5.3 Transmission Electron Microscopy (TEM)

Transmission electron microscopy (Fig. 4.31) is an important technique for studying defects and precipitates (secondary phases) in materials. Much of what is known

[7]Secondary electrons are electrons that are ejected from the target metal atoms after being struck by primary electrons from the electron beam.

about defects would be speculative theory and would have never been verified without the use of TEM, which resolves features in the nanometer range.

Defects such as dislocations can be observed on the image screen of a TEM. Unlike optical microscopy and SEM techniques where sample preparation is rather basic and easy to achieve, sample preparation for TEM analysis is complex and requires highly specialized instruments. Specimens to be analyzed using a TEM must have a thickness of several hundred nanometers or less depending on the operating voltage of the instrument. A properly prepared specimen is not only thin but also has flat parallel surfaces. To achieve this, a thin section (3 to 0.5 mm) is cut out of the bulk material using techniques such as electric-discharge machining (used for conducting samples) and a rotating wire saw, among others. The specimen is then reduced to 50 μm thickness while keeping the faces parallel using machine milling or lapping processes with fine abrasives. Other more advanced techniques such as electropolishing and ion-beam thinning are used to thin a sample to its final thickness.

In the TEM, an electron beam is produced by a heated tungsten filament at the top of an evacuated column and is accelerated down the column by high voltage (usually from 100 to 300 kV). Electromagnetic coils are used to condense the electron beam, which is then passed through the thin specimen placed on the specimen stage. As the electrons pass through the specimen, some are absorbed and some are scattered so that they change direction. It is now clear that the sample thickness is critical: A thick sample will not allow the passage of electrons due to excessive absorption and diffraction. Differences in crystal atomic arrangements will cause electron scattering. After the electron beam has passed through the specimen, it is focused with the objective coil (magnetic lens) and then enlarged and projected on a fluorescent screen (Fig. 4.32). An image can be formed either by collecting the direct electrons or the scattered electrons. The choice is made by inserting an aperture into the back focal plane of the objective lens. The aperture is maneuvered so that either the direct electrons or scattered electrons pass through it. If the direct beam is selected, the resultant image is called a *bright-field image,* and if the scattered electrons are selected, a *dark-field image* is produced.

In a bright-field mode, a region in a metal specimen that tends to scatter electrons to a higher degree will appear dark on the viewing screen. Thus, dislocations that have an irregular linear atomic arrangement will appear as dark lines on the electron microscope screen. A TEM image of the dislocation structure in a thin foil of iron deformed 14 percent at $-195°C$ is shown in Fig 4.33.

4.5.4 High-Resolution Transmission Electron Microscopy (HRTEM)

Another important tool in the analysis of defects and crystal structure is the high-resolution transmission electron microscopy. The instrument has a resolution of about 0.1 nm, which allows viewing of the crystal structure and defects at the atomic level. To grasp what this degree of resolution may reveal about a structure, consider that the lattice constant of the silicon unit cell at approximately 0.543 nm is five times larger than the resolution offered by HRTEM. The basic concepts behind this technique are